PRDM13, A DIRECT DOWNSTREAM TARGET OF PTF1A, REGULATES THE BALANCE OF GABAERGIC NEURONS VERSUS GLUTAMATERGIC NEURONS IN THE DORSAL SPINAL CORD

APPROVED BY SUPERVISORY COMMITTEE

Q. Richard Lu, Ph.D.

Christopher W. Cowan, Ph.D.

Thomas Wilkie, Ph.D.

Jane E. Johnson, Ph.D.

DEDICATION

To my Dad, Mom, and my whole family, for their love, support and devotion throughout my life.

PRDM13, A DIRECT DOWNSTREAM TARGET OF PTF1A, REGULATES THE BALANCE OF GABAERGIC NEURONS VERSUS GLUTAMATERGIC NEURONS IN THE DORSAL SPINAL CORD

by

JOSHUA CHIA-HSI CHANG

DISSERTATION

Presented to the Faculty of the Graduate School of Biomedical Sciences

The University of Texas Southwestern Medical Center at Dallas

In Partial Fulfillment of the Requirements

For the Degree of

DOCTOR OF PHILOSOPHY

The University of Texas Southwestern Medical Center at Dallas

Dallas, Texas

May, 2013

PRDM13, A DIRECT DOWNSTREAM TARGET OF PTF1A, REGULATES THE BALANCE OF GABAERGIC NEURONS VERSUS GLUTAMATERGIC NEURONS IN THE DORSAL SPINAL CORD

Joshua C. Chang, Ph.D.

The University of Texas Southwestern Medical Center at Dallas, 2013

Jane E. Johnson, Ph.D.

A fundamental question in neural development addresses the molecular mechanism for balancing the equilibrium of inhibitory versus excitatory (E/I balance) neurons. The combination of basic helix-loop-helix (bHLH) and homeodomain (HD) transcription factors is essential to generate the E/I balance required for correct functioning of neural networks. During dorsal spinal cord development, the bHLH factor Ascl1 is expressed in progenitors to dI3, dI4, and dI5 (dorsal interneurons 3-5) and is required for the glutamatergic neuronal fate. In contrast, another bHLH factor Ptf1a, is restricted in progenitors to dI4 and is required to specify the GABAergic neuronal fate. Since progenitors to dI4 express both Ascl1 and Ptf1a, some mechanism must exist to repress Ascl1 specification activities in these cells. Given that Ptf1a acts as a transcriptional

activator, I hypothesized that Ptf1a induces a transcriptional repressor as one of its downstream targets to mediate the suppression of glutamatergic lineage genes. A chromatin-remodeling transcription factor, Prdm13 (PRDI-BF1 and RIZ homology domain containing 13), was identified as a direct target of Ptf1a. The expression pattern of Prdm13 reflects that of Ptf1a in the spinal cord, cerebellum, diencephalon, and retina, and Ptf1a is the primary factor required for Prdm13 expression. Furthermore, I demonstrate that Prdm13 functions as a transcriptional repressor to actively suppress the excitatory cell fate by binding to specific cis-elements near the glutamatergic lineage regulatory genes, *Tlx1* and *Tlx3*, to silence their expression. Prdm13 acts through multiple protein/DNA complexes, including a novel complex with Ascl1, to repress Ascl1 activation of *Tlx3*. Prdm13 is also sufficient to induce Pax2 and the GABAergic phenotype. This aspect of Prdm13 function is likely indirect through repression of Tlx1/3 since it is known that Tlx1/3 normally blocks the HD factor Lbx1 that is also involved in GABAergic neuronal specification. Taken together, Prdm13 is a direct target of Ptf1a and is required to suppress the glutamatergic neuronal gene program in GABAergic neurons in the dorsal spinal cord. Therefore, Prdm13 is a novel component of a highly coordinated transcriptional network that provides a missing link in a cell fate decision required for somatosensory processing in the spinal cord.

ACKNOWLEDGEMENT

I thank my mentor Dr. Jane Johnson, for being the awesomest advisor and guiding me to become a better scientist. She has been patient and willing to assist me with my questions, experiments, and presentations. She is always a joy to see and always has her door opened ready for discussion.

I also thank the whole Johnson lab members, present and past, for being such wonderful human beings and making our lab feel like home.

I appreciate all the support and advise from my thesis committee members, Dr. Richard Lu, Dr. Thomas Wilkie, and Dr. Christopher W. Cowan. Every committee meeting discussions were very informative to me.

I thank all my family members for their encouragement and support throughout my life.

TABLE OF CONTENTS

PRIOR PUBLICATION

Chang J.C., Meredith D.M., Mayer P.R., Borromeo M.D., Lai H.C., Ou Y., and Johnson J.E. (2013) Prdm13 mediates the balance of inhibitory and excitatory neurons in somatosensory circuits. *Dev Cell*, (Accepted on February, 2013)

LIST OF FIGURES

LIST OF APPENDIX

LIST OF ABBREVIATIONS

Ascl1	achaete-scute homolog 1
Atoh1	atonal homolog 1
BAC	bacterial artificial chromosome
BAT	brown adipose tissue
BCL	B-cell lymphoma cell
BFI	binding factor I
bHLH	basic helix-loop-helix
BrdU	Bromodeoxyuridine
Brn3a	brain-specific homeobox/POU domain protein 3A
CE	ChIP efficiency
CGE	caudal ganglionic eminence
ChIP	chromatin immunoprecipitation
CNS	central nervous system
CtBP1	C-terminal binding proteins 1
Ctx	cortex
CTZ	cortical transitory zone
DIG	Digoxygenin
DG	dentate gyrus
dI	dorsal interneuron
dIL^{A}	dorsal interneuron late A
dIL^{B}	dorsal interneuron late B
Dll1	deltalike1
Dlx	distal-less
DNA	deoxyribonucleic acid
DRG	dorsal root ganglia
E	embryonic day
e	enhancer
E/I balance	balance of the excitatory versus inhibitory neurons
EnR	engrailed repressor
Evi1	ecotropic virus integration site 1 protein homolog
FACS	fluorescence-activated cell sorting
GABA	γ-Aminobutyric acid
GAD	glutamic acid decarboxylase
GE	ganglionic eminence
GFP	green fluorescent protein
HD	homeodomain
HDAC	histone deacetylases
HH	Hamburger and Hamilton stage
HMTs	histone methyltransferases
HP1	heterochromatim protein-1
HSCs	hematopoietic stem cells
INPs	intermediate neuronal progenitors
IP	immunoprecipitation

ISH	in situ hybridization
Isl	insulin gene enhancer protein
IZ	intermediate zone
Kdm	Lysine-specific demethylase
Kir	inward rectifying potassium channel
Kirrel	Kin of irregular chiasm-like protein
Lbx1	Ladybird homeobox 1
LGE	lateral ganglionic eminence
Lhx	LIM/homeobox protein
LIM	Lin11, Isl-1 and Mec-3
Lmx1b	LIM homeobox transcription factor 1-beta
Mash1	mammalian homolog of achaete-scute complex 1
Mec	mitosis entry checkpoint
MGE	medial ganglionic eminence
mRNA	messenger Ribo Nucleic Acid
MZ	mantle zone
NeuroD	neurogenic differentiation factor 1
Neurog1/2	neurogenin1/2
Nphs	Nephrin
Olig	oligodendrocyte transcription factor
Pax2	paired box gene 2
PBS	phosphate buffered saline
PGC	peroxisome proliferator activated receptor coactivator-1α
PNS	peripheral nervous system
POU	Pituitary specific, Octamer, Unc transcription factor
Prdm13	PRDI-BF1 and RIZ homology domain containing 13
PRDI	positive regulatory domain I
Ptf1a	pancreatic transcription factor 1a
PTF1-J	Ptf1a forms a transcriptional complex with an E-protein and Rbpj
Rbpj	recombining binding protein suppressor of hairless
RGCs	radial glia cells
RIZ	retinoblastoma-interacting zinc finger protein
SCG10	superior cervical ganglion-10
Seg	sequencing
SET	Suppressor of variegation 3-9, Enhancer of zeste and Trithorax
shRNA	small hairpin RNA
SMCs	smooth muscle cells
Tlx	T-cell leukemia homeobox protein
Tuj1	neuron-specific class III beta-tubulin
UTR	untranslated region
vGlut2	vesicular glutamate transporters 2
VP	herpes simplex virus tegument protein
VZ	ventricular zone
WAT	white adipose tissue
ZF	zinc finger

CHAPTER ONE

Introduction

I. Dorsal spinal cord provides the first level of central processing for somatosensation

It is in the dorsal horn where the first level of central somatosensory processing occurs. Primary sensory information from the periphery is conveyed through the dorsal horn of the spinal cord to supraspinal brain regions by ascending efferents including the spinoreticular, spinomesecephalic, and spinohypothalamic tracts, or locally for reflex responses (Liu and Ma, 2011; Ross, 2011; Willis, 2007). Somatosensation initiates when sensory receptors located within peripheral tissues, such as skin, muscles, bones, and joints, are stimulated. The sensory signals including pain, touch, temperature and proprioception are transmitted via primary sensory neurons. These neurons have their cell bodies in the dorsal root ganglia (DRG) and their axons project to the dorsal horn of the spinal cord. Dorsal spinal cord neurons include excitatory projection neurons that relay the sensory information to other spinal cord or brain regions, and a network of excitatory and inhibitory local circuit neurons that mediate the incoming sensory information. Thus, the dorsal horn interneurons are essential for modulating and relaying sensory information that is crucial for sensing our environment and our position within the environment. The balance of the excitatory versus inhibitory neurons (E/I balance), like other neuronal circuitry, is required to integrate and modulate the somatosensory information correctly. Disruption of this E/I balance can lead to sensory disorders such as dyseasthesia, hyperalgesia and allodynia (Fitzgerald, 2005; Tavares and Lima, 2007). Given the importance of the dorsal horn neurons in processing all somatosensory modalities, understanding of how these interneurons are specified during embryogenesis to generate the correct

composition of neurons holds significance for addressing neurological disorders that may arise from disruption of this equilibrium. Yet, even today we are far from understanding the regulatory cascades that control these interneuronal lineages, their migration patterns, axonal targeting, synaptic connections, and neurotransmitter phenotypes. In this study, I identified a zinc finger transcription factor belonging to the PRDM family, which interacts with proneural basic helix-loop-helix (bHLH) transcription factors to regulate downstream homeodomain (HD) transcription factors in order to generate a precise equilibrium of excitatory and inhibitory interneuronal populations.

II. Transcription factors play essential roles in the development of the central nervous system

The development of the central nervous system (CNS) begins as a sheet of neuroepithelial cells. As development proceeds, these neuroepithelial cells are eventually replaced by different neural stem/progenitor cells such as radial glial and/or intermediate neuronal progenitors (INPs). Together, these cells proliferate to give rise to three major cell types, neurons, oligodendrocytes, and astrocytes in the CNS (Merkle and Alvarez-Buylla, 2006). Progenitors are specified in a spatial and temporal dependent fashion, and generate a progressively restricted diverse set of cell types in different time windows. Transcription factors function throughout this process to regulate the various cell types generated. The coordinative interactions between these transcription factors proceed as a dynamic "cocktail", directing neuronal fate determination. Understanding the functional contributions of these transcription factors is crucial to uncover how neuronal progenitors are specified from a complicated heterogeneous environment.

a. Classification of bHLH transcription factors

The bHLH transcription factors are known for controlling the activity of gene expression networks in multiple organ systems where they play critical roles in early cell fate determination and differentiation, cell cycle maintenance, and homeostasis or stress response pathways (Massari and Murre, 2000). As their name implies, bHLH transcription factors are defined by their unique protein structure, which contain two alpha-helices that are separated by a loop of variable length. The two alpha-helices

domain (HLH) is important for protein-protein dimerization either with itself or other HLH proteins. The region contains several basic amino acids directly interact with DNA (Murre et al., 1994). There are several ways to classify the bHLH superfamily. Recent phylogenetic analysis re-evaluates the classifications of these genes from seven different species (human, mouse, rat, worm, fly, yeast, and plant) based on the unbiased sequence comparison across the full-length proteins, and organized this superfamily into six clades. Clade 1 contains only mammalian genes; clades 2-5 have a mixture of species; and clade 6 includes only plant bHLH genes (Stevens et al., 2008). The two bHLH transcription factors, Achaete-scute homolog 1 (Ascl1: previously Mash1) and Pancreas transcription factor 1 subunit alpha (Ptf1a) that I am focusing on in this thesis belong to clade 1, which will be discussed in more detail below (Stevens et al., 2008).

Another way to classify the bHLH superfamily is based on a combination of functional characteristics, such as DNA binding activity, dimerization partners, and expression patterns (Murre et al., 1994). Seven functional subclasses have been identified, class I, II, V, and VI are particularly essential for neuronal development. Class I proteins such as the *Drosophila* daughterless or E-proteins (E12, E47, and E2-2) in vertebrates are ubiquitously expressed and form either homodimers, or heterodimers with class II factors. Class II factors exhibit tissue restricted expression patterns and function as heterodimers with the class I to bind and activate transcription. For example, Ascl1 and Ptf1a1 are involved in the development of the CNS, whereas myogenic factors, such as MyoD and myogenin, are required for muscle development. Class III proteins contain myc related proteins and some interact with the class IV proteins, such as Mad and Max. Members of class V include the Inhibitor of DNA-binding/differentiation proteins (Id) family and Extramacrochaetae (Emc), both of which lack the entire basic segment, and thus do not bind DNA. Instead, these proteins function to dimerize with class I and class II factors thereby inhibiting them from binding to DNA to regulate gene expression. Class VI bHLH proteins contain proline in their basic region and include the Hairy and Enhancer of Split family (Crews, 1998; Murre et al., 1994).

b. Mechanism of bHLH transcription factor action

Studies have shown that bHLH factors bind to a conserved DNA sequence motif, CANNTG, known as an E-box. Solution of the crystal structures for several bHLH factors, including Max, USF, E47, Myod1, and Neurod1, shows that the basic region of each monomer binds to the major groove of each "CAN" half-site (Ellenberger et al., 1994; Ferre-D'Amare et al., 1994; Ferre-D'Amare et al., 1993; Longo et al., 2008; Ma et al., 1994). However, different bHLHs exhibit some preference for a particular combination of the two central bases (Murre et al., 1989a; Murre et al., 1989b). For example, Ascl1 forms high-affinity E-box binding heterooligomeric complexes with E protein E12 and requires its basic region "VARRNERERNR" to interact with a preferred motif as "CAGCTG" for activating downstream target (Fig. 1-1A) (Johnson et al., 1992). In contrast, Ptf1a forms a transcriptional complex (PTF1-J) with an E protein and Rbpj (Recombining binding protein suppressor of hairless) (Beres et al., 2006; Cockell et al., 1989; Krapp et al., 1996; Masui et al., 2007; Obata et al., 2001). The consensus DNA binding site for the PTF1 complex required both an E-box and an Rbpj site (TC-box: TTTCCCA), and both are required to activate transcription (Fig. 1-1B) (Beres et al., 2006; Cockell et al., 1989; Rose and MacDonald, 1997). Importantly, it is the PTF1-J trimer, not the Ptf1a/E protein heterodimer, which is essential for regulating the early neuronal development (Hori et al., 2008; Masui et al., 2007). It is the combination of diverse trans-elements (the transcription factors) and their cis-elements arranged in regulatory regions of genes that provide the complexity needed to regulate the balance of the excitatory versus inhibitory neurons generated to form functioning neuronal circuits.

III. Neuronal specification of excitatory versus inhibitory neurons in CNS

There are two developmental schemes described for the origin of excitatory and inhibitory neurons within a network (Fig. 1-1). In the dorsal spinal cord, both the excitatory and inhibitory neurons arise from progenitor populations within the same region (Gowan et al., 2001; Muller et al., 2005; Nakada et al., 2004). By contrast, in the cortical development, there are distinct origins give rise to these two

major classes of neurons; the inhibitory neurons undergo a long tangential migration from their origin from the ganglionic eminence (GE), where as the excitatory neurons arise from the cortex (Corbin and Butt, 2011; Marin et al., 2000; Merot et al., 2009; Parnavelas, 2002).

a. Neuronal specification in the telencephalon

The neurons of the cerebral cortex can be divided into two categories; the pyramidal neurons that transmit signals to other regions of cortical and subcortical targets using the excitatory neurotransmitter glutamate, and the non-pyramidal neurons that regulate local circuitry using the inhibitory neurotransmitter gamma-aminobutyric acid (Dahm et al.). The excitatory neurons develop within the cortical neuroepithelium from radial glia cells (RGCs), which function as primary progenitors or neural stem cells located in the ventricular zone (VZ) (Kriegstein and Alvarez-Buylla, 2009). Unlike the excitatory pyramidal neurons, the non-pyramidal inhibitory interneurons are derived from the ganglionic eminence (GE), the primordial of the basal ganglia in the ventral telecephalon or subpallium, and migrate tangentially up to the cortex, arriving at their final destination after radial migration across the cortical layers. The GE is divided anatomically into three different regions, the medial (MGE), lateral (LGE), and caudal (CGE), which produce various subtypes of interneurons (Fig. 1-1C, left half). These non-pyramidal neurons are important for modulating the cortical circuit activity, which involves the storage and retrieval of memories, the integration and processing of sensory and motor information, and the regulation of emotion and motivation.

b. Transcription factors regulate neuronal specification in the telencephalon

Genetic mechanisms govern the generation and specification of cortical GABAergic interneurons from the ventral telencephalon. The *Dlx* homeobox genes (Distal-less), including *Dlx1/2* and *Dlx5/6*, encode a family of transcription factors that regulate generation, specification, and migration of cortical interneurons in all regions of GE (Anderson et al., 1997a). In the Dlx1/2 knockout mouse, GABAergic

interneurons fail to migrate out of the GE, thus leading to a reduction of interneurons in the cortex and olfactory bulb and also abnormal striatal differentiation (Anderson et al., 1997b; Bulfone et al., 1998). The proneural factor Ascl1 is expressed in the ventral telencephalon in progenitors to the inhibitory cortical neurons and in progenitors to basal ganglia neurons. Ascl1 mutant mice exhibit defects in neurogenesis in the ventral telencephalon, affecting in particular the generation of neuronal precursor cells in the subventricular zone (SVZ) of the MGE, and the timing of production of SVZ precursors in the LGE. By examining the expression of GAD67 (glutamic acid decarboxylase) and Dlx1, it was found that both genes are less abundant in the intermediate zone (IZ), and are almost completely absent in the MZ, indicating Ascl1 is required for the generation and/or migration of neocortical GABAergic interneurons (Casarosa et al., 1999; Fode et al., 2000).

In contrast to Ascl1, another family of bHLH transcription factors, neurogenin 1 (Neurog1) and neurogenin 2 (Neurog2), are expressed exclusively in cells of the dorsal ventricular zone (VZ), different from the Ascl1, which is expressed in the ventral progenitors (Fig. 1-1C, right half) (Fode et al., 2000; Ma et al., 1997). In the Neurog 2 null mouse, the normal ventrally restricted factor Ascl1 is expanded into dorsal regions. The expanded Ascl1 re-specifies a subpopulation of neurons to Dlx2 expressing vental-like neurons, leaving the general neuronal markers at normal levels (ie SCG10, Superior cervical ganglion-10 and NeuroD, Neurogenic differentiation factor 1). Intriguingly, the expression levels of SCG10 and NeuroD are strongly reduced in Neurog 2 and Ascl1 double knockout mice, indicating that Neurog 2 determines the early born cortical neurons, and that the ectopic up-regulation of Ascl1 can partially compensate for the loss of Neurog 2 in the mutant (Fig. 1-1C). As a result, these data indicate that correct dorsal-ventral patterning of the telencephalon is dependent not only on the interactions of homeodomain genes, but also with the interactions of the bHLH transcription factors (Fode et al., 2000; Rallu et al., 2002). Furthermore, the different excitatory and inhibitory neuronal components of the cortical network are derived from progenitors with distinct spatial origins.

c. Neuronal specification in the spinal cord

A different scheme for the origin of excitatory and inhibitory neurons is used in the spinal cord, and has both subtypes of neurons derived from the same progenitor pool located in the dorsal neural tube (Fig. 1-1D). The transcription factors that regulate neuronal development have been investigated in the spinal cord for decades. Spinal cord, the anatomically simplest and most conserved region of the vertebrate CNS, has been instrumental for understanding the mechanisms that control the progressive acquisition of neuronal specification along the embryonic dorsal-ventral axes. Neurons in the dorsal spinal cord are generated in two phases, six early-born (embryonic day E10-E11.5) interneuron populations defined as dI1-dI6, and two later-born (E11.5-E13) interneuron populations defined as dIL^{A} and dIL^{B}. Neuronal populations dI4 and dIL^{A} become GABAergic inhibitory neurons while the neighboring populations dI5 and dIL^{B} become glutamatergic excitatory neurons (Gross et al., 2002; Muller et al., 2002).

d. Transcription factors regulate neuronal specification in the spinal cord

Two families of transcription factors have stood out as major players in specification of neuronal subtype in the dorsal spinal cord: bHLH and HD proteins (Helms and Johnson, 2003). Proneural bHLH transcription factors define progenitor cell fates in the dorsal neural tube at embryonic day 10 (E10). They specify progenitors as six types of dorsal interneurons, which can be distinguished on the basis of the HD transcription factors they express (Fig. 1-2A). Atonal homolog1 (Atoh1) is expressed in the very dorsal population adjacent to the roof plate in progenitors to dI1 neurons (dI1: dorsal interneuron 1), Neurog1 and Neurog2 are co-expressed in progenitors just ventral to the Atoh1 domain and give rise to dI2. Ascl1 is expressed in the progenitors that will become dI3 to dI5 neurons (Caspary and Anderson, 2003; Helms and Johnson, 2003). Another bHLH transcription factor, Ptf1a, which also determines the cell fate decisions, is restricted to progenitors in the dI4 domain, overlapping with Ascl1 (Fig. 1-2A).

These bHLH transcription factors are not only expressed in distinct progenitor cells but also have distinct functions here as well. In addition to their shared activity in inducing neuronal differentiation, they are both necessary and sufficient to specify the neuronal subtype as defined by expression of HD transcription factors. For example, in Atoh1 mutant mice, dI1 neurons expressing the LIM HD (Lin11, Isl-1 and Mec-3) factors Lhx2 and Lhx9 were lost and instead are replaced by dI2 neurons. That Atoh1 specifies neural progenitors to become dI1 neurons was demonstrated in over expression assays in the chick neural tube where ectopic expression of Atoh1 resulted in an increase in dI1 and a loss of dI2. The opposite was seen when Neurog1 and Neurog2 were mutated or overexpressed (Gowan et al., 2001). This role for bHLH factors was also seen for Ascl1 and Ptf1a (see below), supporting the importance of this class of factors in specifying neuronal subtype in the dorsal spinal cord.

e. bHLH transcription factors specify progenitors in the spinal cord

1. bHLH transcription factor Ptf1a specifies the GABAergic neuronal lineage in CNS

Ptf1a encodes a bHLH transcription factor, Pancreas transcription factor 1 subunit alpha, classified as class II bHLH, and was first identified as one subunit of the PTF1 complex regulating the pancreatic digestive enzyme Elastase (Cockell et al., 1989). However, Ptf1a is expressed early in the pancreas at E11.5, and is required for the pancreas to form. In knockout studies, loss of Ptf1a results in neonatal death and the neonates are associated with below average birth weight, complete failure of pancreatic development, and cerebellar agenesis (Kawaguchi et al., 2002; Krapp et al., 1998; Sellick et al., 2004) (Kawaguchi et al., 2002; Soriano, 1999). During embryogenesis in the CNS, Ptf1a is expressed in the dorsal neural tube, restricted in the dP4 domain (Fig. 1-2C), and also in the developing cerebellum (Fig. 2-3A), diencephalon (Fig.2-3B,C), and retina (Fig. 2-3G). Ptf1a null mice have a complete loss of dI4 and dIL^{A} GABAergic interneurons with a significant increase of excitatory dI5 and dIL^{B} interneurons. Later analysis at E16.5 from the spinal cord showed a loss of Gad1 mRNA expression but an obvious increase of vGlut2. Therefore, Ptf1a is essential for generating these dorsal GABAergic neurons while suppressing the glutamatergic fate (Glasgow et al., 2005; Hori et al., 2008; Huang et al., 2008). Additionally, a point

mutation in Ptf1a, Ptf1a^{W298A}, which interrupts the interaction of Ptf1a and its binding partner Rbpj, also reveals the same phenotypes demonstrating the heterotrimer complex with E-protein and Rbpj is the functional complex in vivo. In summary, the loss of Ptf1a causes a cell fate switch from GABAergic to glutamategic neuronal lineage in the dorsal spinal cord (Glasgow et al., 2005; Hori et al., 2008). Indeed, ectopically expressing Ptf1a in ovo in chick neural tube represses dI3/5 and dIL$_B$ glutamatergic interneurons, and induces dI2/4 and dIL$_A$ GABAergic interneurons (Fig. 1-3B',B'')(Hori et al., 2008).

Ptf1a is also required for the formation of GABAergic neurons in other regions of the nervous system including the developing cerebellum and retina (Dullin et al., 2007; Fujitani et al., 2006; Hoshino et al., 2005; Nakhai et al., 2007; Pascual et al., 2007). Lineage tracing analysis indicated both horizontal and amacrine cells are derived from Ptf1a-expressing precursors but not the photoreceptor cells. Indeed, deletion of *Ptf1a* in the retina dramatically reduces the number of both horizontal and amacrine cells, while producing supernumerary excitatory retinal ganglion cells (Fujitani et al., 2006). An analogous phenotype, fate switching of inhibitory neurons to excitatory neurons, is also seen in cerebellar development. Utilizing the lineage tracing analysis from the Cre knock in *Ptf1a* mice (*Ptf1a$^{Cre/Cre}$;R26R*), in the absence of *Ptf1a*, progenitors failed to develop to Purkinje cells and other GABAergic interneurons, instead, an ectopic expression of glutamatergic granule cells was found (Pascual et al., 2007). Taken together, Ptf1a specifies the GABAergic neurons not only in the dorsal spinal cord, but also in multiple regions within the CNS, such as the embryonic retina and cerebellum.

2. bHLH transcription factor Ascl1 regulates neuronal development in the spinal cord

Ptf1a is not the only bHLH factor that controls the balance of the dI4/dIL^A GABAergic versus dI5/dIL^B glutamatergic neurons in the dorsal neural tube; Ascl1 is also present and earlier than Ptf1a and is in progenitors to both dI4/dILA and dI3/5/dILB. Ascl1 is an ortholog of Achaete-scute genes first identified in Drosophila. Ascl1 is transiently expressed in the VZ in multiple regions of the CNS and PNS (Johnson et al., 1990; Lo et al., 1991), including subsets of cells in the telecephalon, diencephalon, mesencephalon, metencephalon, myelecephalon, and neural tube (Kim et al., 2008; Verma-Kurvari et al.,

1996). *Loss of function of Ascl1 results in dramatic phenotypes in neuronal differentiation and subtype specification in various regions of the nervous system. In the spinal cord, a specification function for Ascl1 was uncovered*. Although Ascl1 is expressed in VZ from dI3 through dI5 domains, in the knockout mice there is a striking loss of only two of these populations. There is a 70% loss of $Isl1^+$ neurons (dI3) and a complete loss of $Lmx1b^+$ neurons (dI5). In contrast, a dramatic increase in dI2 neurons labeled by both Lhx1/5 and Brn3a and also an increase of dI4 neurons labeled by Pax2, which appear to ectopically fill in the gap of the missing dI3 and dI5 neurons was found in the mutant. Furthermore, excess levels of Ascl1 induce expression of homeodomain (HD) factors Tlx1/3, Isl1, and Lmx1b (dI3 and dI5) at the expense of Pax2 (dI4) (Fig. 1-2D-D'') (Helms et al., 2005; Mizuguchi et al., 2006; Wildner et al., 2006). These observations suggested that Ascl1 contributes to the context-dependent regulation of glutamatergic neuronal specification (Helms et al., 2005).

In combination with its role in neuronal cell fate specification, Ascl1 is also well known for its role in neuronal differentiation (Kageyama and Nakanishi, 1997). Gain of function studies indicate Ascl1 induces neuronal differentiation as defined by cell cycle exit, translocation of the cells laterally out of the ventricular zone, and expression of neuronal markers (Nakada et al., 2004). Overexpression of Ascl1 in chick neural tube resulted in the electroporated cells being preferentially located lateral to the VZ in the mantle layer where differentiating neurons reside. These electroporated cells begin to express a neuronal differentiation marker, Tuj1 (neuron-specific class III beta-tubulin); and had exited the cell cycle as determined by the lack of Bromodeoxyuridine (BrdU) incorporation (Nakada et al., 2004). Taken together, in addition to the regulation of neuronal specification, Ascl1 also plays a critical role in promoting the neuronal differentiation in the earlier stage of neural development.

f. HD transcription factors involved in neuronal specification in spinal cord

Homeodomain (HD) transcription factors also play important roles in identifying different subtype of neurons. A classic study by Cheng identified Tlx-class homeobox genes, T-cell leukemia homeobox protein 3 (Tlx3) and its family member Tlx1, in regulating the glutamatergic neuronal cell fate.

Tlx3 and Tlx1 are both expressed in glutamatergic neurons in the developing dorsal spinal cord. Tlx3 is expressed in both dI3 and dI5, whereas Tlx1 is restricted to dI5 (Fig. 1-2A), and both are able to repress the GABAergic cell fate. The loss of Tlx genes causes a concomitant de-repression of generic and region-specific GABAergic markers in prospective glutamatergic cells. The gain of function confirms the results from the Tlx knockout mice studies; ectopic Tlx3 expression is sufficient to repress endogenous GABAergic differentiation and induce formation of glutamatergic cells in developing chick spinal cord (Cheng et al., 2004).

Moreover, another post-mitotic homeobox gene, Ladybird homeobox 1 (Lbx1); actively promotes a GABAergic over a glutamatergic neuron cell fate in the dorsal neural tube. Tlx3 antagonizes Lbx1, which in turn allows a subset of $Lbx1^+$ cells to differentiate into glutamatergic neurons. Even though Lbx1 is expressed in the dI5, the co-existence of Tlx1/3 represses its activity and drives these cells toward glutamatergic fate in the spinal cord (Fig. 1-2D'-D''). Loss of Lbx1 results in a transformation of prospective GABAergic neurons into glutamatergic neurons (Cheng et al., 2005). Indeed, this result was further confirmed by ectopic expressing Lbx1 in the chick neural tube, where an increase of $Pax2^+$ cells was observed in the electroporated side, but only in regions outside of Tlx1/3 expression (Fig. 1-4B-B'',C,D), indicating the endogenous Tlx3 antagonized the overexpression of Lbx1. The output from this regulatory network is the specification of either an excitatory ($vGlut2^+$) or inhibitory ($Gad1^+$) neuronal phenotype, demonstrating the ectopic expression of Lbx1 causes an opposite switch, from glutamatergic to GABAergic neuronal lineage (Cheng et al., 2004; Cheng et al., 2005; Glasgow et al., 2005; Gross et al., 2002; Muller et al., 2002). This cell fate 'switch' activity distinguishes Lbx1 from its downstream target, another HD transcription factor paired box gene 2 (Pax2), which is required for GABAergic differentiation but is incapable of suppressing glutamatergic differentiation (Gross et al., 2002).

In the Pax2 mutant, there is a dramatic reduction of GABAergic marker Gad1, but no effect on the glutamatergic marker vGlut2 in the dorsal spinal cord (Cheng et al., 2004). The co-expression of Pax2 and two other LIM homeodomain transcription factors, Lhx1 and/or Lhx5, provide a transcription factor code for inhibitory neurons, which function together to maintain Pax2 expression in subsets of spinal

inhibitory interneurons and establish a stable GABAergic differentiation program in these cells. The deletion of both *Lhx1* and *Lhx5* in the embryonic cord results in the loss of $Pax2^{+}$ interneurons, which is followed by the decrease of the inhibitory neuronal markers *Gad1* and *Viaat* (Pillai et al., 2007). Although Ptf1a acts as upstream regulator and initiates the expression of several downstream transcription factors in the future inhibitory neurons, Pax2 and Lhx1/5 are required for the inhibitory neuronal cell fate and to determine the inhibitory neurotransmitter, GABA, as well as neuropeptides dynorphin, galanin, *Neuropeptide Y,* nociceptin and enkephalin (Batista and Lewis, 2008; Brohl et al., 2008; Pillai et al., 2007).

IV. Remaining questions for control of neuronal specification in the dorsal spinal cord

One major question is how progenitor cells that express both Ascl1 and Ptf1a give rise to inhibitory neurons where the GABAergic gene program is induced and the glutamatergic gene program is repressed. This is particularly puzzling since both Ptf1a and Ascl1 are transcriptional activators. Thus, some mechanism must exist to repress Ascl1 specification activities when Ptf1a is present. Ptf1a appears sufficient to repress Ascl1 activity since the ectopic expression of Ptf1a represses Tlx1 and Tlx3 (Fig. 1-3B'). I confirmed this prediction by ectopic expression of Ascl1 and Ptf1a simultaneously in the chick neural tube. In this paradigm, Ptf1a was dominant over Ascl1, inhibiting both ectopic and endogenous Tlx1/3 expression while continuing to activate Pax2 (Fig. 1-3C-C'',D,E). Therefore, I hypothesized that Ptf1a induces a transcriptional repressor as one of its downstream targets, and this repressor functions to mediate the suppression of glutamatergic lineage genes. Prior to my thesis work only a few direct targets of Ptf1a had been identified, and none of these provide an understanding of how Ptf1a induces one fate while suppressing the other (Henke et al., 2009; Meredith et al., 2009; Nishida et al., 2010). However, work from the Johnson laboratory combining ChIP-Seq for Ptf1a binding, and RNA-Seq for gene expression in Ptf1a wild type and mutant neural tubes, generated a list of candidate transcription factors that might serve this purpose. I chose to evaluate one of these targets, Prdm13, a zinc finger transcription

factor. I demonstrate Prdm13 function provides a mechanism for the transcriptional repression required to suppress glutamatergic gene expression in the GABAergic lineage.

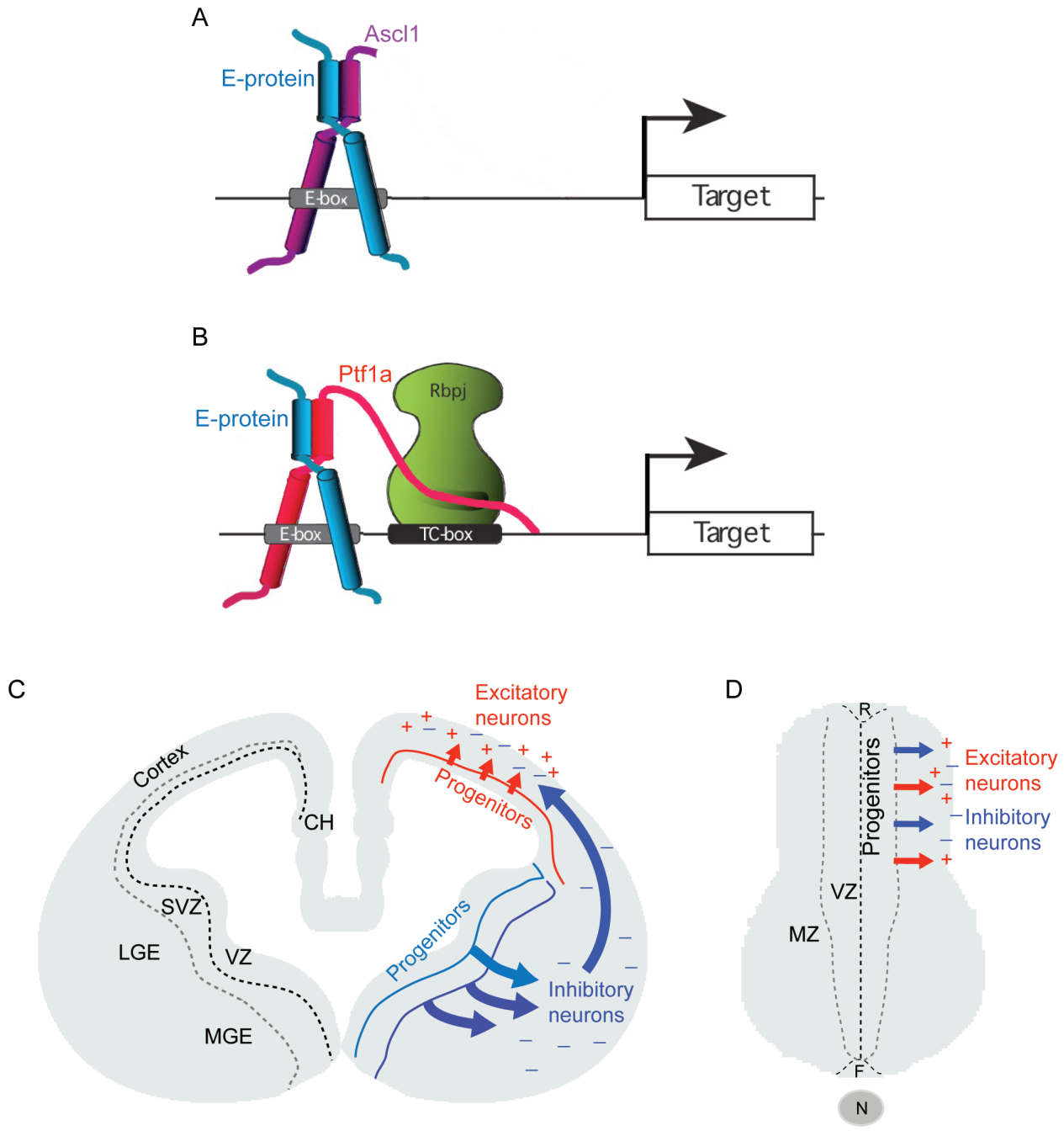

Figure 1-1. Mechanism of bHLH transcription factors.

(A) A diagram depicting the heterodimer formed by the bHLH transcription factor Ascl1 (purple) with its co-factor E-protein (blue). The complex binds to a consensus E-box motif (gray box) to activate transcription of downstream target genes.
(B) A diagram depicting the PTF1-J heterotrimer formed by Ptf1a (red) with an E protein (blue) and Rbpj (green). This complex binds to a consensus PTF1 motif, which contains an E-box (gray box) and a TC-box (dark gray box, Rbpj site).
(C) Diagram of a coronal section from an E13.5 mouse telencephalon showing the distinct origins of the excitatory (red) and inhibitory (blue) neurons.
(D) Diagram of a transverse section from an E10.5 mouse spinal cord showing that excitatory and inhibitory neurons arise from the same progenitor domain.
Abbreviation: ventricular zone, VZ; medial ganglionic eminence, MGE; lateral ganglionic eminence, LGE; subventricular zone, SVZ; cortical hem, CH; mantle zone, MZ; roof plate, R; floor plate, F; notochord, N.

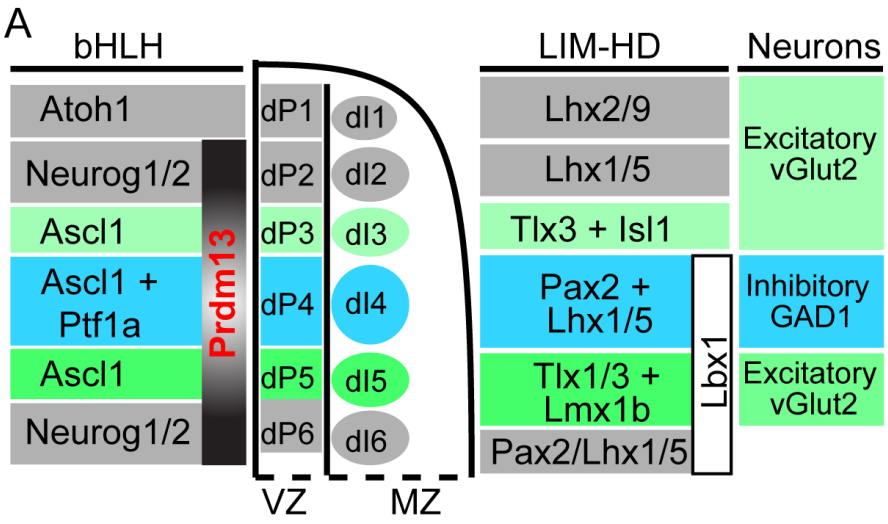
A
bHLH
LIM-HD
Neurons
Atoh1
Neurog1/2
Ascl1
Ascl1 +
Ptf1a
Ascl1
Neurog1/2
Prdm13
dP1
dP2
dP3
dP4
dP5
dP6
dI1
dI2
dI3
dI4
dI5
dI6
VZ
MZ
Lhx2/9
Lhx1/5
Tlx3 + Isl1
Pax2 +
Lhx1/5
Tlx1/3 +
Lmx1b
Pax2/Lhx1/5
Lbx1
Excitatory
vGlut2
Inhibitory
GAD1
Excitatory
vGlut2

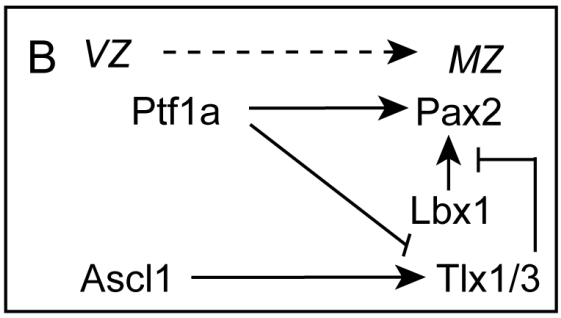
B
VZ
MZ
Ptf1a
Pax2
Lbx1
Ascl1
Tlx1/3

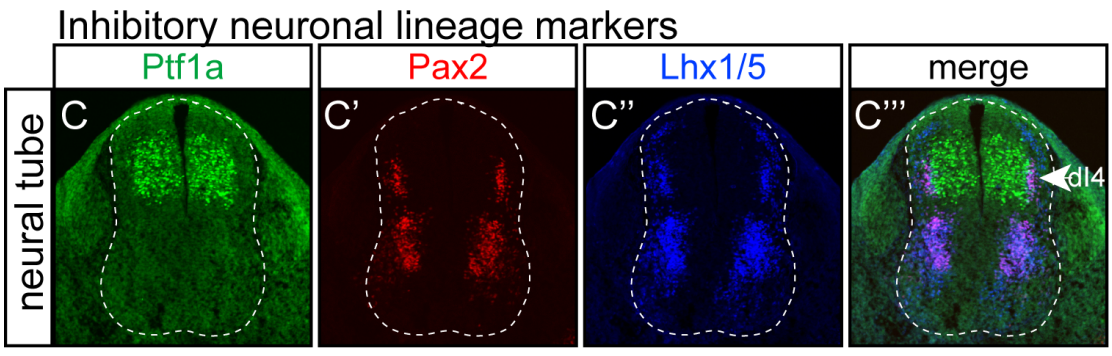
Inhibitory neuronal lineage markers
Ptf1a
Pax2
Lhx1/5
merge
neural tube
C
C'
C''
C'''
dI4

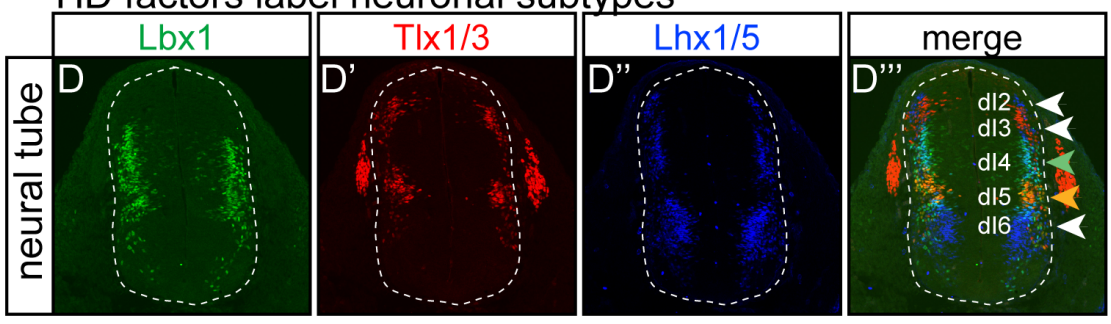
HD factors label neuronal subtypes
Lbx1
Tlx1/3
Lhx1/5
merge
neural tube
D
D'
D''
D'''
dI2
dI3
dI4
dI5
dI6

Figure 1-2. bHLH and HD transcription factors define neuronal subtypes.

(A) Diagram showing the expression pattern and interacting network of bHLH and HD transcription factors in the dorsal spinal neural tube. Notice that the bHLH transcription factor Ascl1 is expressed from dP3 to dP5, whereas Ptf1a is restricted in the dP4 domain. HD transcription factor Tlx1/3 marks dI3 and dI5 neurons, and these neurons will develop as glutamatergic neurons. Pax2 together with Lhx1/5 mark the dI4 as GABAergic neurons. Lbx1 is expressed from dI4 to dI6 in the dorsal spinal cord.
(B) Model for the transcriptional network specifying excitatory versus inhibitory neurons in the dorsal spinal cord at the start of this thesis. Ptf1a, along with Ascl1, act upstream of HD factors such as Pax2 and Lbx1 important in GABAergic lineages, and Tlx1 and Tlx3 important in specifying glutamatergic lineages. To generate glutamatergic neurons from Lbx1 expressing precursor cells, Tlx1 or Tlx3 antagonizes Lbx1 function. In those cells with Lbx1 and Tlx1/3, no Pax2 is expressed and the neurons become glutamatergic neurons. In Lbx1 expressing cells lacking Tlx1/3, Pax2 is expressed and the neurons become GABAergic neurons. Proneural transcription factors are expressed in the progenitors in the VZ, and induce neuronal differentiation, while these cells migrate out to the MZ, they start to express HD transcription factor to further determine their cell fate.
(C) Immunostaining of Ptf1a, Pax2, and Lhx1/5 in the mouse dorsal spinal cord at stage E10.5. Ptf1a, Pax2, and Lhx1/5 are markers for GABAergic lineage neurons. Ptf1a is in the progenitor dP4 domain while Pax2 and Lhx1/5 are in postmitotic cells dI4 domain (white arrow).
(D) Immunostaining of HD transcription factor Lbx1, Tlx1/3, and Lhx1/5 mark neuronal population dI2-dI6. Lbx1 and Tlx1/3 are co-expressed in dI5 (orange arrow), and these cells are Lhx1/5 negative. In Lbx1 cells lacking Tlx1/3, Lhx1/5 is present and labels dI4 neurons (green arrow).

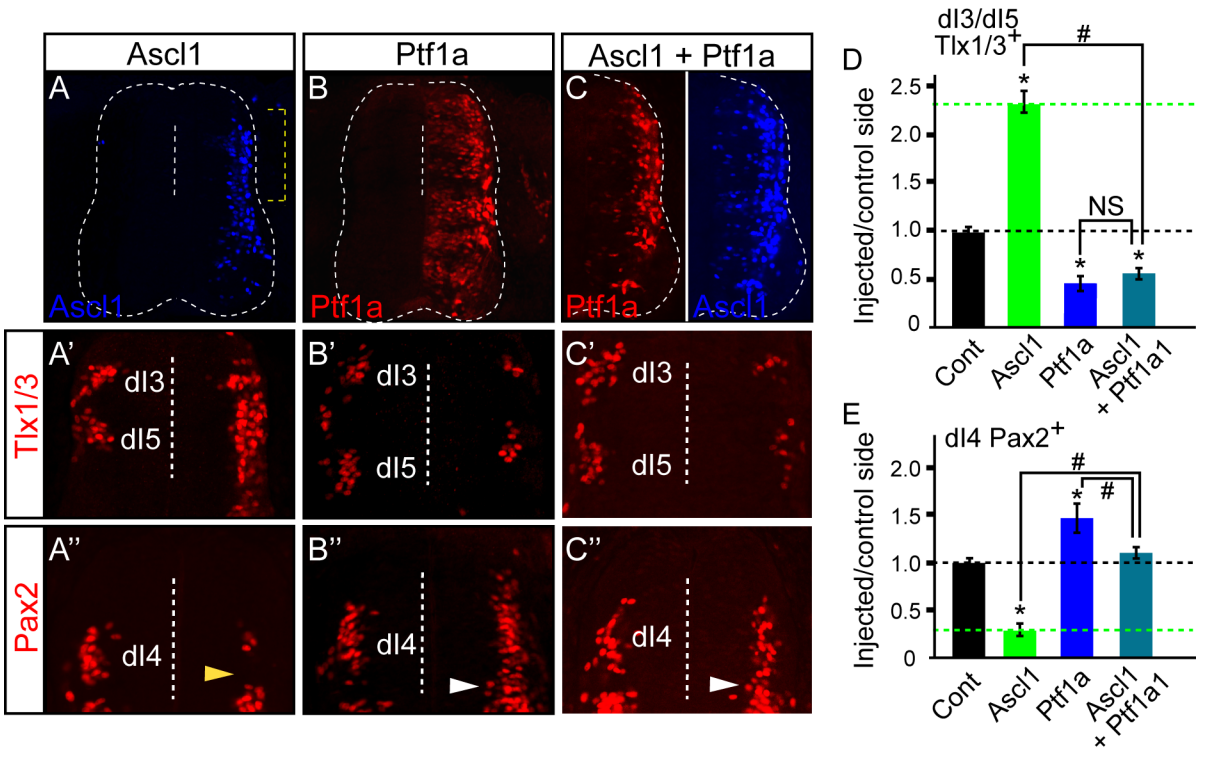

Figure 1-3. Opposing activities of Ascl1 and Ptf1a on neuronal subtype specification.

(A-C) Stage HH12-13 chick embryos were electroporated with expression vectors for Ptf1a and/or Ascl1 and harvested at HH24-25. Transverse sections are shown with the electroporated side on the right. Ascl1 (A,C blue) and Ptf1a (B,C red) immunofluorescence detects the ectopically expressed proteins. Dashed bracket in (A) is the region of the neural tube shown in (A'-C''). Dashed vertical line indicates the ventricle.

(A'-C', D) Dorsal neural tube sections show the dI3 and dI5 neuronal populations marked by Tlx1/3 antibody. (D) is the ratio of Tlx1/3$^+$ neurons on the electroporated side versus the control side showing that overexpression of Ascl1 causes a dramatic increase in Tlx1/3$^+$ neurons (A'), while Ptf1a, or Ascl1 plus Ptf1a, causes a decrease (B', C').

(A"-C", E) Dorsal neural tube sections show the dI4 neuronal populations marked by Pax2 antibody. (E) is the ratio of Pax2$^+$ neurons on the electroporated side versus the control side showing that overexpression of Ascl1 causes a decrease in Pax2$^+$ neurons (A"), while Ptf1a causes an increase (B"). Overexpression of Ptf1a with Ascl1 rescues the Ascl1 induced decrease (C"). Note that ectopic Pax2$^+$ cells (white arrowheads) are found in the dI5 domain not normally expressing Pax2 (yellow arrowhead). More than 6 embryos were quantified for each condition. Error bars are reported as standard error of the mean. Significance with p-values<0.001 is indicated with * between sample and control, and # between samples. NS, not significant.

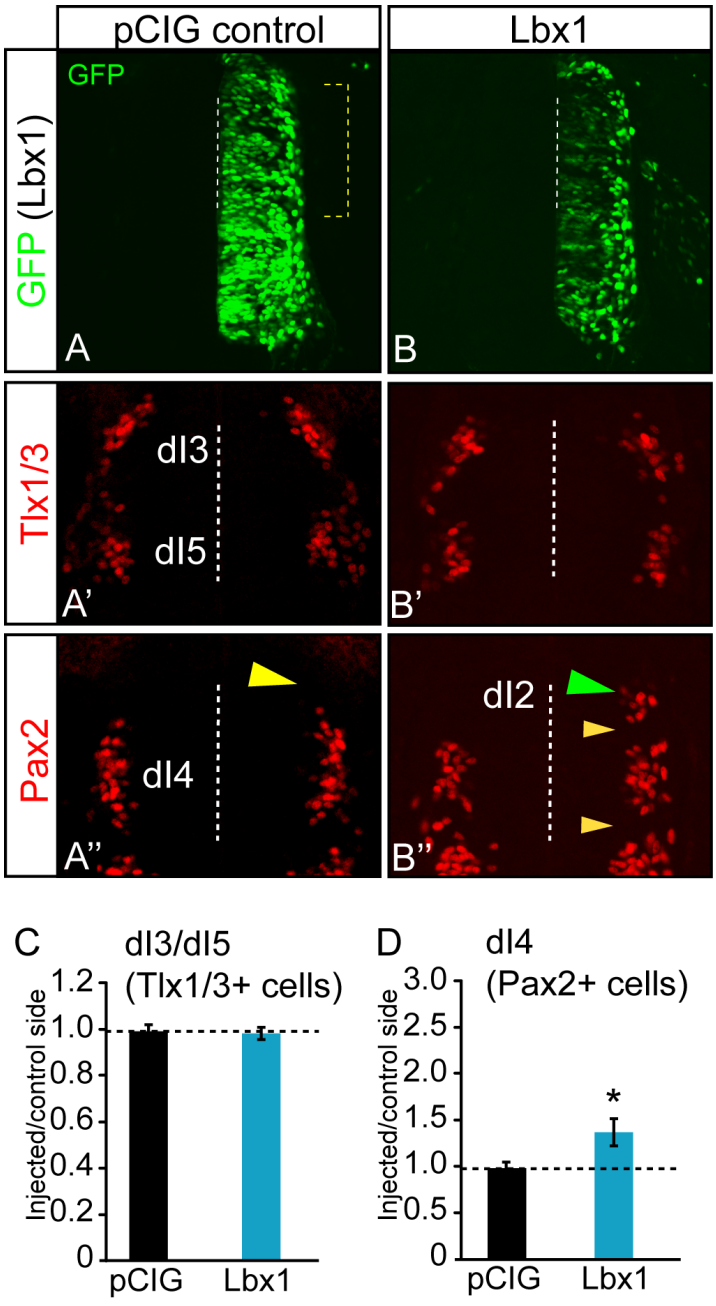

Figure 1-4. Lbx1 induces Pax2 in Tlx1/3-negative cells.

Stage HH12-13 chick embryos electroporated with either an empty pCIG vector as control (A), or an Lbx1 expression vector (B). Transverse sections through stage HH24-25 are shown with the electroporated side on the right. (A-B) GFP (green) indicates the electroporation efficiency along the dorsoventral axis. Dashed braket in (A) is the region of the neural tube shown in (A'-B"). Dashed vertical line indicates the ventricle.
(A'-B', C) A dorsal neural tube section shows the dI3 and dI5 neuronal population marked by Tlx1/3 (red). The overexpression of Lbx1 does not affect the expression of Tlx1/3 (B' and C).

(A”-B”, D) A dorsal neural tube section shows the dI4 neuronal population marked by Pax2 (red). The overexpression of Lbx1 causes ectopic $Pax2^{+}$ cells only in the dI2 domain where Tlx1/3 are not present (B”, green arrowhead). This finding is consistent with Tlx1/3 repressing Lbx1 activity as reported (B”, small yellow arrowheads). More than 6 embryos were quantified for each condition and error bars are reported as standard error of the mean. Asterisk indicates significant difference relative to the pCIG controls with p-value<0.001.

CHAPTER TWO

Prdm13 is a direct downstream target of Ptf1a.

The work presented in this chapter was performed in collaboration with a former graduate student in the Johnson lab, David Meredith. He executed the ChIP-seq and mRNA-Seq experiments as well as the entire bioinformatics analysis (data unpublished). The experiments were also performed with the help of Trisha Savage, a Johnson lab member, who cloned the mutated enhancer reporter constructs (Fig. 2-2F); and Helen Lai, who performed some of the Prdm13 in situ hybridization experiments.

Introduction

A fundamental question in neural development is to understand the molecular mechanism for balancing the number of inhibitory versus excitatory neurons. The combination of basic helix-loop-helix (bHLH) and homeodomain (HD) transcription factors is essential to regulate neuronal specification and promote neuronal differentiation in order to generate a precise neural network in the dorsal neural tube. A bHLH transcription factor, Ptf1a, is essential for the specification of GABAergic neurons in the dorsal spinal cord, cerebellum, hindbrain and retina (Aldinger and Elsen, 2008; Dullin et al., 2007; Glasgow et al., 2005; Hori et al., 2008; Hoshino et al., 2005; Nakhai et al., 2007). However, the downstream targets of Ptf1a that execute these functions to promote inhibitory neurons and suppress excitatory neurons are still unknown.

Since transcription complexes containing Ptf1a function as transcriptional activators and have no known repressor activity (Beres et al., 2006; Hori et al., 2008; Krapp et al., 1996; Krapp et al., 1998;

Masui et al., 2008), a simple model of how Ptf1a promotes inhibitory neurons is that Ptf1a activates GABAergic lineage genes through direct mechanisms, but how Ptf1a suppress glutamatergic lineage genes is still an open question. Ptf1a, along with another bHLH factor, Ascl1, act upstream of HD factors such as Pax2 and Lbx1 important in GABAergic lineages, and Tlx1 and Tlx3 important in specifying glutamatergic lineages, respectively (Batista and Lewis, 2008; Brohl et al., 2008; Cheng et al., 2004; Cheng et al., 2005; Glasgow et al., 2005; Helms et al., 2005; Mizuguchi et al., 2006; Wildner et al., 2006). Ascl1 and Ptf1a both exist in the same domain of progenitors within the dorsal spinal cord, yet how the glutamatergic neuronal gene program is suppressed when Ascl1 is expressed remains unclear (Beres et al., 2006; Hori et al., 2008; Krapp et al., 1996; Krapp et al., 1998; Masui et al., 2008). To uncover the mystery of neuronal specification in these domains, identifying the direct downstream targets of Ptf1a with genetic assays *in vivo* were pursued.

High-throughput deep sequencing, is a cutting edge technology that has been an important innovation for the field of neural development. By massive parallel sequencing of millions of different DNA fragments, we are able to obtain genome-wide chromatin and transcriptional information. The strategy for identifying targets of Ptf1a was to combine chromatin immunoprecipitation sequencing (ChIP-Seq) and mRNA sequencing (mRNA-Seq). mRNA-Seq experiments revealed genome-wide downstream targets by identifying transcripts that were lost in the Ptf1a knockout. Next, ChIP-Seq experiments identified regions of the genome bound by Ptf1a. Together, these experiments identified potential target candidates of Ptf1a. These powerful genomic tools not only demonstrate the DNA binding regions and specific interaction motifs, but also provide a valuable insight into global functions of these regulatory elements mediating transcriptional network.

Prior to this work, only a few genes had been identified as targets of Ptf1a during embryonic development: *Neurog2, Ptf1a, Kirrel2,* and *Nphs1* in the CNS and *Pdx1, Ptf1a,* and *Rbpjl* in the developing pancreas (Henke et al., 2009; Masui et al., 2007; Masui et al., 2008; Meredith et al., 2009; Nishida et al., 2010; Wiebe et al., 2007), and none of these provide an understanding of how Ptf1a induces one fate while suppressing the others. To identify downstream targets of Ptf1a, our laboratory

used a combination of ChIP-Seq and mRNA-Seq assays to probe Ptf1a function in the developing neural tube during early development. Using fluorescence activated cell sorting (FACS) to isolate Ptf1a expressing cells from E11.5 neural tubes from WT and Ptf1a$^{-/-}$ embryos, we performed mRNA-Seq to determine genes that require Ptf1a for expression (Mortazavi et al., 2008). Known targets for inhibitory neuronal lineage genes showed significant decrease of expression level in the Ptf1a mutant when compared to the WT. For example, the mRNA expression level of Lhx1 and Lhx5 were reduced 67- and 75-fold, while Pax2 and Gad1 were reduced by 76- and 130-fold. This result indicates the requirement of Ptf1a for directly regulating GABAergic lineage transcription factors as well as an end state genes required for function of the neurons. Another candidate that also came out of this analysis was a chromatin-remodeling transcription factor, Prdm13, decreased by 4.6-fold (D Meredith, JE Johnson, unpublished data). Together with ChIP-seq experiments that identified 7 Ptf1a bound sites within 60 kb surrounding the *Prdm13* gene, Prdm13 was identified as a potential downstream target of Ptf1a.

Experimental procedures

*Detailed protocols are provided in the Appendix.

Ptf1a Chip-Seq and mRNA-seq

Mutant mouse strains are published. *Ptf1a*^{Cre} (*p48*^{Cre}), where the *Ptf1a* coding region is replaced by the coding for Cre recombinase, was used as the *Ptf1a* null (Kawaguchi et al., 2002). The preparation of the tissues for Ptf1a ChIP-Seq and mRNA-Seq, as well as the experimental process and data analysis were done by David Meredith Ph.D., and was written in his dissertation.

In ovo chick electroporation

Fertilized white Leghorn eggs were obtained from the Texas A&M Poultry Department (College Station, TX) and incubated at 37°C for 48 hours until stage HH12-13 (Hamburger and Hamilton, 1992). Solutions of supercoiled plasmid DNA (1-2.5 μg/μl each) in UltraPure Distilled Water (Invitrogen) and

Trypan Blue (~2%) were injected into the lumen of the closed neural tube. Square-wave current (three 50-ms pulses of 25 mV) was generated using a BTX (San Diego, CA) T820 electroporator connected to 5-mm gold plated electrodes (Timmer et al., 2001). After 48 hours incubation at 37°C, stage HH24-25 embryos were harvested and processed for immunofluorescence or in situ hybridization.

Tissue processing and immunofluorescence

Mouse or chick embryos were dissected in ice-cold PBS, fixed in 4% paraformaldehyde. The time ranges for the embryonic fixation depend on the stage of each embryo, 1 hour for E10.5, 2 hours for E11.5, 6 hours for E12.5, and overnight for any stage above E13.5 embryos, at 4ºC. Fixed embryos were washed three times with PBS at room temperature and sunk in 30% sucrose, embedded in OCT, and cryosectioned at 20 mm.

***In Situ* hybridization**

In situ hybridization (ISH) was performed as per standard protocols*. Digoxygenin (DIG)-labeled antisense RNA probes (1–5 mg/mL) were hybridized overnight at 65°C, incubated with anti-digoxygenin AP antibody (Roche), and then incubated with NBT/BCIP (Roche). The sections were imaged with a Zeiss Discovery Stereomicroscope V12. Specific mouse *Prdm13* probes were cloned by PCR into pBluescript*.

Immunostaining and β-galactosidase (β-gal) staining

5 Ptf1a binding regions were cloned separately into a LacZ reporter vector, Ela1-placZacceptor*. The enhancer-reporter constructs were electroporated into the chick neural tube at HH (Hamburger and Hamilton) stage 12-13 and harvested 48 hours later. Sections were washed twice in cold PBS, and fixed in 4% paraformaldehyde for 30 minutes with follow up washes in PBS. Sections were then stained for β-galactosidase activity by incubation in solution containing 5 mM each K_3[Fe(CN)6] and K_4[Fe(CN)6] and

0.5 mg/ml X-gal (Roche, Indianapolis, IN) at 30°C for several hours or overnight on a shaking platform. Sections were post-fixed in 4% paraformaldehyde for several hours at 4°C.

Immunofluorescence was performed as our laboratory standard protocol (Glasgow et al., 2005; Hori et al., 2008). Immunofluorescence was performed with the specific primary antibodies* listed in the Appendix. Fluorescence imaging was carried out on a Zeiss LSM 510 confocal microscope.

Results

***Prdm13* is a direct downstream target of Ptf1a**

To better understand the transcriptional network that controls the specification of inhibitory and excitatory neuronal subtypes in the dorsal spinal cord, our laboratory identified direct downstream targets of Ptf1a. Targets were defined by intersecting gene lists identified via the combined use of cutting edge technologies of ChIP-seq and mRNA-Seq of uniquely sorted cell populations. For identifying genes whose expression is Ptf1a-dependent, we performed mRNA-Seq (Mortazavi et al., 2008) from Ptf1a lineage cells sorted from neural tubes of *Ptf1a* mutants and heterozygotes at E11.5. These analyses revealed Prdm13, a member of the PRDM class of proteins, whose expression decreased 4.5-fold in the *Ptf1a* mutant, as a particularly interesting target (Fig. 2-1A). Direct targets were defined by intersecting gene lists identified via Ptf1a ChIP-Seq with genes identified as being Ptf1a-dependent using expression profiling of *Ptf1a* mutant neural tubes compared to heterozygote or wildtype tissues. For ChIP-Seq experiments localizing Ptf1a to chromatin in vivo, chromatin from mouse E12.5 neural tube was immunoprecipitated with antibodies to Ptf1a. Tissue from the telencephalon of the same embryos was used as a negative neural control as no Ptf1a is present in this tissue. High-throughput sequencing of these samples, followed by peak detection revealed Ptf1a localized to thousands of sites within the genome (Meredith et al., submitted). Given the importance of the PRDM family of factors to cell fate decisions in other tissues (for review see Fog et al., 2012; Hohenauer and Moore, 2012) and the lack of functional data for Prdm13 (details written in Chapter 3 and 4), I chose to study this factor to determine its function in

neuronal subtype specification in the dorsal neural tube.

ChIP-Seq for Ptf1a identified 7 binding regions surrounding the *Prdm13* gene with in 60 kb (Fig. 2-1A). Ptf1a is a component of a trimeric transcription complex (PTF1) that includes an E-protein and Rbpj. Together, they bind a DNA motif containing an E-box and a TC-box with constrained spacing requirements (Beres et al., 2006; Henke et al., 2009; Hori et al., 2008; Masui et al., 2007). Of the 7 regions surrounding the *Prdm13* gene bound by Ptf1a, 5 contain consensus PTF1 binding motifs (Fig. 2-1B, underlined sequence). To determine whether the PTF1 complex occupies these Ptf1a-bound regions, our laboratory performed ChIP-Seq on neural tube tissue with antibodies to Rbpj (Meredith et al., in revision). Examination of the *Prdm13* locus confirmed that Rbpj co-localizes with Ptf1a in those regions that contain a consensus PTF1 motif (Fig. 2-1A). All five of the PTF1 sites are conserved across mammalian species, and 4 of them are conserved to zebrafish (Fig. 2-1A,B asterisks).

Determination of the enhancer activity

In order to determine if the Ptf1a binding regions are sufficient to direct Ptf1a domain specific Prdm13 expression, 5 of the Ptf1a binding regions (Peak 3-7) located nearest to the *Prdm13* locus were cloned separately into a LacZ reporter vector, Ela1-placZacceptor (Fig. 2-1), or a GFP reporter vector, BgnEGFP-MCSIII (Fig. 2-2). The enhancer-reporter constructs were electroporated into the chick neural tube at HH stage 12-13 and harvested 48 hours later to determine if the enhancer containing the Ptf1a binding site is sufficient to drive restricted Ptf1a domain expression. Only one of the binding sites, the most 5' proximal site (Peak 5) that contains a consensus PTF1-J site (CACATGGAGTGGTTCCCTCA), showed expression that is enriched in the dorsal neural tube. However, it was not restricted to the dI4 domain as would be predicted if it contained sufficient regulatory information (Fig. 2-1E; Fig. 2-2D,D'). The signals from either the β-gal staining or the GFP revealed similar expression pattern to the endogenous Prdm13 pattern in the spinal cord (see Fig. 2-4 B-D). To test if this enhancer is responsive to Ptf1a as would be predicted, Ptf1a was co-electroporated with this construct. Surprisingly, no increase in

expression was detected (data not shown). Furthermore, when either the E-box or the TC-box were mutated, the expression patterns of the reporter remained the same (Fig2. 2-2F,C,H), which suggest additional non-PTF1 transcription factors interact with this cis-element to direct the dorsal restricted.

Another cis-element (Peak 4) located nearest to the 3' of *Prdm13* locus, showed expression in the chick neural tube. This enhancer only contains E-boxes but no TC-box, and it is the least conserved region compared to the other regions (Peak 3-7). It is mainly expresses in dI2 and dI6 labeled with Lhx1/5 (Fig. 2-2C') and the ventral part of spinal cord in the MZ. In contrast to Peak 5, the mutation of all 3 E-boxes disrupted the activity of the Peak 4 enhancer (Fig. 2-2; C yellow arrow compared to I green arrow). Peaks 6/7, located upstream of the 5' end of the *Prdm13* locus, did not give any specific expression in the dorsal spinal cord (Fig. 2-1F-H, Fig. 2-2E,E'), even though they both contain consensus PTF1-J site (Fig. 2-1B) and are highly conserved across mammalian species (Fig. 2-1A,B). The electroporation efficiency was illustrated with a co-electroporated myc expression vector (Fig. 2-2B''-E'',G'-I', red).

Effect of gain and loss of function of Ptf1a on Prdm13 expression

To verify that *Prdm13* is a direct target of Ptf1a, we examined the *Prdm13* expression pattern relative to Ptf1a, and in response to increased or decreased levels of Ptf1a. In mouse embryos, the pattern of *Prdm13* expression is strikingly neural specific and is almost exclusively restricted to Ptf1a domains, the exception being the neural tube where expression is broader and earlier than Ptf1a (Fig. 2-3A-G'). At E11.5, Ptf1a and Prdm13 are present and co-expressed in the dorsal neural tube (Fig. 2-3D,D'; Fig. 2-4A-G), the developing cerebellum (Fig. 2-3A,A'); and in a subset of cells in the diencephalon (Fig. 2-3B-C'). Additionally, *Prdm13* is present in all the neural Ptf1a expression domains examined, but is not detected in the pancreas, the other major site of Ptf1a expression (data not shown). *Prdm13* is also in the developing cerebellum and diencephalon from E11.5 to E13.5 (Fig. 2-4H-N), but is reduced by E14.5 (data not shown). In the retina, expression is seen as early as E12.5 and persists at least to E16.5, the last stage tested (Fig. 2-3G,G', Fig. 2-4K,O). Notably in the caudal neural tube, although *Prdm13* is restricted

to the dorsal region, it appears to be present more broadly in the ventricular zone than Ptf1a (Fig. 2-3D-E'). *Prdm13* overlaps progenitor regions from dI2-dI6 (Fig. 2-3E,E'; Fig. 2-4B,C) and is expressed from E9 to E14.5 (Fig. 2-4A-G). At E13.5 and E14.5, *Prdm13* remains only in a few progenitors in the VZ in the dorsal part of the developing spinal cord (Fig. 2-4F,G). However, even though *Prdm13* appears broader in the neural tube than Ptf1a, it is enriched in the Ptf1a domain.

To evaluate the requirement for Ptf1a in Prdm13 expression, *Ptf1a* null embryos were examined. In *Ptf1a* null embryos, *Prdm13* is essentially abolished in rostral domains (Fig. 2-3A"-C"), indicating that expression of *Prdm13* in these regions is dependent on *Ptf1a*. Within the caudal neural tube, *Prdm13* mRNA is reduced only at the lateral border of the ventricular zone where Ptf1a is expressed (Fig. 2-3D'-E'', arrowheads), suggesting that additional, Ptf1a-independent mechanisms must regulate *Prdm13* in this region, consistent with the cis-element reporter assay results. I also tested whether ectopic expression of Ptf1a could induce Prdm13. In the chick, *Prdm13* is expressed in the ventricular zone of the dorsal neural tube (Fig. 2-5B, control side), and ectopic expression of Ptf1a via in ovo electroporation resulted in a dramatic increase in endogenous c*Prdm13* mRNA levels on the electroporated side (Fig. 2-5A,B).

I also evaluated whether the gain or loss of Prdm13 alters expression of Ptf1a. For the most part, Ptf1a was unaffected by altering levels of Prdm13 (Fig. 2-5 C-F). However, this result was variable in that in the Prdm13 overexpression experiments about 20% of the embryos appeared to have an increase in Ptf1a mRNA levels, and 20% had a decrease (data not shown). This variability might result from multiple functional contributions of Prdm13 during early development, such as regulating proliferation (Chittka et al., 2012; Davis et al., 2006).

In summary, the neural restricted patterns of *Prdm13* and Ptf1a are strikingly similar with a major component of *Prdm13* expression being Ptf1a-dependent. Taken together with the ChIP-Seq results, we conclude that *Prdm13* is a neural specific, direct downstream target of Ptf1a.

Discussion

Utilizing high throughput deep sequencing performed *in vivo*, our laboratory identified a zinc finger transcription factor Prdm13 as a direct downstream target of Ptf1a. Prdm13 contains a PR domain, defined by the positive regulatory domain I-binding factor 1 (PRD1-BF1) and retinoblastoma-interacting zinc finger protein 1 (RIZ1), followed by four clustered zinc finger domains at the amino-terminus (Davis et al., 2006; Huang, 2002; Jenuwein, 2001; Kinameri et al., 2008; Kouzarides, 2002). Several studies have shown that PRDM family members are essential for regulating both cell proliferation and cell fate decisions in non-neural systems, and some have been described as proto-oncogenes or tumor suppressors in different contexts (Deng and Huang, 2004; Nguyen et al., 2003; Nishikawa et al. 2010; Nishikawa et al., 2007; Watanabe et al., 2007). Molecular dissection of the related family member Prdm6 showed that the PR domain and zinc fingers are both sufficient to mediate transcriptional repression, and regulate smooth muscle cell proliferation versus differentiation (Davis et al., 2006). Furthermore, Prdm16 was shown to be required for the survival, cell-cycle regulation, and self-renewal in neuronal progenitor cells (Chuikov et al.; Horn et al., 2009), and regulates cell fate specification between skeletal myoblasts and brown adipocytes (Fruhbeck et al., 2009; Kajimura et al., 2009; Kajimura et al., 2010; Seale et al., 2008). Intriguingly, Prdm16 can function as an activator or a repressor of transcription depending on cofactors present (Kajimura et al., 2010; Kajimura et al., 2008; Seale et al., 2007). Taken together, these data suggest Prdm13 is a strong candidate for regulating the inhibitory/excitatory neuronal balance downstream of Ptf1a. Indeed, since Ptf1a functions to suppress markers of excitatory neurons like Tlx3, but Ptf1a itself functions as transcriptional activator (Rose et al., 1994; Wiebe et al., 2007), I hypothesized that Prdm13 is the direct downstream mediator of Ptf1a that functions to repress transcription of genes found in excitatory neurons which I tested in Chapter 3.

The in situ hybridization results showed the expression pattern of Prdm13 in the dorsal spinal cord is not restricted to the Ptf1a domain (Fig. 2-3D-E'). Prdm13 remains in the VZ while Ptf1a is gone at E11.5 (Fig. 2-3D-D''''), and it expressed in the VZ at least till E14.5 (Fig. 2-4), indicating that Prdm13

might have a broader function in neuronal specification than just its function in the Ptf1a lineage, and might be involved for regulating the proliferation and/or differentiation of those progenitors.

In the cis-elements studies, only one (Peak 5) of the enhancer regions is sufficient to drive the expression reflecting the endogenous Prdm13 expression pattern. There are several lines of evidence that suggest that other factors regulate Prdm13 expression in a Ptf1a independent manner. First, the Peak 5 enhancer drives reporter expression to the dorsal part of the spinal cord, but is not enriched in the Ptf1a domain (dI4) (Fig. 2-2D-D''). Second, Prdm13 expression is maintained in the ventricular zone in the Ptf1a -/- (Fig. 2-3 D',D'). Third, intriguingly, the overexpression of Ptf1a with this enhancer reporter did not increase the signals either broader or stronger, suggesting that additional repressor might limit the expression through this element simultaneously (data not shown). Fourth, even when the E-box or TC-box was disrupted, this cis-element retained its activity to drive reporter expression (Fig. 2-2G,H). Lastly, given the early expression of Prdm13 at E9 (Fig. 2-4A), when there is no detectable Ptf1a mRNA expression in the dorsal spinal cord at this stage (data not shown), other early neuronal transcription factors might regulate the expression of Prdm13 through this cis-element. Together, these results indicate that the strength/efficiency of this cis-element (Peak 5) in response to Ptf1a is weak. Therefore, it may not be the primary Ptf1a regulatory element, but other transcription factors may also be regulating Prdm13 expression through this region.

Another enhancer region that was tested, the Peak 4 enhancer (Fig. 2-1A,B), also drives expression of either LacZ or GFP in the spinal cord, but a bit more extended towards the ventral part. Interestingly, the GFP signals are highly co-localized with the Lhx1/5^{+} neurons (Fig. 2-2C'). The reporter is expressed strongly in the dI2 and dI6, and a subset of neurons in the dI4, although this region does not contain any potential PTF1 binding motifs. Together with the Prdm13 mRNA expression pattern in the spinal cord, where there is a higher expression level in the dI2, dI4, and dI6 (Fig. 2-4B,C), suggests that this enhancer region (Peak 4) is important to drive the expression of Prdm13 independent to Ptf1a. This observation should be verified by additional experiments, where this Peak 4 enhancer reporter could be co-expressed with Ptf1a in the neural tube. Strikingly, the disruption of the 3 E-boxes in this region totally

diminished its activity, indicating that potentially other bHLH transcription factors in addition to Ptf1a likely interact with this cis-element for modulating its activity. According to the pattern (Fig. 2-2C', Fig. 1-1A), transcription factors such as Ngn1 or Ngn2 might be interesting transcription factors to further investigated in the regulation of Prdm13 expression. While the tested enhancer regions Peak 3-7, did not reveal a uniquely Ptf1a responsive enhancer element, Peak 1 and 2 were not yet tested. Given the possibility that Prdm13 might have multiple functional contributions in the developing CNS, various trans- or cis-elements are required for regulating the expression of Prdm13 is evident from my analysis. Thus, further investigating these cis-elements are important to uncover the regulation of early neuronal development.

Nevertheless, I identified a zinc finger transcription factor Prdm13 as a direct downstream of Ptf1a since Ptf1a binds to multiple regions surrounding the *Prdm13* gene, both transcription factors are expressed in highly overlapping domains throughout the CNS, and the gain and loss of Ptf1a showed that it is necessary and sufficient to induce the expression of *Prdm13*.

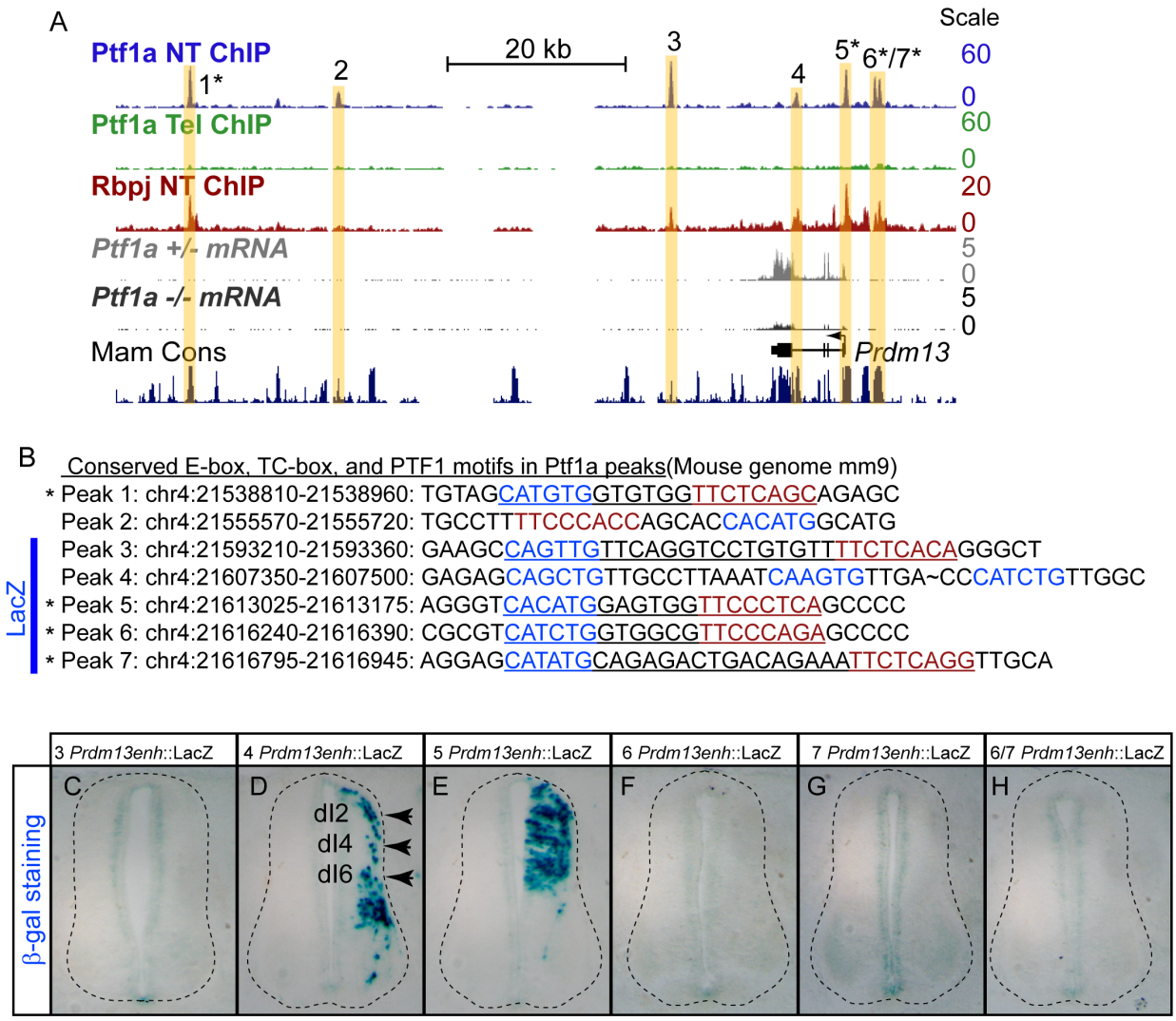

Figure 2-1. Prdm13 is a direct downstream target of Ptf1a.

(A) The mouse genomic region surrounding *Prdm13* showing ChIP-seq data for Ptf1a from E12.5 neural tube (blue) and telencephalon (green) or Rbpj from neural tube (red), and RNA-seq from FACS isolated Ptf1a lineage cells from E11.5 *Ptf1a*+/- (gray) or *Ptf1a*-/- embryos (black). Seven Ptf1a peaks are highlighted with yellow bars. The location of the *Prdm13* transcript is shown, as is a histogram of mammalian conserved regions (UCSC Genome Browser).
(B) Sequence under the apex of each Ptf1a ChIP-seq peak. Genomic coordinates for DNA regions Peaks 1-7 showing the E-box (blue), TC-box (red), and the PTF1 motifs (underlined) were examined. Asterisk indicates those peaks that are conserved from mouse to zebrafish and contain the consensus PTF1 motif. Blue bar indicated the cis-elements that were tested in the LacZ repoter assay in chick neural tube.
(C-H) Peaks 3-7 were tested in LacZ reporter constructs in chick neural tube, and analyzed with β-Gal staining on transverse sections. (D) Peak 4 cis-element located in the intron of *Prdm13* locus, contains activity to drive the expression of lacZ in dI2, dI4, and dI6, and also some parts of the ventral neural tube (arrows). (E) Peak 5 cis-element, which is located to the transcription start site of *Prdm13*, drives LacZ expression in the dorsal neural tube. (C, F-H) Other cis-elements lack the activity to drive the expression in the neural tube.

A Ptf1a peaks tested in GFP reporters (blue: E-box; red: TC-box)

Peak 4: GAGAGCAGCTGTTGCCTTAAATCAAGTGTTGA~CCCATCTGTTGGC
* Peak 5: AGGGTCACATGGAGTGGTTCCCTCAGCCCC
* Peak 6: CGCGTCATCTGGTGGCGTTCCCAGAGCCCC
* Peak 7: AGGAGCATATGCAGAGACTGACAGAAATTCTCAGGTTGCA

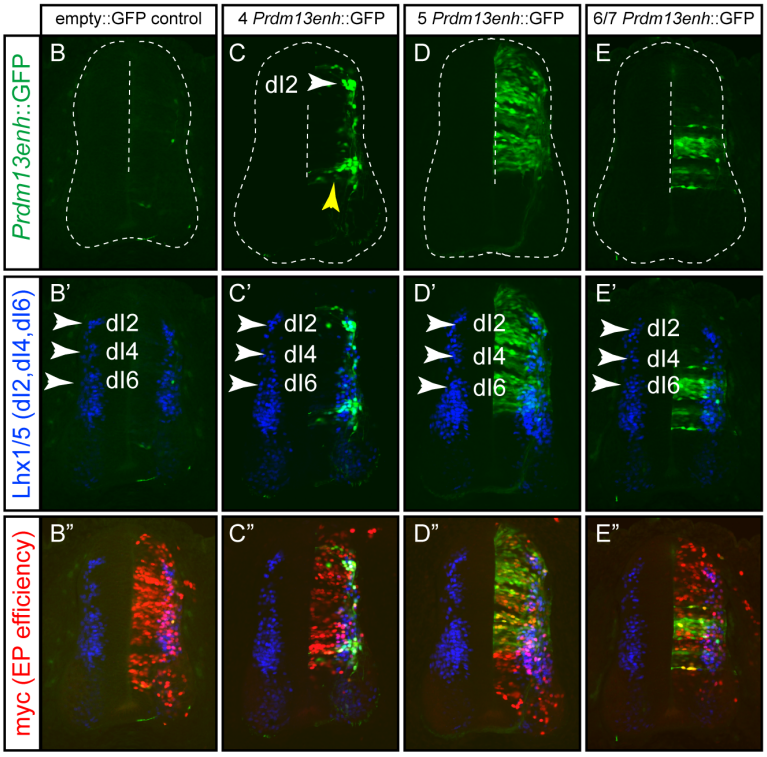

F Ptf1a peaks tested in GFP reporters
(blue: E-box; red: TC-box; green: mutation)

Peak 5: AGGGTCACATGGAGTGGTTCCCTCAGCCCC
m5 mE-box: AGGGTTACTATGAGTGGTTCCCTCAGCCCC
m5 mTC-box: AGGGTCACATGGAGTGGTTATAACCGCCCC

Peak 4: GAGAGCAGCTGTTGCCTTAAATCAAGTGTTGA~CCCATCTGTTGGC
m4 m3E-box: GAGAGTACTATTTGCCTTAAATTACTATTTGA~CCTACTATTTGGC

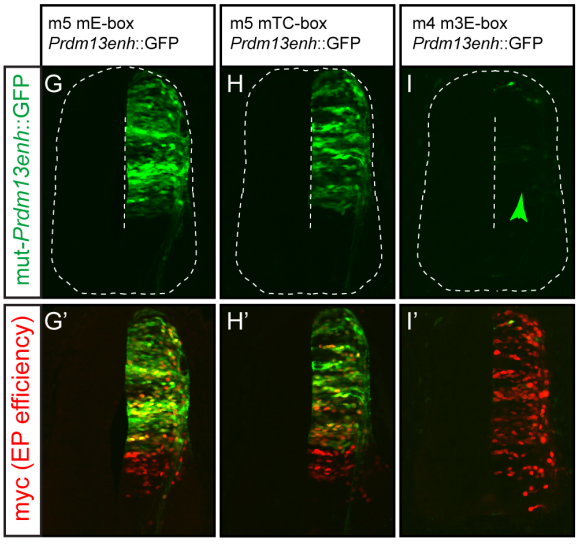

Figure 2-2. Peak 4 enhancer requires E-boxes for its activity.

(A) Sequence under the apex of each Ptf1a ChIP-seq peak that was tested in the GFP reporter assay. DNA regions 4-7 showing the E-box (blue), TC-box (red), and the PTF1 motifs (underlined) that were examined. Asterisk indicates those peaks that are conserved from mouse to zebrafish and contain the consensus PTF1 motif.
(B-B') Empty GFP reporter construct shows no background when electroporated in the chick neural tube.
(C-C') Peak 4 enhancer GFP reporter (*4 Prdm13enh*::GFP) contains the activity to drive GFP expression in the dI2, dI4, and dI6 in the dorsal spinal cord (C'), mimicking the results with the LacZ reporter (Fig. 2-1d).
(D-D') Peak 5 enhacer GFP reporter (*5 Prdm13enh*::GFP) drives the GFP expression in the dorsal spinal cord (D'), mimicking that seen with the LacZ reporter (Fig. 2-1E).
(E-E') Peak 6/7 enhacer GFP reporter (*6/7 Prdm13enh*::GFP) contains some activity to drive the GFP expression in the dI6 domain (E'), not seen with the LacZ reporter (Fig. 2-1H).
(B''-E'') The myc immunostaining indicates the electroporation efficiency.
(F) Sequence under the apex of each Ptf1a ChIP-seq peak that was tested for mutated enhancer regions in the GFP reporter assay. DNA regions 4 and 5 showing the E-box (blue), TC-box (red), the PTF1 motifs (underlined), and the mutated E-box or T-box (green) that were examined.
(G-H') The mutation of either E-box (G) or TC-box (H) does not alter the activity of Peak 5 enhancer.
(I-I') The mutation of all three E-boxes in the Peak 4 enhancer disrupted activity of the enhancer (Compare green arrow to the yellow arrow in Fig. C).
(G'-I') The myc immunostaining indicates the electroporation efficiency.

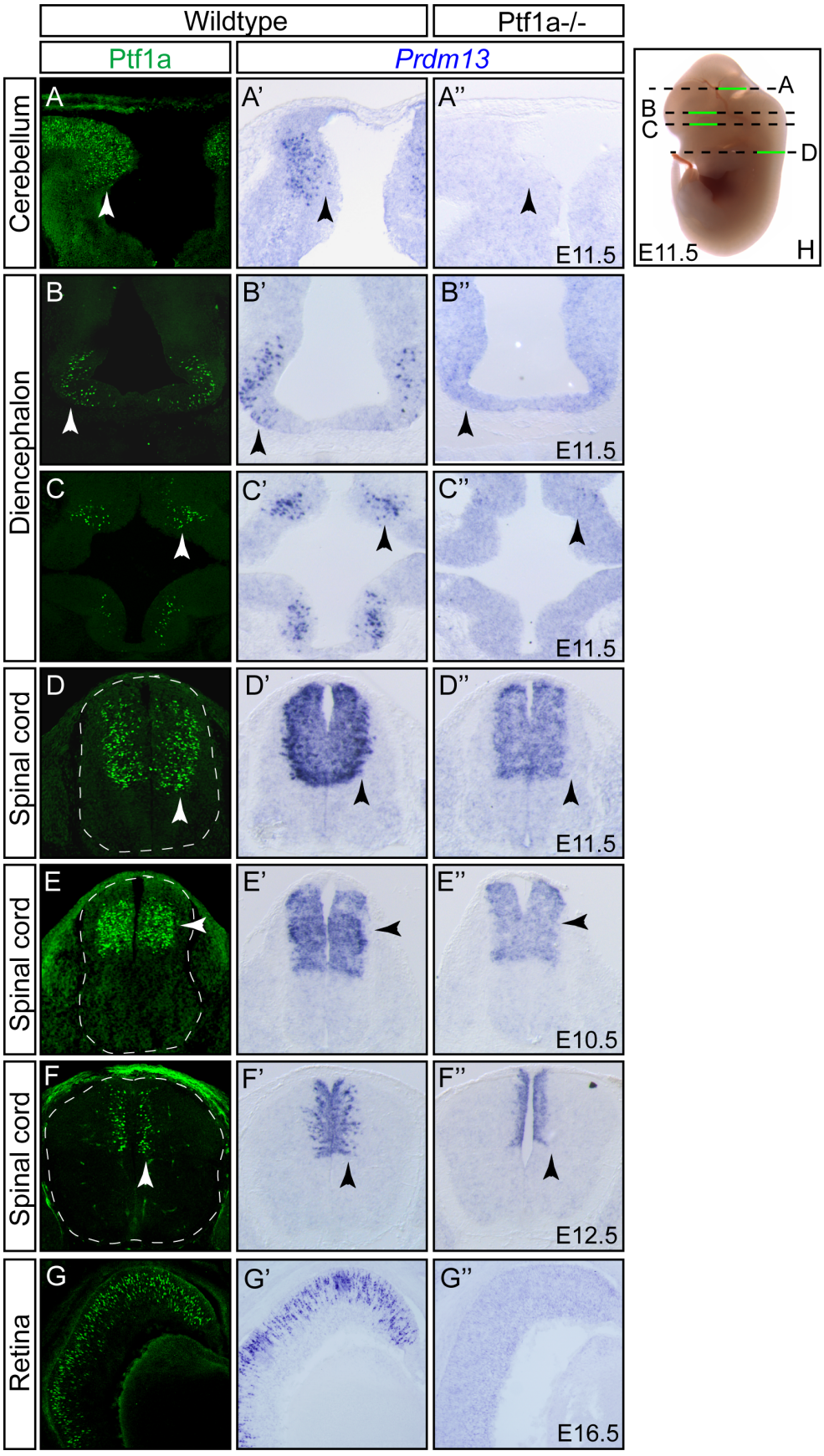
Wildtype
Ptf1a-/-
Ptf1a
Prdm13
Cerebellum
Diencephalon
Spinal cord
Spinal cord
Spinal cord
Retina
A
A'
A''
B
B'
B''
C
C'
C''
D
D'
D''
E
E'
E''
F
F'
F''
G
G'
G''
E11.5
E11.5
E11.5
E11.5
E10.5
E12.5
E16.5
A
B
C
D
E11.5
H

Figure 2-3. Ptf1a-dependent expression of Prdm13 in the CNS.

(A-D") Cross sections through regions indicated in mouse E11.5 show Ptf1a immunofluorescence (A-G), and *Prdm13* mRNA by *in situ* hybridization in wildtype (A'-D') and *Ptf1a-/-* (A"-D"). Note that although in cerebellum and diencephalon *Prdm13* mRNA is almost completely lost in the *Ptf1a* mutant, in the spinal cord, only the lateral domain that reflects the Ptf1a pattern is lost (arrows).
(E-F'') Cross sections through either E10.5 (E) or E12.5 (F) spinal cord show Ptf1a immunofluorescence (E-F), and *Prdm13* mRNA by *in situ* hybridization in wildtype (E'-F') and *Pt1a-/-* mutant mice (E"-F'').
(G-G'') Cross sections through E16.5 retina show Ptf1a immunofluorescence (G), and *Prdm13* mRNA by *in situ* hybridization in wildtype (G') and *Pt1a-/-* mutant mice (G").
(H) Diagram of section planes for images shown in (A-D).

Expression pattern of Prdm13 in developing spinal cord

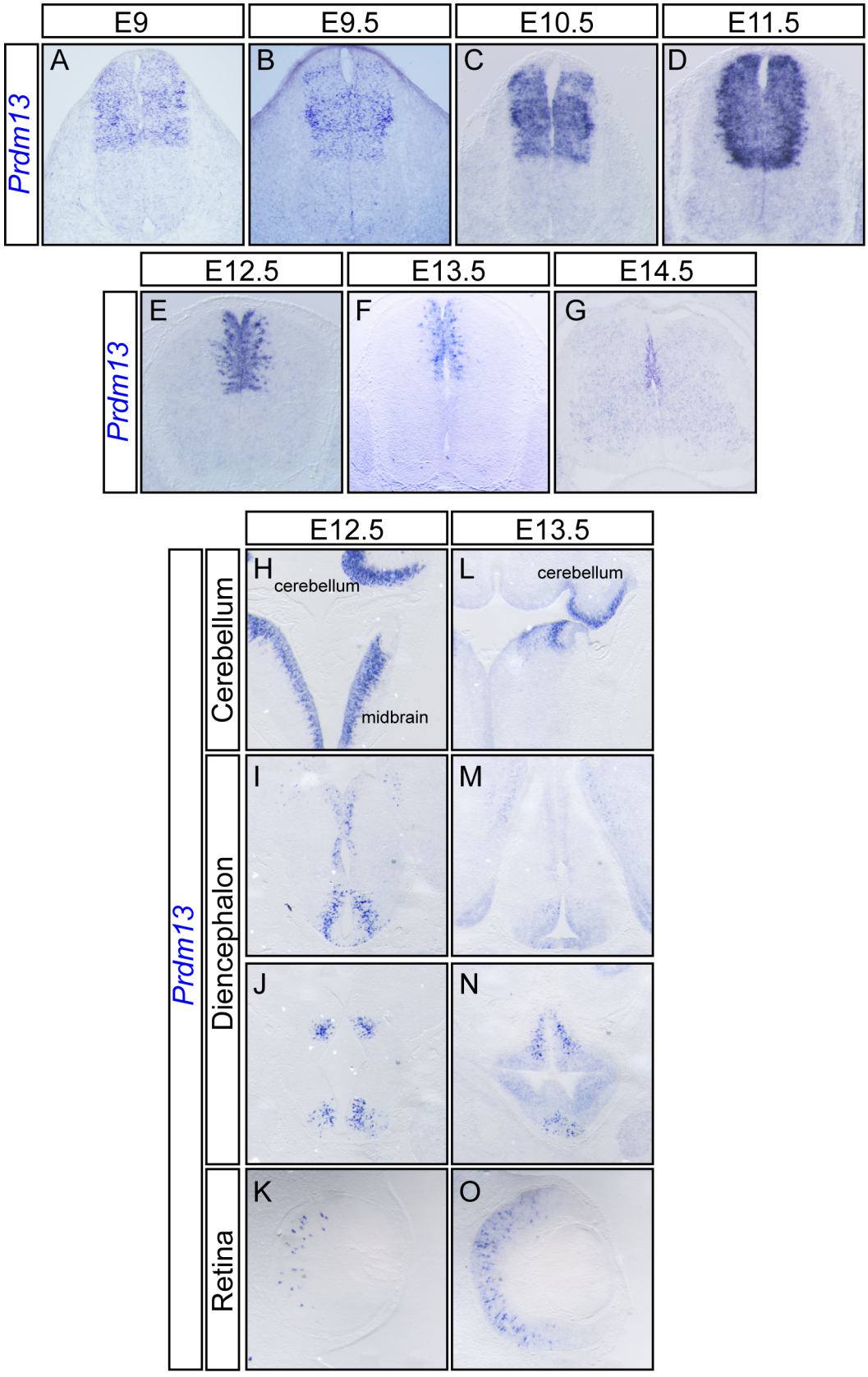

Figure 2-4. *Prdm13* expression in the CNS at multiple embryonic stages.

(A-G) Transverse sections through mouse E9 to E14.5 spinal cords show *Prdm13* mRNA expression patterns by *in situ* hybridization in wildtype embryos. Prdm13 starts to express as early as E9 (A) in the ventricular zone in the dorsal spinal cord with enrichment in regions lateral to the Ptf1a domain from E9.5 till E11.5 (A-D). By E14.5, *Prdm13* mRNA is almost gone, reflecting the diminished proliferative zone (G).
(H-O) *In situ* hybridization shows *Prdm13* mRNA expression pattern in E12.5 (H-K) and E13.5 (L-O) throughout the CNS. At stage E12.5 and E13.5, Prdm13 is in the developing cerebellum and hindbrain (H, L), diencephalon (I, J, M, N), and retina (K, O).

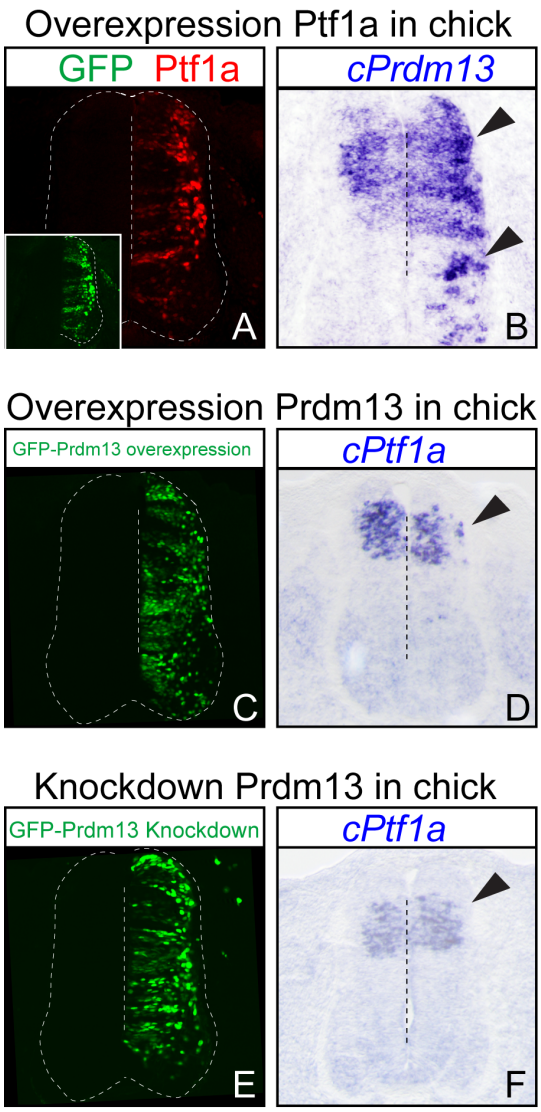

Figure 2-5. Ptf1a induces *Prdm13* in the chick spinal cord.

(A-B) Overexpression of mouse Ptf1a (A, red) in chick neural tube induces c*Prdm13* mRNA (B, arrowheads) relative to the control side. Inset: GFP indicates the electroporation efficiency.
(C-D) Overexpression of mouse Prdm13 (C, GFP-Prdm13) in chick neural tube does not alter the expression of c*Ptf1a* mRNA (D, arrowheads) relative to the control side.
(E-F) The knockdown of the endogenous chick *Prdm13* (E, GFP) in chick neural tube does not change the expression level of c*Ptf1a* mRNA (F, arrowheads) relative to the control side.

CHAPTER THREE

Prdm13 specifies the GABAergic neuronal lineage in the spinal cord

Introduction

The dorsal spinal cord provides the first level of somatosensory processing and requires a balanced excitatory and inhibitory neuronal network. The dorsal horn neurons in these circuits integrate somatosensory information coming into the spinal cord from dorsal root ganglia neurons, before it is relayed to supraspinal brain regions or locally for reflex responses. Given the importance of the dorsal horn neurons in processing all somatosensory modalities, understanding how these neurons are specified during embryogenesis to generate the correct composition of neurons holds significance for addressing neurological disorders that may arise from disruption of this equilibrium. Here we identify a new component of the transcriptional machinery that controls how neurons in the somatosensory circuit are generated during development.

The bHLH transcription factors in neuronal subtype specification highlight a fundamental question in the generation of neuronal diversity. A transcription factor with the ability to re-direct the fate of a cell requires two activities; it must activate lineage specific gene expression, and it must repress expression of genes in the alternate lineage. One of the class II bHLH transcription factors, Ptf1a, is essential for GABAergic while suppressing glutamatergic neuronal cell-fates in the developing dorsal spinal cord (Fig.1-1), as well as in the cerebellum and retina (Fujitani et al., 2006; Glasgow et al., 2005; Hoshino et al., 2005; Nakhai et al., 2007; Pascual et al., 2007). Specification of the GABAergic inhibitory neurons (dI4) requires Ptf1a and the HD factors Lbx1 and Pax2; in contrast, Ptf1a suppresses the HD factor Tlx3, a factor required for glutamatergic excitatory neurons (dI3/5) (Cheng et al., 2004; Cheng et

al., 2005; Glasgow et al., 2005) (Fig.1-1). How Ptf1a induces the GABAergic phenotype but represses the glutamatergic phenotype is still unknown. Here I identify a PRDM class transcription factor, Prdm13, as the missing component through which Ptf1a can suppress genes in the glutamatergic lineage in the dorsal spinal cord.

Prdm13 belongs to the PRDM family, which contains 16 orthologs in rodents and 17 orthologs in primates; this is due due to gene duplication of Prdm7/9 after divergence of a common ancestor. All members, except Prdm11, contain a PR domain followed by one or several zinc finger domains. A variant zinc finger binding domain called a zinc knuckle, which is likely involved in protein-protein interaction, was identified in some PRDM class factors (Fig. 3-1 blue box)(Fog et al., 2012; Hohenauer and Moore, 2012; Kinameri et al., 2008). Prdm13 contains a PR domain (PRDI-BF1 and RIZ homology domain) at the N-terminus followed by four zinc fingers of which three are clustered at the C-terminus (Fig. 3-1). PRDI-BF1 (positive regulatory domain I–binding factor 1), which is now commonly called Prdm1 (PR domain-containing 1), and RIZ1 (retinoblastoma-interacting zinc finger protein), now called Prdm2, together named the PR (PRDI-BF1-RIZ1 homologous) domain (Cheng et al.; Huang et al., 1998; Nishikawa et al., 2007; Watanabe et al., 2007; Xie et al., 1997). The PR domain is related to the catalytic SET domains (named after the *Drosophila* factors Suppressor of variegation 3-9, Enhancer of zeste and Trithorax) that define a large group of histone methyltransferases (HMTs) known as transcriptional silencers (Huang et al., 1998; Schneider et al., 2002). In contrast to the SET domain containing proteins, only Prdm2, 8, and 9, so far, have been shown to possess intrinsic HMTase activity (Eom et al., 2009; Hayashi et al., 2005; Kim et al., 2003). Although there are no functional studies on Prdm13, its mRNA expression was shown to be within the dorsal region of VZ in the neural tube (Kinameri et al., 2008) in a pattern reflecting that of Ptf1a (Fig. 1-1). Therefore, Prdm13 is a potential candidate to mediate inhibition of glutamatergic lineage in GABAergic neurons downstream of Ptf1a.

PRDM family members are known to regulate several processes related to cell proliferation (Chittka et al., 2012; Davis et al., 2006), differentiation (Nishikawa et al.; Su et al., 2009), and specification during development (Brzezinski et al., 2010; Fruhbeck et al., 2009; Katoh et al., 2010; Seale

et al., 2008; Vincent et al., 2005). They control gene expression through modification of the chromatin state at promoter and/or enhancers of their target gene by using either intrinsic enzymatic activity towards histones or recruitment of interaction partners (Fog et al., 2012; Hohenauer and Moore, 2012). One of the most thoroughly studied PRDM members, Prdm16, specifies brown fat fate while suppressing white fat or muscle lineages (Kajimura et al., 2010; Seale et al., 2008). Prdm16 expression was highly enriched in brown adipose tissue (BAT) when compared to white adipose tissue (WAT). In order to induce the BAT downstream gene expression, Prdm16 functions as a transcription activator that directly interacts with PPARγ-coactivator-1α (peroxisome proliferator activated receptor, PGC-1α) to activate transcription and specify BAT (Seale et al., 2007). Conversely, Prdm16 expression in white fat precursors or in myoblasts robustly represses gene expression, mediated through its direct binding to C-terminal binding proteins (CtBP1), which are well-known co-repressors. These results indicate that Prdm16 is a co-regulatory protein that can function as a bidirectional switch in brown fat development through multiple protein-protein interactions (Kajimura et al., 2009; Kajimura et al., 2008). Interestingly, mice overexpressing Prdm16 in adipose tissues are resistant to high fat diet-induced obesity and display increased glucose clearance and energy expenditure. Therefore, medical treatment that could increase Prdm16 expression or stability is a potential therapeutic for obesity or diabetes (Seale et al., 2011). Surprisingly, Prdm16 not only plays a role in specifying BAT, but also is involved in early hematopoiesis together with another PRDM member, Prdm3. There are two pools of hematopoietic stem cells (HSCs): quiescent long-term HSCs (LT-HSCs) and proliferating short-term (ST-HSCs). Both Prdm3 and Prdm16 are essential for the earliest processes of hematopoiesis. The knockout of *Evi1*, a gene together with *Mds1* as a complex locus (*MECOM*) encodes Prdm3 (Zhang et al., 2011), results in simultaneous loss of Prdm3. Evi1 (ecotropic virus integration site 1 protein homolog) deletion causes a severe reduction in hematopoietic stem/progenitor cells but is compatible with differentiation of progenitors once they are formed (Goyama et al., 2008). The recent generation of Prdm3 knockout mice that retain Evi1 expression has revealed that loss of Prdm3, but not Evi1, results in loss of the quiescent LT-HSCs (Zhang et al., 2011). Similar to Prdm3, Prdm16 is also required for HSC homeostasis; and Prdm16 overexpression produces a decrease of

apoptosis and a relative increase of HSC number, and increased reconstitution ability (Aguilo et al., 2011; Deneault et al., 2009).

In the nervous system, Prdm1 specifies photoreceptor over bipolar neuron fate (Brzezinski et al., 2010; Katoh et al., 2010). The bipolar cells and photoreceptor cells are both derived from HD transcription factor Chx10 positive precursors. Overexpession of Prdm1 reduces the number of bipolar cells and increases the number of photoreceptor cells (Brzezinski et al., 2010; Katoh et al., 2010). In contrast, overexpression of Chx10 induced photoreceptor cells over bipolar cells (Livne-Bar et al., 2006). Furthermore, Prdm1 was found to interact with multi cis-elements surrounding *Chx10* locus *in vivo*, and represses the expression of a *Chx10* enhancer reporter *in vitro* (Brzezinski et al., 2010; Katoh et al., 2010).

Recently, PRDM factors have been shown to regulate axon outgrowth and targeting. Prdm8 forms a transcriptional complex with the Olig-related transcription factor Bhlhb5, and mediates the repression of a target gene, Cadherin-11, to regulate axonal targeting in the dorsal telencephalon (Ross et al., 2012). Moreover, in zebrafish, a gene-trap mutant that contains a disrupted Prdm14 showed shortened axons in caudal primary motorneurons resulting in defective embryonic movement. Prdm14 binds to the promoter region of Islet2, a known transcription factor required for caudal primary motorneuron development, and regulates the activation of islets for precise axon outgrowth (Liu et al., 2012).

Despite the emergence of PRDM family members as important regulators of neural development, to date very little is known about their roles in cell fate specification and differentiation in the CNS. In this study, we identify Prdm13 as a critical component that regulates the neuronal cell-fate branch point distinguishing the dI4 and dI3/5 neuronal lineages in the dorsal spinal cord. In particular, we show that Prdm13 expression and function phenocopies that of Ptf1a in the CNS, where Prdm13 is both necessary and sufficient to promote $Pax2^{+}$/GABAergic neuronal fate over $Tlx1/3^{+}$/glutamatergic neuronal fate in the dorsal spinal cord. My findings put Prdm13 at the center of the bHLH and HD transcription factor cascade that governs cell fate decisions, and its function is central to the generation of a balanced circuitry of excitatory and inhibitory neurons required for somatosensory information processing.

Experimental procedures

Plasmid description

FLAG-tagged Prdm13 and variations used for expression in the chick neural tube were inserted into the pCIG vector, which drives expression through a combined CMV early enhancer/chicken β-actin promoter and contains an IRES-NLS-GFP (Megason and McMahon, 2002). Different truncations of Prdm13 were also FLAG-tagged and cloned into the pCIG vector. Mutations of the zinc finger domains in Prdm13 contains point mutations of each zinc finger as: mZ1: C185A, H207A; mZ2: C622A, H638A; mZ3: C650A, H666A; Z4: C679A, H695A. Ptf1a and Ascl1 expression constructs used pMiWIII as previously described (Hori et al., 2008; Nakada et al., 2004). The engrailed repressor (EnR) (Smith and Jaynes, 1996) or the VP16 activator (Triezenberg et al., 1988) were fused at the C-terminal end of Prdm13 in pMiWIII. Lbx1 construct was a gift from Muller (Muller et al., 2002). All constructs used were sequence verified.

The pSilencer 1.0-U6 vector (Ambion) was used in knock down experiments where several sets of 21-mer oligonucleotides were selected from chick *Ptf1a* or *Prdm13* mRNA sequences (listed in the SEP). Additionally, shRNA targeting *DSred* was used as control (Rao et al., 2004). The shRNA constructs were co-electroporated with pCIG so the GFP could be used to assess electroporation efficiency. The knockdown efficiency was further verified by in situ hybridization with specific mRNA probes to chick *Ptf1a* or *Prdm13*. The absence of cell death was verified by the absence of Caspase3 expression (data not shown).

In ovo chick electroporation

As described in Chapter 2.

Immunofluorescence and In Situ hybridization

Immunofluorescence was performed as previously described (Glasgow et al., 2005; Hori et al., 2008). A list of primary antibodies used is listed in SEP. Fluorescence imaging was carried out on a Zeiss LSM 510 confocal microscope. For each experiment, multiple sections from at least six different embryos were analyzed and used for quantification. Cell counting was blind to the condition and was performed manually using ImageJ. The quantitative results are presented as a ratio of the number of marker positive cells on the electroporated side divided by the number on the non-electroporated side. Only sections with confirmed high efficiency expression across the dorsal ventral axis were used in the analysis. Mean GFP pixel intensity for *eTlx1/3::GFP* expression was measured by ImageJ. Significant differences between control and experimental samples were calculated using a two-tailed two-sample equal variance (homoscedastic) Student's t test (* indicates $P < 0.001$) in Microsoft Excel. SEM is shown.

In situ hybridization was performed as previously described (Lai et al., 2011). Chick *Gad1* and *vGlut2* (Cheng et al., 2004), and chick *Ptf1a* (gift T. Reh) probes were used. Plasmids for generating chick and mouse *Prdm13* probes were cloned by PCR into pBluescript with the primers listed in SEP.

Results

Prdm13 phenocopies Ptf1a function in the dorsal neural tube

The neural restricted patterns of *Prdm13* and Ptf1a are strikingly similar with a major component of *Prdm13* expression being Ptf1a-dependent; together with the ChIP-Seq results, we conclude that *Prdm13* is a neural specific, direct downstream target of Ptf1a. To begin to uncover the function of Prdm13 during neural development, I misexpressed mouse Ptf1a and Prdm13 in chick neural tubes at stage HH12-13 via in ovo electroporation. One of the advantages of the in ovo electroporation paradigm is that for each section of each embryo there is a control for the number of cells that are present at that stage, and at that level of the neural tube. To help control for electroporation differences, GFP was

included in every electroporation and only sections that efficiently express GFP across the dorsal ventral axis were used for the analysis. In some cases, I showed the GFP as evidence for the quality of the electroporations (Fig. 3-2A,C,D). The exogenous expression was confirmed by specific immunofluorescence for Ptf1a and mRNA in situ hybridization for *Prdm13* (Fig. 3-2B-D). Transverse sections of thoracic neural tube were collected at HH24-25 and examined by immunofluorescence for alterations in neuronal sub-type specification relative to the non-electroporated side. Ectopic expression of either Ptf1a or Prdm13 dramatically decreased the number of Tlx1/3 positive cells (2.5 and 2.0-fold, respectively) while increasing the number of dI4 Pax2 positive cells (1.5-fold in each case) relative to the non-electroporated side (Fig. 3-2B'-C'',E-F). Electroporation of empty vector, in contrast, did not alter the number of the neurons generated in either population (Fig. 3-2A'-A'', E-F). Co-electroporation of Prdm13 and Ptf1a together more strongly induced Pax2 expression to 2.3-fold than the control pCIG empty vector (Fig. 3-2D''-F).

A closer look at the pattern of $Pax2^+$ neurons in the Ptf1a and Prdm13 electroporated neural tubes revealed that the normal dI5 gap between dI4 and dI6 was filled with $Pax2^+$ cells (Fig. 3-2 compare A'' with B''-C'', arrows). This suggested that the ectopic expression of Ptf1a and Prdm13 alter the fate of progenitor cells, an interpretation consistent with previous conclusions from analysis of the *Ptf1a* knock out mouse (Glasgow et al., 2005). Indeed, closer examination of the dI3-dI5 domain revealed that Prdm13 electroporated cells are strongly biased to a $Pax2^+$:$Tlx1/3^-$ fate (Fig. 3-2G-N). In the empty vector control, 34% of the dorsal GFP^+ cells were $Tlx1/3^+$. When Ptf1a, Prdm13, or both were ectopically expressed, GFP^+:$Tlx1/3^+$ cells were rarely seen and the percentage dropped to 2-4% (Fig. 3-2H-J). In contrast, the number of dorsal GFP^+:$Pax2^+$ cells increased from 12% in the control to 39-40% with ectopic Ptf1a or Prdm13 (Fig. 3-2L-M). The percentage increased to 53% GFP^+/$Pax2^+$ cells when Ptf1a and Prdm13 were introduced simultaneously, consistent with the collaborative effect noted above (Fig. 3-2N). I confirmed that the loss of $Tlx1/3^+$ cells and enrichment of $Pax2^+$ cells is not an artificial result of selective cell death,

as assayed by immunostaining for Caspase 3 (data not shown). These findings indicate both Ptf1a and its target Prdm13 can alter the fate of progenitor cells and bias them to the $Pax2^+$/inhibitory neuronal lineage.

Similar trends were seen with additional markers for dorsal interneuron populations including Isl1/2 (dI3), Lmx1b (dI5), and Lhx1/5 (dI2, dI4, dI6) (Fig. 3-3A-C). When Prdm13 was ectopically expressed in the chick neural tube, there was a 2.4-fold decrease of $IsI1/2^+$ cells, indicating the reduction of dI3 interneurons in the dorsal spinal cord (Fig. 3-3A',C). LIM HD transcription factor Lmx1b is shown to be required for the formation of dI5 interneurons in the dorsal spinal cord (Ding et al., 2004); here again, ectopic expression of Prdm13 reduces the $Lmx1b^+$ cells down to 2.5-fold. These additional markers confirmed the Tlx1/3 analysis (Fig. 3-3B',C). Moreover, although there is an increase of the $Lhx1/5^+$ cells (Fig. 3-3E',C), when calculating the $Pax2^-$ and $Lhx1/5^+$ cells as the dI2 interneurons, there is a significant decrease the number of those cells (data not shown). This suggests that even though both Pax2 and Lhx1/5 are GABAergic lineage markers (Batista and Lewis, 2008; Huang et al., 2008; Pillai et al., 2007), Prdm13 seams to induce specifically dI4 over dI2 interneurons.

Prdm13 together with Lbx1 specifies GABAergic neurons

Because other members of the PRDM family are primarily repressors, we hypothesized that Prdm13 might induce Pax2 by indirect means, such as by relieving repression by another factor. For example, derepression of Lbx1, which induces Pax2 in the absence of Tlx1/3 (Cheng et al., 2005; Gross et al., 2002), might account for the increase in Pax2 levels seen with Prdm13 misexpression. Indeed, Lbx1 was also induced by ectopic expression of Ptf1a and Prdm13, particularly in regions dorsal to its native domain (Fig. 3-2O-S, arrows). Since Ptf1a and Prdm13 also inhibit Tlx3 in the dI3 domain, the induction of Pax2 may be indirect through the unopposed activity of ectopic Lbx1. Indeed, ectopic expression of Lbx1 in the chick neural tube induces Pax2, but only in regions outside of Tlx1/3 expression (Fig. 3-4B'', green arrows), but not in the dI3 and dI5 domains (yellow arrows). Intriguingly, together with the ectopic expression of Prdm13, a dramatic increase of Pax2+ cells was observed in the electroporated side (Fig. 3-

4D',D'',F). Electroporation of empty vector, in contrast, did not alter the number of the neurons generated in either population (Fig. 3-4A-A'', E-F). The output from this regulatory network is the specification of either an excitatory (vGlut2$^+$) or inhibitory (Gad1$^+$) neuronal phenotype (Cheng et al., 2004; Cheng et al., 2005; Glasgow et al., 2005; Gross et al., 2002; Muller et al., 2002).

Prdm13 and Ptf1a determine the inhibitory over excitatory neurons

In the dorsal neural tube, Tlx1/3 cells give rise to *vGlut2*$^+$ excitatory neurons, and Pax2 cells give rise to *Gad1*$^+$ inhibitory neurons. To determine whether Ptf1a and Prdm13 are sufficient to modulate the neurotransmitter phenotypes as well, we performed mRNA in situ hybridization for *Gad1* and *vGlut2* on the electroporated neural tubes. An increase in *Gad1 and* decrease in *vGlut2* confirms that the ectopic Pax2 expressing neurons from Ptf1a and Prdm13 overexpression adopt a GABAergic identity (Fig. 3-3TA'-D'', arrows indicating dI3 and dI5 regions with ectopic *Gad1* or reduced *vGlut2*). Thus, Prdm13 serves a similar function as Ptf1a by promoting the Pax2$^+$ GABAergic lineage and suppressing the Tlx1/3$^+$ glutamatergic lineage (Fig. 3-3H).

Knockdown of Ptf1a or Prdm13 leads to a reduction of Pax2$^+$ cells

To gain further insight into the role of Prdm13 in neuronal specification, we generated specific short hairpin RNAs (shRNA) to knockdown endogenous Ptf1a or Prdm13 in the chick neural tube. Constructs containing shRNAs to *Ptf1a*, *Prdm13*, or *DsRed* (control) were electroporated as above (Fig. 3-5A-C), and mRNA in situ hybridization was performed to verify knockdown (Fig. 3-5M-P, black arrows). Reduction of Ptf1a and Prdm13 levels led to a marked decrease in the number of Pax2$^+$ cells (1.7 and 2.0-fold for Ptf1a and Prdm13, respectively) (Fig. 3-5B''-C'', E). There was a modest increase in the number of Tlx1/3$^+$ cells with Prdm13 knockdown; however, in the Ptf1a knockdown there was no significant difference (Fig. 3-5B'-C',D). Electroporation of control shRNA did not alter the expression of

Tlx1/3 or Pax2 (Fig. 3-5A',A'',D,E). There was no increase in cell death in electroporated hemicords as detected by Caspase3 expression (data not shown). Misexpression of mouse Ptf1a or Prdm13 with their respective shRNA constructs rescued the knockdown phenotypes, demonstrating specificity of the shRNA (Fig. 3-5Q-T). These results demonstrate that Prdm13, like Pft1a, is required to generate the correct number of $Pax2^+$ neurons in the dorsal spinal cord.

In summary, from both gain and loss of function experiments in chick neural tube, Prdm13 phenocopies Ptf1a by inducing $Pax2^+$/GABAergic neurons and suppressing the $Tlx1/3^+$/glutamatergic neurons. My findings demonstrate that Prdm13 is a novel component of a highly coordinated transcriptional network necessary to mediate the balance of inhibitory versus excitatory neurons generated in the dorsal neural tube.

Ptf1a requires Prdm13 to increase $Pax2^+$ and decrease $Tlx1/3^+$ cells

Results detailed above strongly suggest that Prdm13 functions as a downstream effector of Ptf1a during neuronal sub-type specification. If Prdm13 is required for Ptf1a activity, then knocking down Prdm13 when Ptf1a is ectopically expressed should abrogate Ptf1a activity. Indeed, the increase in $Pax2^+$ cells and the decrease in $Tlx1/3^+$ cells normally seen with ectopic Ptf1a expression was inhibited when Prdm13 was simultaneously knocked down (Fig. 3-6B'-C'',F,G, blue bar compares with red bar), and the numbers of $Pax2^+$ and $Tlx1/3^+$ cells approximated control levels (Fig. 3-6F-G, compare with black bar). Conversely, knockdown of Ptf1a did not affect the activity of ectopically expressed Prdm13, consistent with Ptf1a acting upstream of Prdm13 (Fig. 3-6D'-E'',F,G). These experiments support the requirement for Prdm13 as a downstream effector of Ptf1a. In other words, Ptf1a requires Prdm13 to specify the GABAergic interneurons in the dorsal spinal cord (Fig. 3-6H).

Prdm13 requires its zinc finger motifs for activity and acts as a repressor

The PRDM transcription factors are characterized by a PR domain and a variable number of zinc fingers, but the functional contribution of each of these domains remains unclear for any given member of the family (for review see Fog et al., 2012; Hohenauer and Moore, 2012). To better understand the mechanism behind Prdm13 function, I generated mutants of Prdm13 shown in diagram Fig. 3-7A, total 9 different truncations of Prdm13 were tested for their activity in chick neural tube (Fig. 3-7B-M). Although the PR domain has been shown to be critical for the function of other PRDM family members, this domain was dispensable for Prdm13 activity, as the truncated form of Prdm13 containing the four zinc fingers (Z1234: aa185-754) retained full activity (Fig. 3-7H-H'',N,O). The PR domain alone did not do anything to alter neuronal specification (Fig. 3-7D-D'',N,O). The domain containing the last three zinc fingers 2-4 (Z234) was sufficient for a majority of Prdm13 activity for suppression of Tlx1/3 (Fig. 3-7I'-M',N,O); however, the truncations (488Z234 and 611Z234) that miss the amino acid before 488 of Prdm13 lost its activity to induce Pax2 (Fig. 3-7L'-M'',N,O). This indicates that the region between the Z1 and Z234 might contribute to the stability or protein-protein interaction for Prdm13 activity, although it is predicted mostly as low-complexity regions. Interestingly, the half truncated of Z1234 (Z1) (Fig3-8A), which only contains the first zinc finger seems to have some activity on its own, at least for suppressing Tlx1/3 (Fig. 3-7E'). This suppression is unique to the dI3 domain, labeled with Brn3a and Isl1/2, as Z1 does not affect the dI5 domain, labeled with Brn3a but not Isl1/2 (Fig. 3-8B,B',E). In contrast, the other half of the Z1234, 466Z234 (Fig3-8A), reduces the number of Tlx1/3^{+} cells in both domains with similar efficiency (Fig. 3-8C,C',E). Thus, Prdm13 requires at least two distinct zinc finger containing domains for proper function, and it may repress Tlx1/3 through two separable mechanisms.

Furthermore, in order to understand more about the functional contribution of these zinc finger domains, I performed different point mutations to disrupt each zinc finger (Fig. 3-9 A). As predicted from the previous Prdm13 truncation assays, the loss of either Z1 or Z234 disrupts the specification activity of Prdm13 (Fig. 3-9E,F). Although mutation of Z1 or Z234 each completely disrupted the ability to induce

Pax2, they only partially disrupted Tlx1/3 repression (Fig. 3-9,B'-C'',E,F). Complete disruption of both phenotypes was seen when all four zinc fingers were mutated (Fig. 3-9D',D'',E,F). Taken together, it is clear that the zinc fingers themselves are required for Prdm13 activity since mutations designed to disrupt these domains also disrupted Prdm13 function.

Discussion

A balance of excitatory and inhibitory neuronal input is crucial for normal nervous system function (McCormick and Contreras, 2001; Persico and Bourgeron, 2006). For the dorsal spinal cord, disruption of this balance may underlie neurological disorders affecting the somatosensory system such as hyper- or hypo-algesia since dorsal horn neurons serve as the first level of processing of this information from the periphery. During development, the initial specification of these neurons occurs from neighboring and interspersed progenitors in the dorsal neural tube ventricular zone just as they are transitioning to post-mitotic neurons. The network of transcription factors required for specification of different neuronal subtypes includes a cascade of transcription factors of the bHLH and HD families. Prior to this study, Ptf1a was known to induce Pax2/GABAergic and repress Tlx1/3/glutamatergic specific neuronal lineages. However, it was not known how this transcriptional activator could repress transcription of genes in the glutamatergic lineage seen in this process of cell-fate specification. Here, I identified Prdm13, a zinc finger containing transcription factor that provides a missing link in the cell fate decision required for somatosensory processing in the spinal cord. Prdm13, as a transcriptional repressor required downstream of Pft1a, provides the mechanistic insight into how Ptf1a functions to regulate this cell fate switch.

Network of transcription factors balancing the numbers of dorsal spinal cord inhibitory and excitatory neurons

Work from multiple laboratories has demonstrated the essential role for HD transcription factors, in addition to bHLH factors, in specifying neurons in the dorsal spinal cord (Brohl et al., 2008; Cheng et al., 2004; Cheng et al., 2005; Gross et al., 2002; Huang et al., 2008; Muller et al., 2002; Xu et al., 2008). It is within this known network of transcription factors that I now place Prdm13. Important HD players in specification and balance of the dI4/dIL^{A} and dI5/dIL^{B} populations include Lbx1, Pax2, Tlx1, Tlx3, Isl1, Isl2, Lmx1b, Lhx1, and Lhx5. Lbx1 is present in precursors to both GABAergic and glutamatergic neurons in dI4/dIL^{A} and dI5/dIL^{B}, respectively, although it is required only for the GABAergic phenotype. To generate glutamatergic neurons from Lbx1 expressing precursor cells, Tlx1 or Tlx3 is needed to antagonize Lbx1 function (Cheng et al., 2005). In those cells with Lbx1 and Tlx1/3, no Pax2 is expressed and the neurons become glutamatergic (Cheng et al., 2004; Cheng et al., 2005). In Lbx1 expressing cells lacking Tlx1/3, Pax2 is expressed and the neurons become GABAergic (Fig. 3-6H). The bHLH factors generally function upstream of these HD factors (Fig. 7A-B). Ascl1 is in proliferating progenitors to both glutamatergic and GABAergic neurons, but at early stages it is required for Tlx1/3 and Lmx1b expression, at least in the first wave of neurogenesis in this region (Helms et al., 2005; Mizuguchi et al., 2006). In contrast, Ptf1a is present in a subset of the Ascl1 domain and is required for inducing Pax2 and suppressing Tlx1/3, and thus, is essential in generating the balance of these neurons in the dorsal spinal cord (Glasgow et al., 2005; Hori et al., 2008; Mizuguchi et al., 2006). Ptf1a has been clearly shown to have transcriptional activator function (Beres et al., 2006), and it induces lineage markers for inhibitory neurons such as Pax2, and Gad1 (Fig. 3-2B'', E'). However, how Ptf1a suppresses Tlx1/3 and other glutamatergic lineage markers was not understood. Identifying Prdm13 as a downstream target of Ptf1a provides a mechanism for how Ptf1a can repress lineage specific gene expression (see model Fig. 3-6H).

Prdm13 belongs to the PRDM family and contains a PR domain and 4 zinc finger domains (Fig. 3-1). Most of the family members were defined as transcription silencers (for review see Fog et al., 2012; Fumasoni et al., 2007), therefore, I speculate that Prdm13 functions as a repressor in this respect and

induces Pax2 in an indirect way. Thus, Prdm13 serves to repress expression of Tlx1/3, and releases inhibition of Lbx1 function and induction of the Pax2/GABAergic lineage. I found Prdm13 also induces Lbx1 expression indirectly, explaining how ectopic Pax2 was detected in the dI3 domain, since the Lbx1 activity would be unopposed by Tlx3. However, when ectopically expressing Prdm13, the increase of $Lbx1^+$ cells is less than the $Pax2^+$ cells in the dI1 to dI3 (Fig. 3-2C'',Q), indicating Prdm13 may have multiple pathways for inducing GABAergic lineage neurons. Indeed, when ectopically expressed, both Lbx1 and Prdm13 cause a dramatic 2.6-fold increase of the $Pax2^+$ cells, a significantly higher fold change than when each is ectopically expressed (Fig. 3-4 compare B'',C'' to D'',F). All these results suggest that Prdm13 is critical to specify neuronal cell fates, and whose function connects that of the bHLH factor Ptf1a with the downstream HD factors Lbx1, Tlx1/3, and Pax2 to generate the correct number of GABAergic and glutamateric neurons.

The PRDM family of factors is interesting in the variety of mechanisms they reportedly use to regulate transcription (for review Fog et al., 2012; Hohenauer and Moore, 2012). They contain two major recognizable motifs, the PR domain and zinc finger domains. The PR domain is similar to the SET domain found in histone lysine methyltransferases, and thus, some members of the PRDM family have been shown to have this enzymatic activity. However, the sequence homology between PR domains and the SET domain reveals that the PR domain of Prdm13 is substantially divergent. Molecular dissection of the related family member Prdm6 showed that the PR domain and zinc fingers are both sufficient to mediate transcriptional repression, and regulate smooth muscle cell proliferation versus differentiation (Davis et al., 2006). Here, I show that the PR domain is dispensable for Prdm13 activity in our assays, since a truncated Prdm13 (amino acids 185-754) that lacks the PR domain but contains all four zinc fingers (Z1234) is sufficient to induce $Pax2^+$ cells and repress Tlx1/3 at levels similar to that seen with the full-length protein. Intriguingly, the first zinc finger domain (Z1) and the last three zinc finger domains (Z234) have different activities in suppressing Tlx1/3. The domain containing zinc fingers 2-4 (208Z234, 399Z234, 466Z234) was sufficient for a majority of Prdm13 activity; however, the region containing zinc finger 1 (Z1) seems to have some activity on its own, at least for suppressing Tlx1/3 (Fig. 3-7N,O). This

suppression is unique to the dI3 domain, as Z1 does not affect Tlx1/3 expression in the dI5 domain (Fig. 3-8). In contrast, Z234 reduces the number of Tlx1/3^{+} cells in both domains with similar efficiency. Thus, uncovering the mechanism used by Prdm13 for neuronal specification must focus on the zinc finger containing domains of the protein.

Indeed point mutations that disrupt the structure of all four zinc finger domains (mZ1234) completely abolish the ability of Prdm13 to suppress Tlx1/3 and induce Pax2 (Fig. 3-9). This mutated Prdm13-mZ1234 may even function as a dominant negative protein since it slightly induces Tlx3 and suppresses Pax2 (Fig. 3-9E,F). Significantly, these observations mimic results from the truncated Prdm13 assay, where both the first zinc finger domain (Z1) and the last 3 zinc finger domains (Z234) play a partial role in regulating neuronal specification. When either of them was mutated (mZ1 and mZ234), they both reduced the number of Tlx1/3+ cells down to 1.4-fold and 1.3-fold respectively, but fail to induce Pax2 (Fig. 3-9E,F). As expected, all these zinc finger domains are highly conserved throughout evolution (data not shown), supporting a critical function for these regions.

Despite the emergence of PRDM family members as important regulators of neural development, to date very little is known about their roles in cell fate specification and differentiation in the CNS. Here, I identify Prdm13 as a critical component of the transcription network that regulates neuronal diversity and the excitatory/inhibitory balance in the dorsal spinal cord. In particular, I show that Prdm13 expression and function phenocopies that of Ptf1a in the CNS, where Prdm13 is both necessary and sufficient to promote Pax2^{+}/GABAergic neuronal fate over Tlx1/3^{+}/glutamatergic neuronal fate in the dorsal spinal cord. However, the mechanisms of how Prdm13 suppresses the glutamatergic lineage genes remain unclear. In the next chapter, I report me findings on how Prdm13 suppresses Tlx1 and Tlx3, in order to repress the glutamatergic neuronal cell fate.

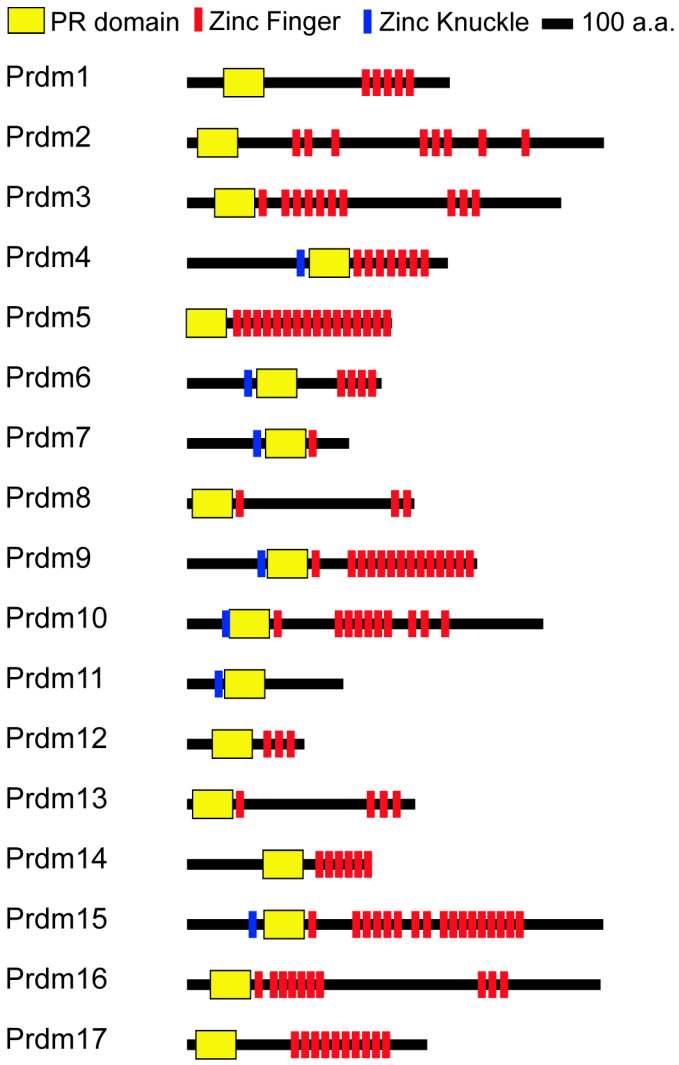

Figure 3-1. PRDM family protein domain organization.

(A) The protein domain organization each human PDM family member is illustrated. Only the longest or most likely isoform of each PRDM member is shown. The location of the PR domain is shown as a yellow box, the zinc finger domains are shown as red boxes, and while the protein-protein interaction zinc knuckle domain is shown in blue.

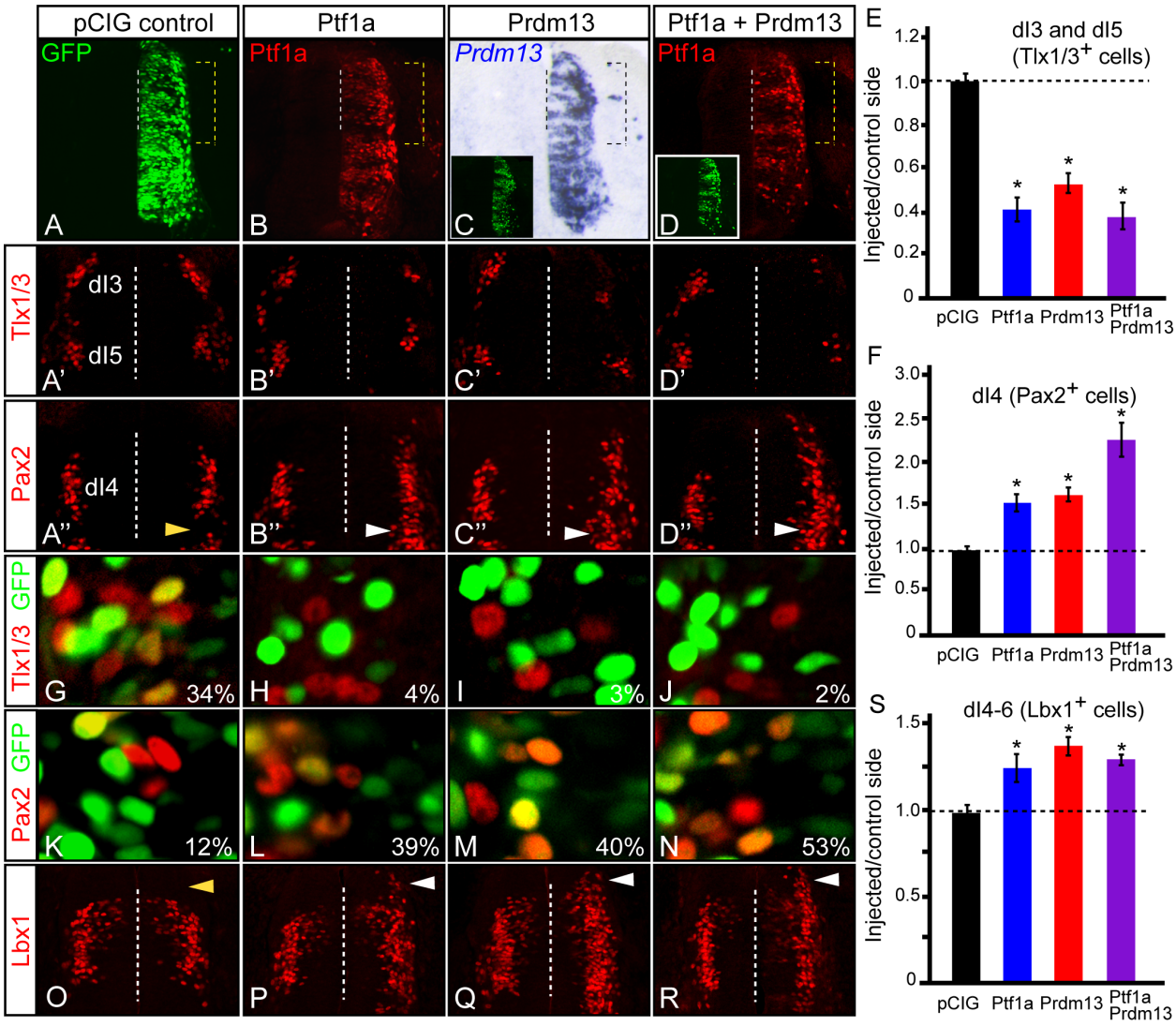

Figure 3-2. Ptf1a and Prdm13 induce inhibitory and suppress excitatory neuronal markers.

Stage HH12-13 chick embryos were electroporated with empty vector (control), Ptf1a, Prdm13, or both Ptf1a and Prdm13. Transverse sections through stage HH24-25 are shown with the electroporated side on the right.
(A-D) GFP (green) shows electroporation efficiency along the dorsoventral axis. Ptf1a immunofluorescence detects the ectopically expressed protein (B, red) and *Prdm13* is detected by *in situ* hybridization (C). Dashed bracket in (A-D) is the region of the neural tube shown in (A'-D", O-R).
(A'-D', E) Dorsal neural tube sections from (A-D) indicate the dI3 and dI5 neuronal populations marked by Tlx1/3. Dashed vertical line indicates the ventricle. (E) is the ratio of Tlx1/3$^+$ neurons on the electroporated side versus the control side showing that overexpression of Ptf1a and Prdm13 cause a dramatic decrease in Tlx1/3$^+$ neurons relative to control.

(A”-D”, F) Dorsal neural tube sections from (A-D) showing the dI4 neuronal population marked by Pax2. (F) is the ratio of $Pax2^+$ neurons above dI6 on the electroporated side versus the control side showing Ptf1a and Prdm13 cause a dramatic increase in these neurons relative to control. Note that ectopic $Pax2^+$ cells (white arrowheads) are found in the dI5 domain not normally expressing Pax2 (yellow arrowhead). (G-N) Electroporated cells, visualized by GFP, co-localized with Tlx1/3 (G-J) or Pax2 (K-N). The percentage of GFP cells that co-express Tlx1/3 or Pax2 in the dorsal mantle zone is shown. Ectopic expression of Ptf1a and/or Prdm13 reduces the percentage of Tlx1/3:GFP double positive cells from 34% to 2-4%, and increases Pax2:GFP double positive cells from 12% to 39-53%.
(O-S) Dorsal neural tube sections from (A-D) showing the dI4-6 neuronal populations marked by Lbx1. (S) is the ratio of $Lbx1^+$ neurons on the electroporated side versus the control side showing that Ptf1a and Prdm13 overexpression cause an increase in $Lbx1^+$ neurons relative to control. The white arrowheads indicate ectopic Lbx1 expression detected in the dI3 region not normally expressing Lbx1 (compare to control (O) yellow arrowhead).

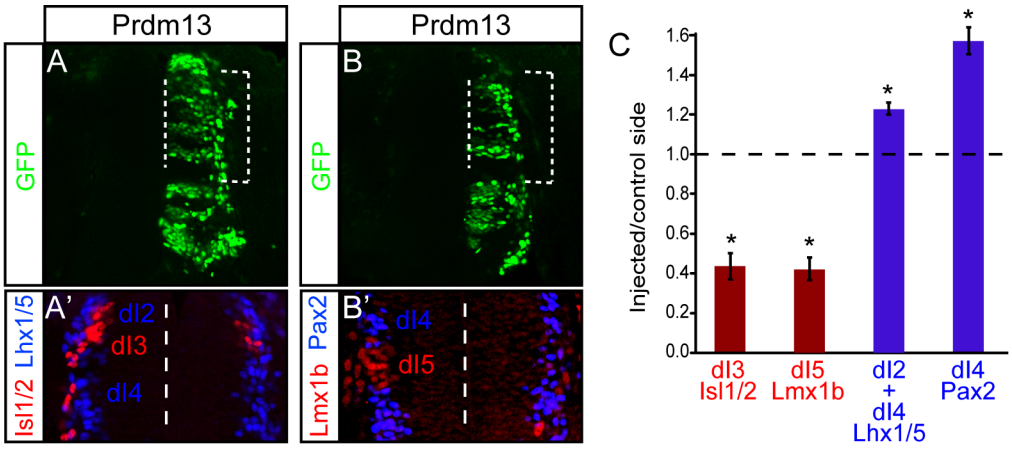
Prdm13
Prdm13
A
B
GFP
GFP
A'
B'
dI2
dI3
dI4
dI4
dI5
Isl1/2 Lhx1/5
Lmx1b Pax2
C
Injected/control side
1.6
1.4
1.2
1.0
0.8
0.6
0.4
0.2
0.0
dI3 Isl1/2
dI5 Lmx1b
dI2 + dI4 Lhx1/5
dI4 Pax2

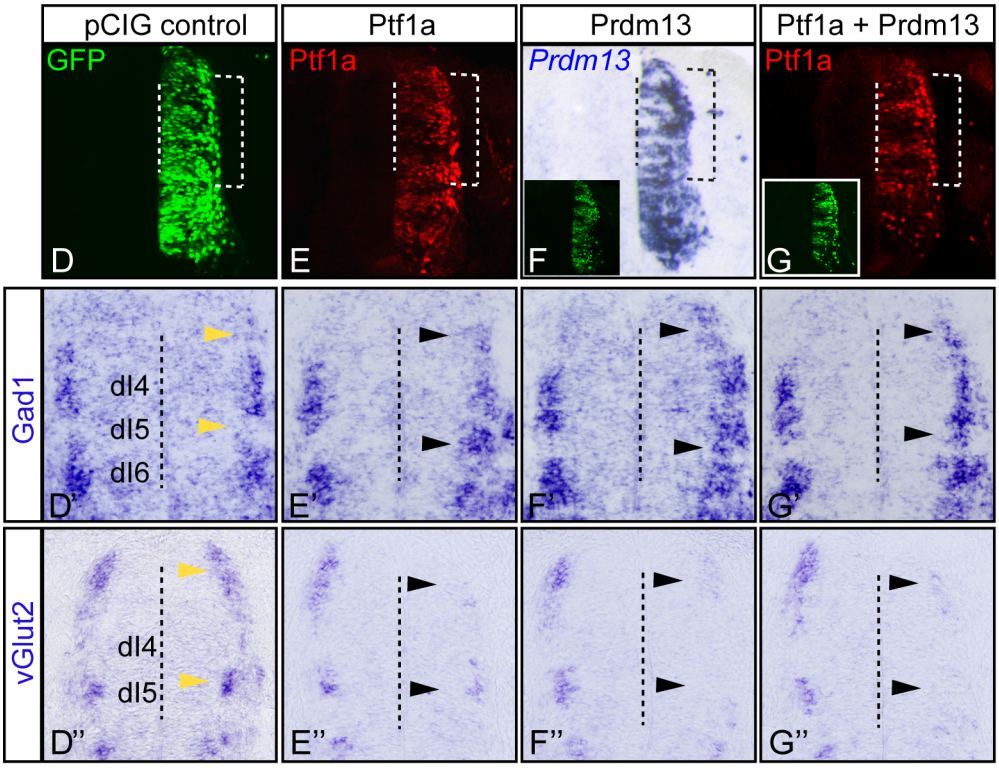
pCIG control
Ptf1a
Prdm13
Ptf1a + Prdm13
GFP
Ptf1a
Prdm13
Ptf1a
D
E
F
G
Gad1
dI4
dI5
dI6
D'
E'
F'
G'
vGlut2
dI4
dI5
D''
E''
F''
G''

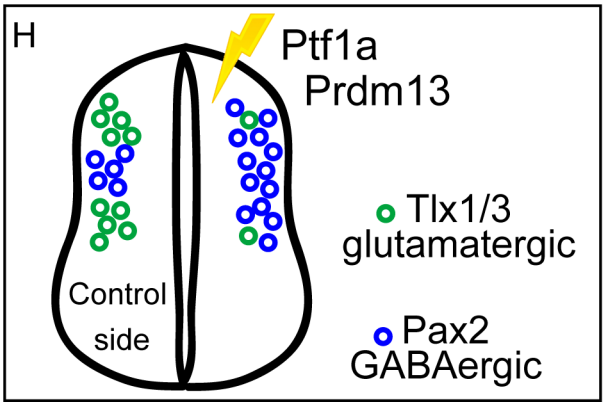
H
Ptf1a
Prdm13
Tlx1/3
glutamatergic
Pax2
GABAergic
Control
side

Figure 3-3. Prdm13 induces GABAergic and suppresses glutamatergic phenotypes.

Stage HH12-13 chick embryos were electroporated with empty vector (control), Ptf1a, Prdm13, or both Ptf1a and Prdm13. Transverse sections through stage HH24-25 are shown with the electroporated side on the right.
(A-B, D-G) GFP (green) shows the electroporation efficiency along the dorsoventral axis. Ptf1a immunofluorescence detects the ectopically expressed protein (E, red) and *Prdm13* is detected by *in situ* hybridization (F). Dashed bracket in (A-B, D-G) is the region of the neural tube shown in (A'-B', D-G''). Inset: GFP indicates the electroporation efficiency.
(A') Dorsal neural tube section showing the dI3 neuronal population marked by Isl1/2 (red), and dI2 and dI4 neuronal populations marked by Lhx1/5 (blue).
(B') Dorsal neural tube section showing the dI5 neuronal population marked by Lmx1b (red), and dI4 and dI6 neuronal populations marked by Pax2 (blue).
(C) The ratio of Isl1/2 (dI3) and Lmx1b (dI5) excitatory neurons (red) on the electroporated side versus the control side indicates that Prdm13 causes a dramatic decrease in the number of these neurons relative to empty vector control. The ratio of Lhx1/5 (dI2/dI4) and Pax2 (dI4) inhibitory neurons (blue) on the electroporated side versus the control side indicates that Prdm13 causes a significant increase in the number of these neurons relative to empty vector control.
(D-G'') *In situ* hybridization with *Gad1* or *vGlut2* probes showing that Ptf1a and Prdm13 overexpression increase *Gad1* and decrease *vGlut2* (black arrowheads) when compared to either the empty vector control (yellow arrowheads) or the control side in each neural tube.
(H) Diagram summarizing the overexpression phenotypes indicating overexpression of either Ptf1a or Prdm13 could both induce GABAergic neurons and suppress glutamatergic neurons.
More than 6 embryos were quantified for each condition and error bars are reported as standard error of the mean. Asterisks indicate significance with p-values<0.001.

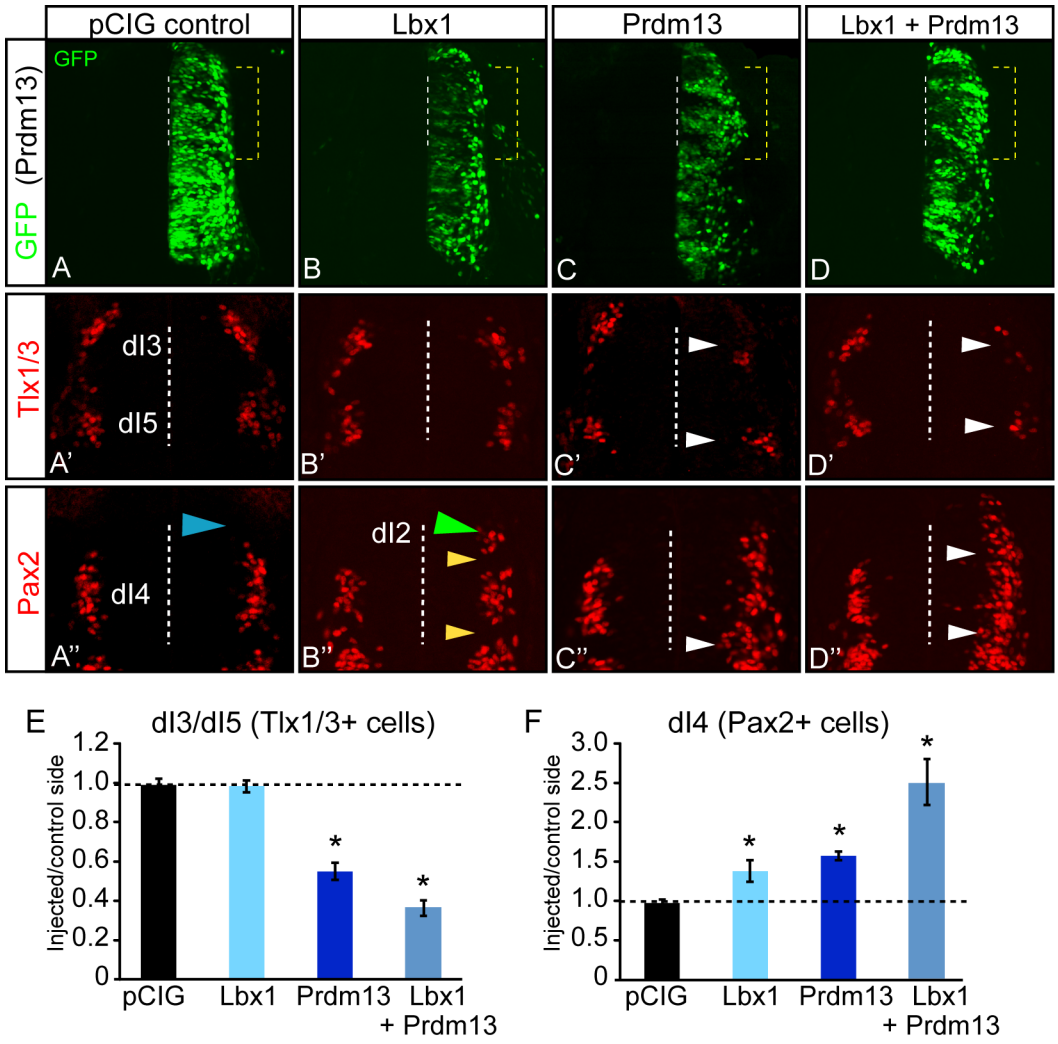

Figure 3-4. Prdm13 together with Lbx1 dramatically induce GABAergic neurons.

Stage HH12-13 chick embryos were electroporated with empty vector (control), Lbx1, Prdm13, or both Lbx1 and Prdm13. Transverse sections through stage HH24-25 are shown with the electroporated side on the right.
(A-D) GFP (green) shows electroporation efficiency along the dorsoventral axis. Dashed bracket in (A-D) is the region of the neural tube shown in (A'-D'').
(B-B'', E, F) The overexpression of Lbx1 does not affect the expression of Tlx1/3 (B' and E), but causes ectopic Pax2^{+} cells only in the dI2 domain where Tlx1/3 are not present (B", green arrowhead).
(C-C'', E, F) The electroporated side versus the control side shows the overexpression of Prdm13 causes a dramatic decrease in Tlx1/3^{+} neurons (C' E), and a dramatic increase of Pax2^{+} cells (C'', white arrowheads, F)
(D-D'', E, F) Co-electroporation of Prdm13 and Lbx1 decreases the Tlx1/3^{+} neurons (D', E), and dramatically increases the Pax2^{+} cells (D''), notice ectopic Pax2^{+} cells filling up the gap in dI3 and dI5 domains (D'', white arrowheads compare with B'', yellow arrowheads).
More than 6 embryos were quantified for each condition and error bars are reported as standard error of the mean. Asterisk indicates significant difference relative to the pCIG controls with p-value<0.001.

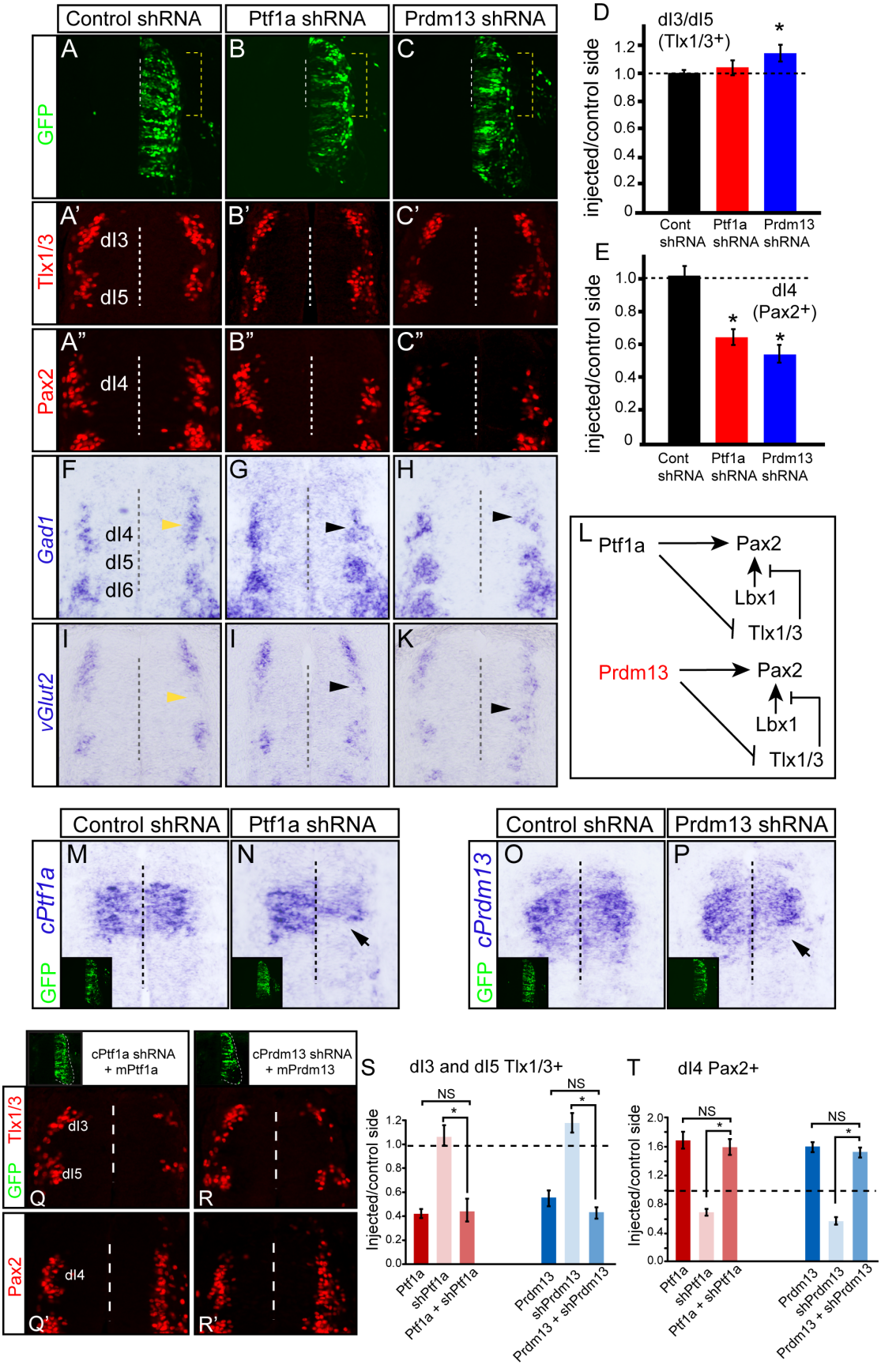
Control shRNA
Ptf1a shRNA
Prdm13 shRNA
GFP
Tlx1/3
Pax2
Gad1
vGlut2
dI3
dI4
dI5
dI6
D
dI3/dI5 (Tlx1/3+)
injected/control side
Cont shRNA
Ptf1a shRNA
Prdm13 shRNA
E
dI4 (Pax2+)
L
Ptf1a
Pax2
Lbx1
Tlx1/3
Prdm13
cPtf1a
cPrdm13
cPtf1a shRNA + mPtf1a
cPrdm13 shRNA + mPrdm13
S
dI3 and dI5 Tlx1/3+
T
dI4 Pax2+
NS
Ptf1a
shPtf1a
Ptf1a + shPtf1a
Prdm13
shPrdm13
Prdm13 + shPrdm13

Figure 3-5. Ptf1a and Prdm13 are required for generating inhibitory neurons.

Stage HH12-13 chick embryos were electroporated with shRNA to knockdown Ptf1a or Prdm13. Transverse sections through stage HH24-25 are shown with the electroporated side on the right.
(A-C) GFP indicates the electroporation efficiency along the dorsoventral axis. The dashed bracket is the region shown in (A'-C'').
(A'-C', D) Immunofluorescence for Tlx1/3 shows a slight increase in the number of dI3/dI5 neurons when Prdm13 is knocked down compared to control shRNA. Asterisk indicates p-value<0.05.
(A''-C'', E) Immunofluorescence for Pax2 shows a significant decrease in the number of dI4 neurons when Ptf1a or Prdm13 are knocked down compared to control shRNA. Asterisk indicates p-value<0.001.
(F-H) *In situ* hybridization for *Gad1* shows a reduction when Ptf1a or Prdm13 are knocked down (black arrowheads) but not with the control shRNA (yellow arrowhead).
(I-K) *In situ* hybridization for *vGlut2* shows ectopic expression in the electroporated side (I, K, black arrowheads) when Ptf1a or Prdm13 are knocked down but not with the control shRNA (yellow arrowhead).
(L) Diagram showing the model of both Ptf1a and Prdm13 are required to induce $Pax2^{+}$ cells and suppress $Tlx1/3^{+}$ cells in the dorsal spinal cord.
(M-P) *In situ* hybridization with either chick *Ptf1a* or *Prdm13* probes indicate the knockdown efficiency (black arrows). Control shRNA did not alter their expression. Inset: GFP indicates the electroporation efficiency.
(Q-R) Rescue of Ptf1a and Prdm13 shRNA knockdown phenotypes. Immunofluorescence for Tlx1/3 shows the phenotype of the knockdown constructs is rescued by the overexpression of Ptf1a or Prdm13 evident as a decrease in the number of Tlx1/3 neurons on the electroporated side. Inset: GFP indicates the electroporation efficiency.
(Q'-R') Rescue of Ptf1a and Prdm13 shRNA knockdown phenotypes. Immunofluorescence for Pax2 shows the phenotype of the knockdown constructs is rescued by the overexpression of Ptf1a or Prdm13 evident as an increase in the number of Pax2 neurons on the electroporated side.
(S-T) Quantification of the rescue experiments shown in (Q-R') relative to overexpression or shRNA experiments from Figs. 3,4. The asterisk indicates p-value<0.001. NS, not significant.

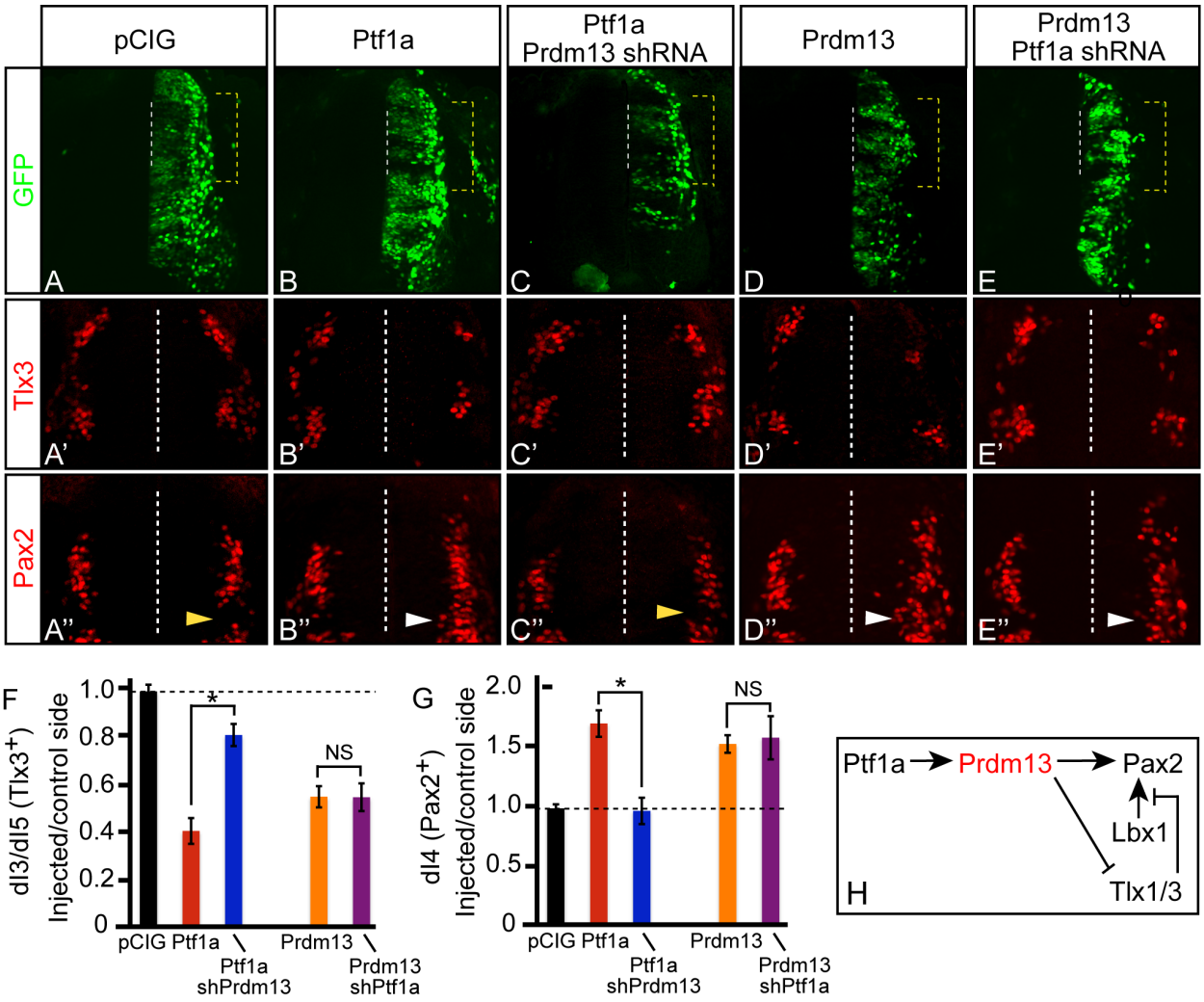

Figure 3-6. Ptf1a requires Prdm13 to specify inhibitory neurons and suppress excitatory neurons.

Stage HH12-13 chick embryos were electroporated with (A) Empty vector (control), (B) Ptf1a, (C) Ptf1a and Prdm13 shRNA, (D) Prdm13, (E) Prdm13 and Ptf1a shRNA, to modulate levels of Ptf1a and Prdm13. Transverse sections through stage HH24-25 are shown with the electroporated side on the right.
(A-E) GFP (green) shows the electroporation efficiency along the dorsoventral axis. The dashed bracket is the region of the neural tube shown in (A'-E'').
(A'-E', F) Immunofluorescence for Tlx1/3 marks dI3/dI5 neurons. The ability of Ptf1a to suppress the number of Tlx1/3$^+$ neurons requires Prdm13, but the activity of Prdm13 does not require Ptf1a.
(A''-E'', G) Immunofluorescence for Pax2 marks dI4 neurons. The ability of Ptf1a to increase the number of Pax2$^+$ neurons requires Prdm13, but the activity of Prdm13 does not require Ptf1a. White arrowheads indicate ectopic Pax2$^+$ cells not found normally in the dI5 domain (marked by yellow arrowheads).
More than 6 embryos were quantified for each condition and error bars are reported as standard error of the mean. Significance with p-values<0.001 is indicated with * between sample and control. NS, not significant.
(H) Diagram illustrates the model of Ptf1a requires Prdm13 to specify Pax2$^+$ neurons and suppress the Tlx1/3$^+$ neurons in the dorsal spinal cord

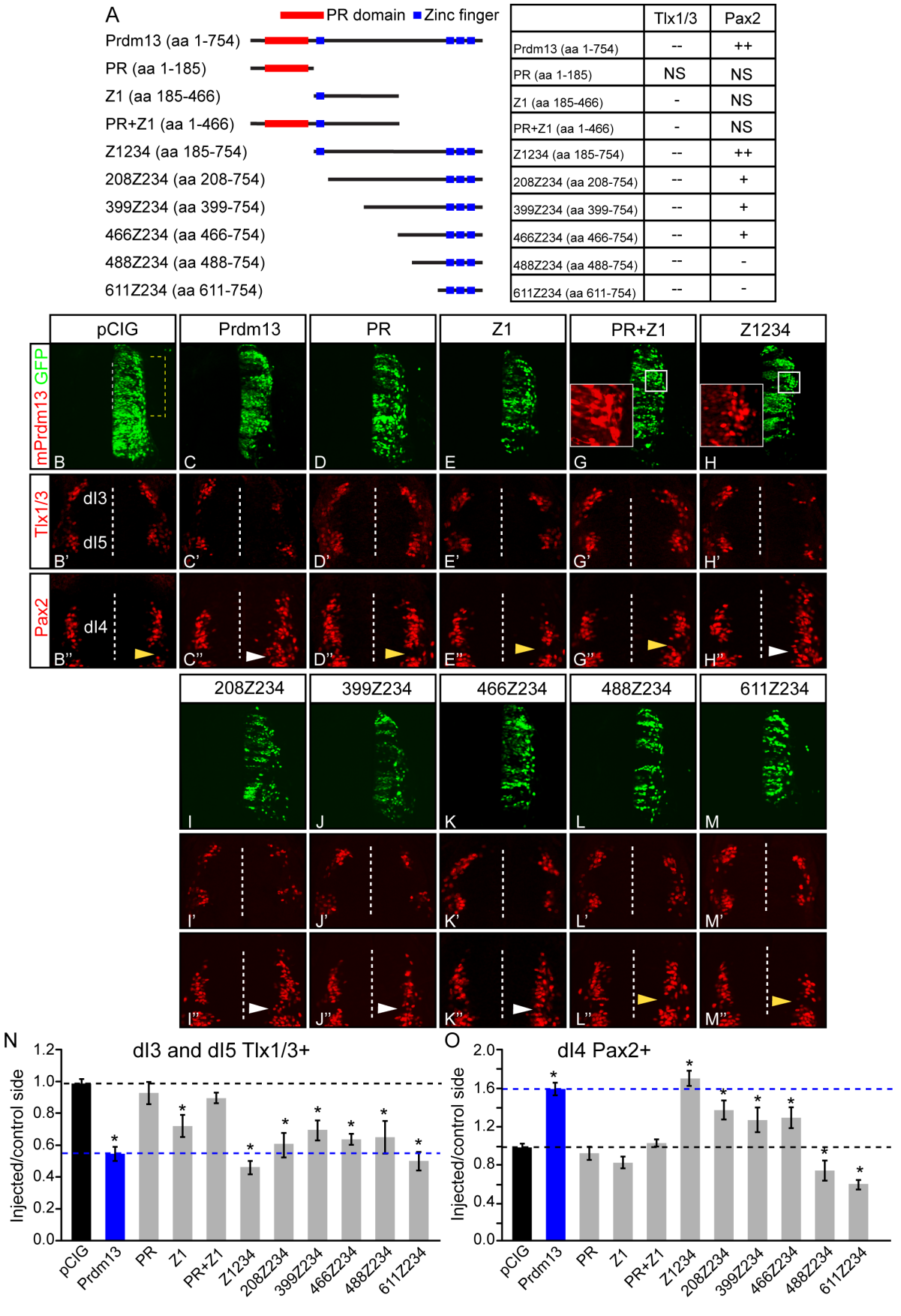

	Tlx1/3	Pax2
Prdm13 (aa 1-754)	--	++
PR (aa 1-185)	NS	NS
Z1 (aa 185-466)	-	NS
PR+Z1 (aa 1-466)	-	NS
Z1234 (aa 185-754)	--	++
208Z234 (aa 208-754)	--	+
399Z234 (aa 399-754)	--	+
466Z234 (aa 466-754)	--	+
488Z234 (aa 488-754)	--	-
611Z234 (aa 611-754)	--	-

Figure 3-7. The zinc finger containing domains of Prdm13 are sufficient for activity.

(A) Diagram of the Prdm13 mutations tested. PR domain (red boxes) and Zn finger domains (blue boxes) are indicated.
(B-M) GFP (green) indicates the electroporation efficiency along the dorsoventral axis. Dashed bracket in (B) is the region of the neural tube shown in (B'-M''). Dashed vertical line indicates the ventricle. Insets in (G,H) are immunofluorescence for the ectopic mutated Prdm13 showing Z234 contains information for nuclear localization of the protein.
(B'-M') Immunofluorescence for Tlx1/3 marks dI3/dI5 neurons.
(B''-M'') Immunofluorescence for Pax2 marks dI4 neurons. White arrowheads indicate ectopic $Pax2^{+}$ cells not found normally in the dI5 domain (marked by yellow arrowheads).
(N and O) Quantification of experiments by immunofluorescence for Tlx1/3 (B'-M') and Pax2 (B''-M''). The black dashed line indicates the control ratio of injected/control side of 1. The blue dashed line indicates the phenotype of the full-length Prdm13. The PR domain is dispensable for Prdm13 activity whereas the zinc finger domains can recapitulate activity of the full-length protein. More than 6 embryos were quantified for each condition and error bars are reported as standard error of the mean. Asterisks indicate significance with p-values<0.001.

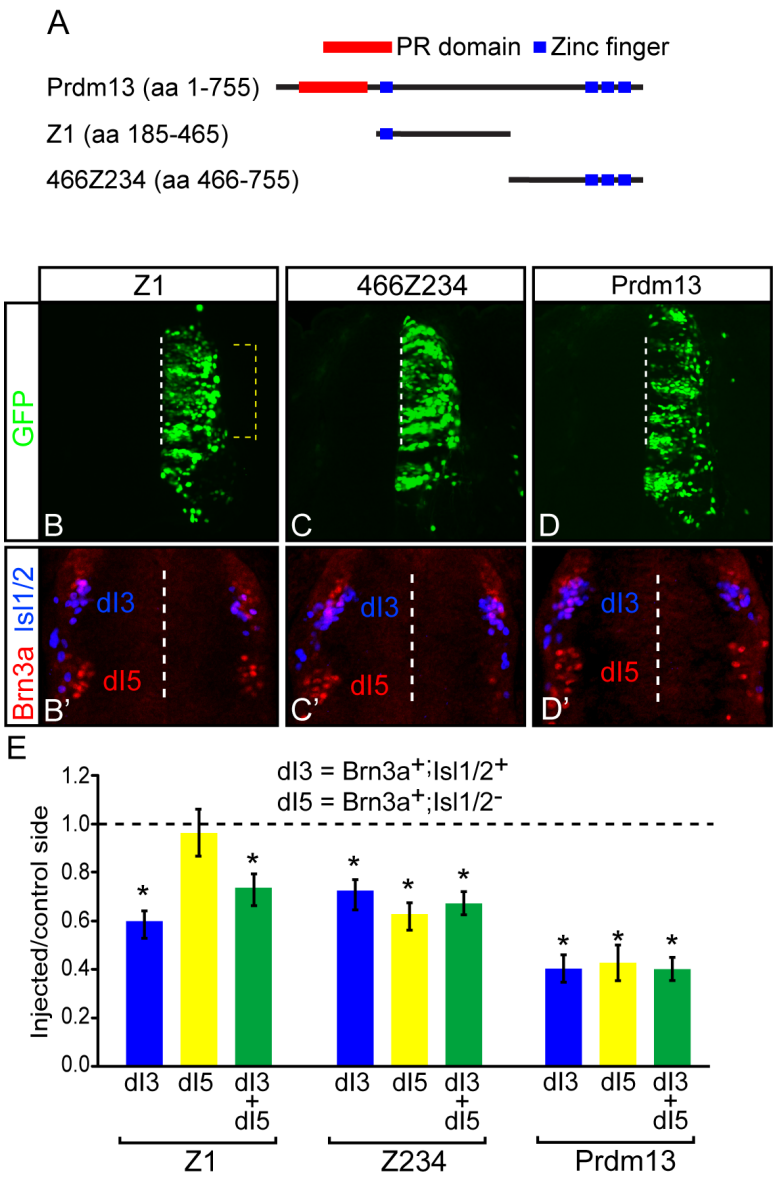

Figure 3-8. Z1 and Z234 contain different activity to suppress dI3 and/or dI5 glutamatergic neurons.

(A) Diagram of the Prdm13 mutations tested. PR domain (red boxes) and Zn finger domains (blue boxes) are indicated.
(B-D') Z1, 466Z234, and the full length Prdm13 were electroporated, and markers Isl1/2 and Brn3a were used to distinguish dI3 and dI5. Isl1/2^{+};Brn3^{+} marks dI3 (blue/pink) and Brn3a^{+};Isl1/2^{-} marks dI5 (red). GFP shows electroporation efficiency.
(E) Quantification of the results from (B'-D'). The Z1 partial protein retains the ability to reduce the number of dI3 neurons but had no significant effect on dI5. In contrast, Z234 was sufficient to reduce the number of both dI3 (blue/pink) and dI5 (red) neurons almost as much as the full length Prdm13. The control experiments show a ratio of 1 (dashed line). More than 6 embryos were quantified for each condition. Asterisk indicates pvalue< 0.001 as compared to controls (ratio 1).

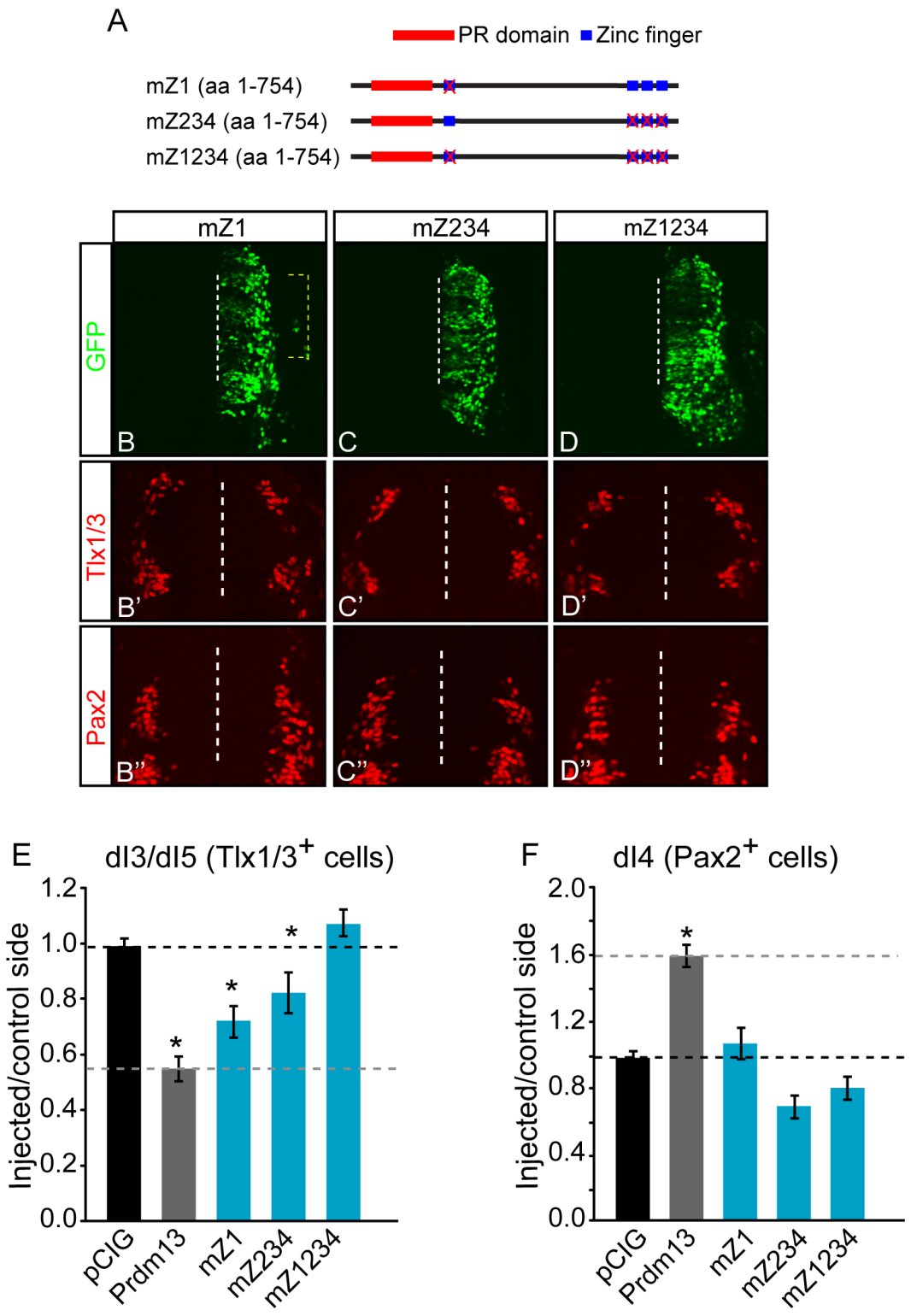
A
PR domain
Zinc finger
mZ1 (aa 1-754)
mZ234 (aa 1-754)
mZ1234 (aa 1-754)
mZ1
mZ234
mZ1234
GFP
Tlx1/3
Pax2
B
C
D
B'
C'
D'
B''
C''
D''
E
dI3/dI5 (Tlx1/3+ cells)
Injected/control side
1.2
1.0
0.8
0.6
0.4
0.2
0.0
pCIG
Prdm13
mZ1
mZ234
mZ1234
F
dI4 (Pax2+ cells)
2.0
1.6
1.2
0.8
0.4
0.0

Figure 3-9. The zinc finger domains in Prdm13 are required for suppressing Tlx1/3.

(A) Diagram of the Prdm13 mutations tested. PR domain (red boxes) and Zn finger domains (blue boxes) are indicated.
(B-D) Stage HH12-13 chick embryos were electroporated with Prdm13 with mutated zinc finger domains mZ1, mZ234, and mZ1234. Transverse sections through stage HH24-25 are shown with the electroporated side on the right. GFP (green) shows electroporation efficiency along the dorsoventral axis. Dashed bracket in (B) is the region of the neural tube shown in (B'-D'').
(B'-D', E) Dorsal neural tube sections from (B-D) indicate the dI3 and dI5 neuronal populations marked by Tlx1/3. Dashed vertical line indicates the ventricle. (E) is the ratio of $Tlx1/3^+$ neurons on the electroporated side versus the control side showing that the mutations of the zinc finger domains in Prdm13 diminished the activity of Prdm13 to suppress Tlx1/3.
(B"-D", F) A dorsal neural tube sections from (B-D) show the dI4 neuronal population marked by Pax2. (F) is the ratio of $Pax2^+$ neurons above dI6 on the electroporated side versus the control side showing the mutations of the zinc finger domains in Prdm13 reduce its ability to induce Pax2.

CHAPTER FOUR

Multi-mechanisms of Prdm13 repressing glutamatergic lineage

The work presented in this chapter was performed in collaboration with a former post-doctoral fellow in the Johnson lab, Paul Mayer, and a fellow graduate student, Yi-Hung Ou, for the Co-immunoprecipitation experiments. The ChIP-Seq experiment was performed with the help of Mark Borromeo, a Johnson lab graduate student.

Introduction

Chapter 2 and 3 detail the evidence for Prdm13 as a direct downstream target of Ptf1a, and its role in mediating neuronal specification in the dorsal spinal cord. Prdm13 phenocopies the gain and loss of function of Ptf1a by increasing the number of $Pax2^{+}$/GABAergic neurons and decreasing the number of $Tlx1/3^{+}$/glutamatergic neurons in the chick dorsal spinal cord. Epistasis experiments confirm Prdm13 functions downstream of Ptf1a, and Ptf1a requires Prdm13 for its function in neuronal specification. Furthermore, Prdm13 induces inhibitory interneurons indirectly through repressing transcription of dI5/dILB control genes Tlx1/3, relieving the block on Lbx1, a HD factor required to specify GABAergic interneurons. Thus, balancing the excitatory and inhibitory interneurons in dorsal spinal cord circuitry requires not only bHLH and HD factors but also at least one member of the PRDM family, Prdm13, to modify bHLH function and to directly regulate HD transcription. Here, I performed a combination of techniques, including in ovo chick electroporation, *in vivo* ChIP-Seq, and *in vitro* biochemical assays, to uncover the mechanism behind Prdm13 function in these processes.

Prdm13 belongs to the Prdm super family, known to regulate multiple transcriptional mechanisms involved in cell proliferation, differentiation, and specification during development (Bikoff et al., 2009; Fog et al., 2012; Hohenauer and Moore, 2012). The PR domain has 20-30% identity to the SET domain found in a class of histone methyltransferases (HMTs) that function to silence transcription. Recent studies showed Prdm2, 8, and 9 exhibit intrinsic HMT activity (Derunes et al., 2005; Eom et al., 2009; Hayashi et al., 2005; Kim et al., 2003). Other members recruit histone modifying enzymes to mediate their function. These co-factors include HMTs, which induce repressive chromatin states by methylation of histone lysines, the enzyme Prmt5 (protein methyltransferase 5), which methylates arginines to repress transcription, and Lsd1 (lysine-specific demethylase 1, Kdm1a), which mainly promotes repression through erasure of activating H3K4 (histone H3 lysine 4) methylation (Ancelin et al., 2006; Chittka et al., 2012; Eckert et al., 2008; Su et al., 2009). Furthermore, histone deacetylases (HDAC), which promote transcriptional repression, are also involved in the PRDM transcriptional regulation.

For example, although lacking the intrinsic HMT activity, Prdm6 was shown to bind HDAC1, -2, and -3 (histone deacetylases), HP1-β (heterochromatim protein-1β), and G9a HMT (histone methyltransferase) *in vitro* (Davis et al., 2006). Interestingly, the PR domain primarily mediates the binding ability of Prdm6 to G9a, yet both the PR and zinc finger domains are individually sufficient to repress transcription by recruiting HDAC1, -2, -3, and p300 (Davis et al., 2006). Prdm1/Blimp-1 can also recruit HDAC1 and HDAC2 (Yu et al., 2000). Strikingly, in contrast to Prdm6, the zinc finger domains of Prdm1 recruit histone H3 lysine methyltransferase G9a to assemble silent chromatin over the interferon beta promoter, and this activity remains when the PR domain is deleted (Gyory et al., 2004). Prdm1 also interacts with a Lysine-specific demethylase Lsd1 (Kdm1a) forming a repressor complex, and binds to the cis-elements of *CIITA* gene to regulate the plasma cell differentiation (Su et al., 2009). Data mined from the BioGRID suggest that another lysine-specific demethylase, Kdm5b, which functions as a transcriptional repressor, binds to human Prdm13 (Zhou et al., 2009).

Except Prdm11, most PRDM members contain one or several zinc finger domains after the PR domain, which contribute a diverse complexity of mechanisms for PRDM proteins to regulate transcription. Zinc finger domains are well known to interact with either DNA or other proteins (Brayer and Segal, 2008; Wolfe et al., 2000). Although there are 20 different types of zinc finger domains, each categorized by the structure of their zinc stabilizing amino acid sequence (Brayer and Segal, 2008; Krishna et al., 2003), the PRDM members contain the classic zinc finger, Cys2-His2 (C2H2) type. C2H2 zinc finger domains often contain tandem repeats connected by short peptides known as the linker. Base on the repeated number of zinc fingers, these proteins can be divided to mainly four classes as single, triple, multiple-adjacent, and separated-paired C2H2 zinc finger proteins (Iuchi, 2001). Most of the zinc finger proteins contain a well-conserved linker, TGEKP, in between adjacent zinc fingers, which is required for DNA interaction (Nunez et al., 2011; Wolfe et al., 2000). The linker in the second and third zinc finger domains of Prdm13 is TGYKP, which contains one amino acid different from the classic DNA binding linker. In this study, I have no evidence to support Prdm13 directly binds to DNA, hence, whether Prdm13 directly interacts with DNA or not remains unclear.

Consistant with PRDM proteins being transcription factors, they are localized to the nucleus and in multiple cases, it has been shown that the zinc finger domains are required for this. For example, Prdm6 and Prdm8 localized to the cytoplasma when their zinc finger domains were truncated (Davis et al., 2006; Eom et al., 2009); indeed, Prdm13 requires its zinc finger domains for nuclear localization as well (Fig. 3-7G,H). Because of the well known DNA interaction activity of zinc finger domains, specific motifs bound by several PRDM members have been determined. Utilizing the electrophoretic mobility shift assay (EMSA), the most C-terminal six zinc finger domains of Prdm5 are required for direct DNA interaction (Duan et al., 2007). Prdm9 directly interacts with a specific binding motif known as "CCTCCCTGCCCAC", which is a hotspot for initiating recombination in human and mouse (Baudat et al., 2010; Berg et al., 2010; Segurel et al., 2011). Prdm1 directly binds to the motif "AAGTGAAAGTG" that was found in regions surrounding its downstream targets, such as *c-myc* and *CIITA* (Kuo and Calame, 2004). Other studies have utilized genome-wide ChIP-Seq assays and bio-informatic analysis to identify

the specific binding motifs of PRDM members. Prdm14 ChIP-Seq from mouse embryonic stem cells (mESCs) revealed a specific Prdm14 interacting cis-element as "TTAGAGACCC", and further validated it by *in vitro* DNA-pull down experiments (Ma et al., 2011). Although several C2H2 zinc finger domains were shown to interact with specific GC-rich motifs (Brayer and Segal, 2008; Razin et al., 2012; Wolfe et al., 2000), the known binding sites for PRDM members seem to be diverse, which might reflect different sequence repeats within the zinc finger domains in the PRDM proteins.

Intriguingly, Prdm8, which shares the highest similarity in the PR domain to Prdm13, does not show any evidence of direct DNA interaction so far (Ross et al., 2012). Instead, Prdm8 requires its obligate partner, a bHLH transcription factor bHLHb5, to bind to DNA. A specific binding motif of bHLHb5 was identified as "CATATGCT" (E-box), and this sequence was required for this complex to repress Cadherin-11, generating consequences for neural circuit development (Ross et al., 2012). One difference between Prdm8 and Prdm13 is the arrangement of the zinc finger domains with Prdm8 predicted to not have the correct configuration. However, there are no mechanistic studies of Prdm13 to date.

In this study, I demonstrate Prdm13 interacts with specific cis-elements to repress the glutamatergic lineage genes *Tlx1* and *Tx3*. This repression is executed through multiple-mechanisms: one is Ascl1-dependent, where Prdm13 switches Ascl1 from activator to repressor; another is Ascl1-independent, where Prdm13 directly represses Tlx1.

Experimental procedures

Chromatin Immunoprecipitation and RNA Sequencing (ChIP-Seq and RNA-Seq)

The tissue source for ChIP was mouse E11.5 neural tubes. Negative tissues for control included telencephalon for Prdm13 ChIP and limbs for Ascl1 ChIP, from the same embryos when neural tube was extracted. ChIP was performed as previously described (Holmstrom et al., 2011; Masui et al., 2007), with details in the Appendix. Mark Borromeo performed the Ascl1 ChIP experiments. Notably, the Prdm13

ChIP was treated with formaldehyde along with an additional long-arm cross-linker, ethylene glycol-bis (succinimidyl succinate), to increase the ChIP efficiency (Zeng et al., 2006). A mouse monoclonal antibody used for Ascl1 ChIP was purchased from BD Pharmingen. Lab generated antisera against full-length Prdm13 were used for Prdm13 (TX970, rabbit anti-Prdm13), details provided in the Appendix. NEBNext ChIP-Seq Sample Prep Master Mix Set 1 was used for library generation. Detailed methods and primers used for ChIP qPCR are listed in Appendix. ChIP efficiency (CE) was calculated relative to input as CE = $(2^{Ct\ input\ -\ Ct\ ChIP})$ x DF x 100%, where DF is the dilution factor between input and ChIP sample.

Plasmid description

FLAG-tagged Prdm13 and variations used for expression in the chick neural tube were inserted into the pCIG vector, which drives expression through a combined CMV early enhancer/chicken β-actin promoter and contains an IRES-NLS-GFP (Megason and McMahon, 2002). Prdm13 mZ1234 contains point mutations in each zinc finger (Z1;C185A, H207A, Z2;C622A, H638A, Z3;C650A, H666A, Z4;C679A, H695A), and the truncated mutations of Prdm13 were all cloned into the pCIG vector. Ascl1 expression construct used pMiWIII as previously described (Hori et al., 2008; Nakada et al., 2004). The engrailed repressor (EnR) (Smith and Jaynes, 1996) or the VP16 activator (Triezenberg et al., 1988) were fused at the C-terminal end of Prdm13 in pMiWIII. The *eTlx1::GFP* and *eTlx3::GFP* reporter constructs include mm9 coordinates (*eTlx1*, chr19:45217747-45218583) and (*eTlx3*, chr11:33134077-33134502), respectively, cloned into a GFP reporter cassette with a β-globin basal promoter (Lai et al., 2011). All constructs used were sequence verified. The pSilencer 1.0-U6 vector (Ambion) was used in knock down experiments where several sets of 21-mer oligonucleotides were selected from chick *Prdm13* mRNA sequences (listed in the Appendix). The shRNA constructs were co-electroporated with pCIG so GFP could be used to assess electroporation efficiency.

In ovo chick electroporation

Fertilized white Leghorn eggs were obtained from the Texas A&M Poultry Department (College Station, TX) and incubated at 37°C for 48 hours until stage HH12-13 (Hamburger and Hamilton, 1992). Solutions of supercoiled plasmid DNA (1-2.5 μg/μl each) in UltraPure Distilled Water (Invitrogen) and Trypan Blue were injected into the lumen of the closed neural tube, and embryos were electroporated as previously described (Timmer et al., 2001). After 48 hours incubation at 37°C, stage HH24-25 embryos were harvested and processed for immunofluorescence or in situ hybridization.

Immunofluorescence and In Situ hybridization

Immunofluorescence was performed as previously described (Glasgow et al., 2005; Hori et al., 2008). A list of primary antibodies used is listed in Appendix. Fluorescence imaging was carried out on a Zeiss LSM 510 confocal microscope. For each experiment, multiple sections from at least six different embryos were analyzed and used for quantification. Cell counting was blind to the condition and was performed manually using ImageJ. The quantitative results are presented as a ratio of the number of marker positive cells on the electroporated side divided by the number on the non-electroporated side. Only sections with confirmed high efficiency expression across the dorsal ventral axis were used in the analysis. Mean GFP pixel intensity for *eTlx1/3::GFP* expression was measured by ImageJ. Significant differences between control and experimental samples were calculated using a two-tailed two-sample equal variance (homoscedastic) Student's t test (* indicates $P < 0.001$) in Microsoft Excel. SEM is shown. In situ hybridization was performed as previously described (Lai et al., 2011). Mouse *Prdm13* probes were cloned by PCR into pBluescript with the primers listed in Appendix.

Co-immunoprecipitation (performed by Paul Mayer Ph.D.)

HEK293T cells were transfected with Flag-tagged Prdm13, and myc-tagged Ascl1 or Hook3 (control) (Walenta et al., 2001) expression constructs using FuGene 6 (Roche Life Sciences), and collected 48 hours later. Anti-Flag antibodies conjugated to protein A/G beads (Santa Cruz) were added to cleared lysate. Co-immunoprecipitation was assessed by western blot using anti-myc (A-14, Santa Cruz, 1:2000).

Results

Prdm13 suppresses generation of Tlx1/3$^+$ neurons by antagonizing Ascl1 activity

The bHLH factor Ascl1 specifies opposing programs (dI3 and dI5) to Ptf1a and Prdm13 at this stage (Fig. 4-1A) (Brohl et al., 2008; Helms et al., 2005; Mizuguchi et al., 2006; Nakada et al., 2004), and given that the expression pattern of Ascl1 highly overlaps with Prdm13 in the dorsal spinal cord (Fig. 4-1B-C), we hypothesized that Prdm13 might function through interfering with Ascl1 activity. Ascl1 is expressed in dI3 to dI5, with a weaker expression in the dI4, opposite than the pattern of Prdm13 (Fig. 4-1B). According to the mRNA expression level of Prdm13, it is highly enriched in the dI4, more so than dI2 and dI6, but also is present in dI3 and dI5 (Fig. 4-1C).

I tested this hypothesis by co-electroporating Ascl1 and Prdm13 into the chick neural tube. Ectopic Ascl1 results in a dramatic increase of Tlx1/3$^+$ neurons and a loss of Pax2$^+$ neurons (Fig. 4-2C-C'',K,L). Strikingly, when Ascl1 and the full length of Prdm13 are expressed simultaneously, Ascl1 is no longer able to induce Tlx1/3. Instead, we observed a 3.3-fold decrease in Tlx1/3$^+$ neurons and a 1.6-fold increase in Pax2$^+$ cells relative to the control side, similar to what is seen with Prdm13 misexpression alone (Fig. 4-2D-D'',K,L, compare with Fig. 4-2C'-C'',K,L). To explore how Prdm13 antagonizes Ascl1, I determined which domain of Prdm13 protein retained this activity. As predicted, the PR domain was dispensable whereas Z1234 recapitulated the activity of full-length Prdm13 (Fig. 4-2I-I'' compare with

Fig. 4-2D-D''K,L). When Z1 (Fig. 4-2A, first zinc finger domain of Prdm13) was co-expressed with Ascl1, it neutralized the number of Tlx1/3^{+} neurons down 2-fold compared to the Ascl1 overexpression alone (Fig.4-2C',F',K), and could partially rescue the number of Pax2^{+} neurons when compared to the empty pCIG vector as control (Fig.4-2B'',F'',L). However, the antagonizing effect of 466Z324 (Fig. 4-2A, last three zinc finger domains) to Ascl1 is twice as strong as Z1 (Fig.4-2,K,L). Therefore, the truncation containing the Z234 (466Z234) retains the majority of the activity, but Z1 has some activity and seemed to neutralize the effects of ectopic Ascl1 (Fig. 4-2E-H'', K,L).

Interestingly, Prdm13 not only dominates the neuronal specification when co-expressed with Ascl1, but it also seems to inhibit the ability of Ascl1 to promote neuronal differentiation (Fig. 4-2, C compare with D). The progenitors electroporated with Ascl1 alone, appearing as the GFP^{+} cells (Fig. 4-2C, green or blue cells), differentiated and migrated to the MZ at the lateral part of spinal cord (Fig. 4-2C). This specific phenotype is due to the activity of Ascl1 in inducing neuronal differentiation (Nakada et al., 2004). However, when Prdm13 is co-expressed, the GFP^{+} cells are not biased in the MZ, but are evenly spread in the medial to lateral axis in the spinal cord (Fig. 4-2D, green or blue cells), indicating Prdm13 blocks the neuronal differentiation activity of Ascl1. Thus, at least in this overexpression assay, Prdm13 suppresses Ascl1 activity in both its functions: neuronal differentiation and neuronal subtype specification.

Manipulation of Prdm13 expression level does not alter endogenous Ascl1 levels (Fig. 4-2M-N',O); therefore, Prdm13 antagonizes Ascl1 activity without inhibiting expression of Ascl1 itself. Thus, while Ascl1 is expressed in both progenitors to dI4 and dI5 neurons, it is the presence or absence of enriched Prdm13 levels that dictate the decision between these cell fates. As a result, in the dI4 domain, Prdm13 inhibits the activity of Ascl1 to induce Tlx1/3, consequentially releasing Lbx1 to specify the progenitors differentiating as GABAergic interneurons (Fig. 4-2P).

Prdm13 functions as a repressor

Members of the PRDM family of factors have been reported to function either as transcriptional repressors or activators depending on the cellular context (Fog et al., 2012; Hohenauer and Moore, 2012). According to the results above, if Prdm13 antagonizes Ascl1 and suppresses *Tlx1/3* in order to indirectly induce GABAergic lineage genes; it should function as a transcriptional repressor. To determine whether the neuronal specification activity observed with Prdm13 reflects its function as a transcriptional repressor or an activator, I fused it with the engrailed repressor (EnR) (Smith and Jaynes, 1996) or with the VP16 activator (Triezenberg et al., 1988) and tested these chimeric proteins for activity in the chick neural tube (Fig. 4-3A). The activity of Prdm13-EnR was indistinguishable from that of wild-type Prdm13 in that the number of Tlx1/3^{+} neurons was dramatically reduced while Pax2^{+} neurons increased (Fig. 4-3E-E'',F,G compare with Fig. 4-3C-C'',F,G). In contrast, expression of Prdm13-VP16 resulted in a decrease in Pax2^{+} cells. Prdm13-VP16 also slightly repressed Tlx1/3, although the effect was much less pronounced than that of Prdm13-EnR or Prdm13 (Fig. 4-3D-D'',F,G). Taken together, Prdm13 appears to exert its effects by acting as a transcriptional repressor, an activity that requires its zinc finger domains to suppress the glutamatergic lineage genes.

Prdm13 directly represses *Tlx1/3* expression

One model for Prdm13 repression of Tlx1/3 expression is through a direct mechanism. To test this model, I used ChIP-Seq to determine if Prdm13 localizes to chromatin *in vivo* near *Tlx1* and *Tlx3* genes. I performed ChIP-Seq with antibodies to Prdm13 using chromatin from E11.5 neural tubes. I found Prdm13 enriched at regions upstream of both the *Tlx1* and *Tlx3* genes (Fig. 4-4A,B yellow bars). No enrichment was detected with these antibodies in chromatin isolated from E11.5 mouse telencephalon tissue where Prdm13 is absent confirming specificity of the antibody (Fig. 4-4A,B). Furthermore, Prdm13 was not found within a 60-300 kb region surrounding the GABAergic lineage genes, such as *Pax2*, *Lhx1*, and *Lhx5*, consistent with Prdm13 induction of these genes being indirect (Fig. 4-4E-G). Enrichment of

the *Tlx1* and *Tlx3* regions was confirmed in ChIP-qPCR experiments. Again, results yielded a 10-fold and 3-fold enrichment of the *Tlx1* and *Tlx3* sites respectively in neural tube when compared with telencephalon tissue, and no enrichment was found with a control genomic region (Fig. 4-4C). These data suggest that Prdm13 inhibits glutamatergic identity by binding near the glutamatergic specified genes *Tlx1 and Tlx3,* and directly repressing their transcription. This, in turn, may facilitate Lbx1-mediated induction of Pax2 and GABAergic neuronal specification (see Fig. 4-2P for model).

Prdm13 directly forms a complex with Ascl1 to repress *Tlx3* expression

To explore how Prdm13 antagonizes Ascl1, we asked whether Ascl1 was also found at the Prdm13 bound *Tlx1* and *Tlx3* sites. ChIP with Ascl1 antibodies from E11.5 neural tubes showed significant enrichment at the *Tlx3* site but not the *Tlx1* (Fig. 4-4D). This enrichment was similar to that seen with a known target of Ascl1, *Dll1*, used as a positive control in this case (Castro et al., 2006). Enrichment at the *Tlx3* site was not detected from limb tissue where Ascl1 is not expressed or from a control genomic region (Fig. 4-4D). This finding suggests a model whereby Ascl1 binds and activates expression of *Tlx3*, but when Prdm13 levels increase downstream of Ptf1a, a novel transcriptional repressor complex that includes Ascl1 and Prdm13 is formed. However, no enrichment was found at the *Tlx*1 site, indicating Ascl1 regulates Tlx1 in an indirect way (Fig. 4-4D). Therefore, I demonstrate that Prdm13 has multiple mechanisms to suppress the glutamatergic lineage control genes, *Tlx3* and *Tlx1*. Since Ascl1 and Prdm13 both bind to the same site near *Tlx3* locus *in vivo*, I hypothesize that Prdm13 forms a repression complex with Ascl1 to regulate the expression of Tlx3. Supporting this hypothesis, specific binding between Ascl1 and Prdm13 is detected in co-IP experiments when epitope-tagged versions of the proteins are expressed in HEK 293 cells (Fig. 4-4H). This interaction was not found with the controls, including a myc-tagged Hook3 (Fig. 4-4H), or a myc-tagged RGS16 (data not shown), indicating the specific interaction between Prdm13 and Ascl1, but not random proteins or the myc tag.

Multiple mechanisms of Prdm13 suppresses glutamatergic lineage genes

Two distinct mechanisms, one Ascl1-dependent and one Ascl1-independent, are suggested for Prdm13 suppression of the glutamatergic gene expression program in cells fated to become GABAergic neurons (see Fig. 4-6 model). To verify that Prdm13 and Ascl1-bound regions function as enhancers, I tested reporter constructs derived from the *Tlx1* and *Tlx3* genomic loci (Fig. 4-5A,G yellow bars). *eTlx1::GFP* and *eTlx3::GF*P (enhancer regions cloned into GFP reporter vector) reporters were electroporated into the chick neural tube at HH12-13 and assayed 48 hours later. Strikingly, *eTlx3::GFP* was largely restricted to the dI3 and dI5 domains and *eTlx1::GFP* to the dI5 domain reflecting the expression of their respective gene loci (Fig. 4-5B,B',H,H'). Furthermore, co-electroporation of the reporter constructs with Ascl1 resulted in a dramatic induction of *eTlx3::GFP* and only a slight induction of *eTlx1::GFP*, consistent with Ascl1 localizing to *Tlx3* but not *Tlx1* (Fig. 4-5C,I). This dramatic activation of *eTlx3::GFP* by Ascl1 was abrogated when Prdm13 was also expressed (Fig. 4-5E,K). Misexpression of Prdm13 alone with the reporter constructs similarly inhibited their activity in dI3 and dI5 domains (Fig. 4-5D white bracket, J). This further supports the previous observation that Ascl1 directly regulates Tlx3 but indirectly regulates Tlx1. Thus, in addition to identifying enhancers for *Tlx1* and *Tlx3* that are directly repressed by Prdm13, I identified a novel Ascl1/Prdm13 containing repressor complex that directly represses the *Tlx3* but not the *Tlx1* enhancer (see Fig. 4-6 model).

Discussion

The current understanding of the transcriptional network that controls the balance of the dI4/dILA GABAergic versus dI5/dILB glutamatergic neurons in the dorsal neural tube has Ptf1a, along with another bHLH factor Ascl1, acting upstream of HD factors such as Pax2 and Lbx1 important in GABAergic lineages, and Tlx1 and Tlx3 important in specifying glutamatergic lineages (Batista and Lewis, 2008; Brohl et al., 2008; Cheng et al., 2004; Cheng et al., 2005; Glasgow et al., 2005; Helms et al., 2005; Mizuguchi et al., 2006; Wildner et al., 2006). Utilizing in ovo chick electroporation, *in vivo* ChIP-

Seq, and biochemical assays, I identify Prdm13 as a direct target of Ptf1a and uncover a mechanism for how Ptf1a induces one cell fate while suppresses the other.

Mechanisms of Prdm13 action in neuronal specification

The PRDM family of factors is interesting in the variety of mechanisms they reportedly use to regulate transcription (for review Fog et al., 2012; Hohenauer and Moore, 2012). Zinc finger domains in other PRDM factors have been shown to be involved in a variety of activities including DNA binding, protein-protein interaction, intrinsic HMT activity, and recruitment of other histone-modifying protiens (Fog et al., 2012; Hohenauer and Moore, 2012). Prdm1, 3, 5, 9, and 14 can directly bind DNA (Fog et al., 2012). In contrast, Prdm8, which shows the highest similarity to Prdm13, does not directly bind DNA but rather binds chromatin in a complex with Bhlhb5 (Ross et al., 2012). Results from Prdm13 ChIP indicate it localizes with chromatin, but like Prdm8, it may do so indirectly. This is supported by three findings in our data. First, for efficient ChIP, a long-arm cross-linker compound treatment, ethylene glycol-bis (succinimidyl succinate) (Zeng et al., 2006) was required. Second, no zinc finger type binding motif was identified from the ChIP-Seq results in regions bound by Prdm13 (data not shown). And most importantly, we provide evidence for Prdm13 interacting with Ascl1 to repress Ascl1 target genes (Fig. 4-5). These results do not exclude the possibility that Prdm13 also binds DNA directly, and this may be the mechanism for repressing Tlx1 (Fig. 4-6 model). Indeed, Prdm13 contains two zinc fingers not present in Prdm8, and a linker (TGYKP) between zinc fingers 2 and 3 in Prdm13 is similar to the canonical zinc finger DNA binding linker TGEKP (Dovat et al., 2002; Wolfe et al., 2000). Thus, Prdm13 may repress its targets by direct and indirect binding to DNA.

I demonstrate here that Prdm13 is a key factor in ensuring that glutamatergic lineage genes are silenced during generation of GABAergic neurons. Prdm13 suppresses the glutamatergic lineage and induces the GABAergic lineage through transcriptional repression of the glutamatergic specifier factors Tlx1 and Tlx3 (Fig. 4-6). This is supported by: First, ectopically expressed Prdm13 reduces the number of

Tlx1/3^{+} cells in the dorsal neural tube (Fig. 3-2). Second, Prdm13 functions as a transcriptional repressor (Fig. 4-3). Third, Prdm13 occupies genomic regions near both the *Tlx1* and *Tlx3* genes in sequence conserved across mammalian species (Fig. 4-4). Finally, Prdm13 bound *Tlx1* and *Tlx3* regions have enhancer activity that was blocked by ectopic Prdm13 (Fig. 4-5D,J). Since Prdm13 was not localized to the *Pax2*, *Lhx1/5*, or *Lbx1* genes (Fig. 4-4 and data not shown), and Prdm13 is acting as a transcriptional repressor, the increase in expression of these GABAergic lineage genes upon overexpression of Prdm13 is likely indirect. Indeed, induction of Pax2 can be explained by Prdm13's direct suppression of Tlx1 and Tlx3, known to block Lbx1 induction of Pax2 as mentioned above (Cheng et al., 2005) (see Model Fig. 4-6).

Switching Ascl1 from transcriptional activator to repressor

Ascl1 was the first mammalian proneural bHLH factor identified (Johnson et al., 1990). Over the last two decades it has been shown to be essential in the development of multiple neural and neuroendocrine lineages, particularly during early stages of differentiation from progenitors (Bertrand et al., 2002). Most recently it was identified as an essential component of a transcription factor cocktail that can directly reprogram or transdifferentiate fibroblasts to neurons (Yang et al., 2011). At a mechanistic level, Ascl1 heterodimerizes with E-proteins (such as Heb and E2a), binds DNA, and activates transcription (Johnson et al., 1992). Interactions with the global co-activator p300, a histone acetyltransferase, have been reported (Yamamoto et al., 2001). My current findings suggest Ascl1 makes a repressor complex with Prdm13, switching Ascl1 from an activator to a repressor with respect to the glutamatergic specifier gene *Tlx3*.

Multiple lines of evidence support this model (Fig. 4-6). First, Ascl1 and Prdm13 localize to the same genomic location upstream of the *Tlx3* gene. Intriguingly, only near the binding site of Tlx3 locus but not the Tlx1 locus, indicating different mechanisms may be used by Prdm13 to repress glutamatergic genes. Second, Ascl1 and Prdm13 co-immunoprecipitate, revealing a specific interaction, since binding to random proteins, such as RGS16 (data not shown) or Hook3 (Fig. 4-4H), was not detected. Interestingly,

different domains of Prdm13 seem to have preferential interaction with Ascl1. The PR and Z1 truncated Prdm13 interacts stronger than the Z234 (data not shown). Indeed, Z1 (truncated Prdm13) could partially inhibit Ascl1 to induce Tlx1/3, and also disrupts Ascl1 function to stimulate differentiation (Fig. 4-2F-F'',K,L). However, since the PR domain itself did not repress Ascl1 activity, while Z234 (466Z234) does (Fig. 4-2K,L), there is still more to learn about these interactions. A last line of evidence supporting the model in Fig. 4-6 has Ascl1 inducing expression of the Tlx1 and Tlx3 enhancer reporters, activities repressed by Prdm13. Noticeably, the induction of GFP signals were extremely strong when Ascl1 was co-expressed with the *eTlx3::GF*P reporter; consistent with a direct regulation by Ascl1 through this cis-element. Indeed, results from EMSA (electrophoretic mobility shift assay) demonstrated direct interaction of Ascl1 to a double E-box located within this region (AGCAGGTGCCAGCTGTA) (data not shown). However, we did not observe any super shift when Prdm13 was also added in this assay (data not shown), a finding that would have strengthened the model. In contrast to the *eTlx3::GF*P reporter, the *eTlx1::GF*P reporter expressed a weaker GFP signal even with the expression of Ascl1, consistent with an indirect induction by Ascl1 (Fig. 4-4).

Thus, via direct interactions with Ascl1, Prdm13 is instrumental to silencing the gene program for the glutamatergic fate as cells progress towards the GABAergic neuronal lineage in the dorsal spinal cord. Combining Ascl1 with factors such as Prdm13 and/or Ptf1a may direct the reprogramming of fibroblasts to specific types of neurons. In summary, PRDM factors utilize diverse mechanisms to modulate transcription, and broadly function in progenitor populations to control lineage decisions. This study places Prdm13, a zinc finger transcription factor, in a critical role connecting the neuronal specification functions of bHLH and HD factors, and highlights the importance of silencing transcription of gene programs in the opposing lineage.

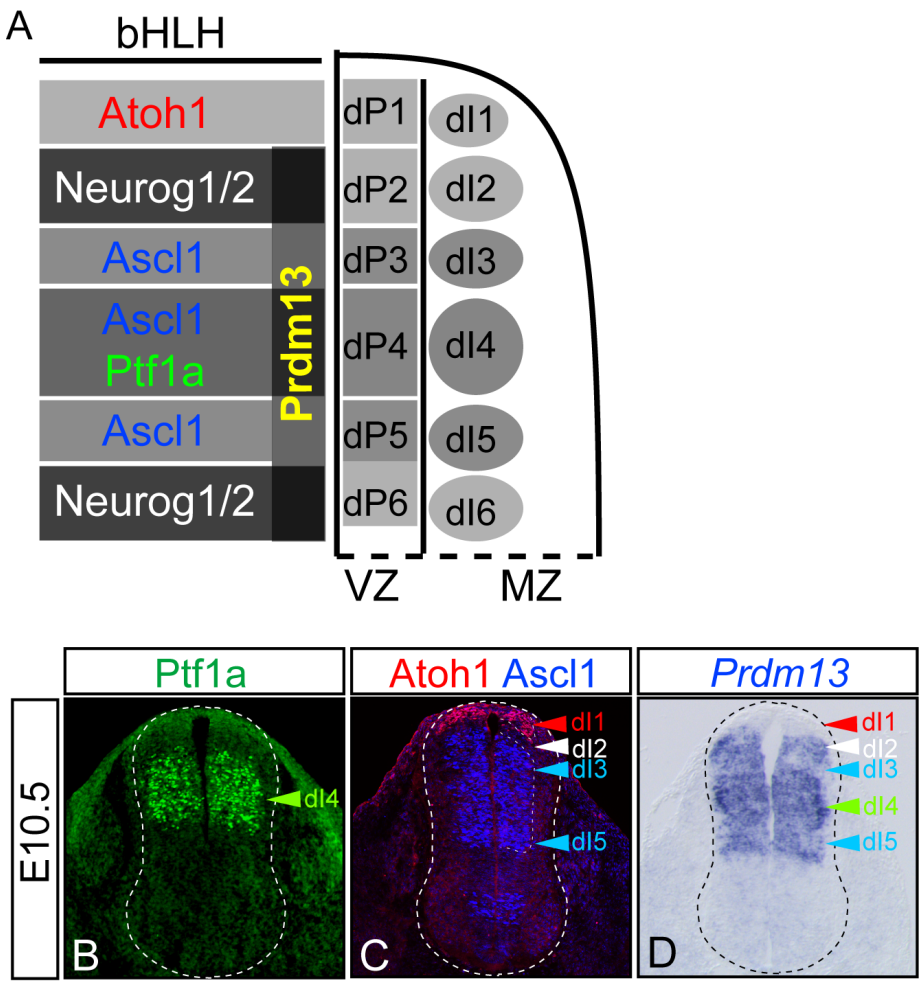

Figure 4-1. Prdm13 and Ascl1 are present in overlapping.

(A) Diagram showing the expression pattern of bHLH and Prdm13 transcription factors in the dorsal spinal neural tube.
(B-D) Immunostaining of Ptf1a (B), Ascl1 (C), and *in situ* hybridization of *Prdm13* (D) on the same mouse embryo but adjacent sections of spinal cord at E10.5 demonstrate their expression patterns. The bHLH transcription factor Ascl1, is expressed from dP3 to dP5 (C, dashed bracket, blue arrows), whereas Ptf1a is restricted in the dP4 domain (B, green arrow). Prdm13 is expressed from dI2 to dI6, and its expression level is enriched in dI2, dI4, and dI6 domains (D).

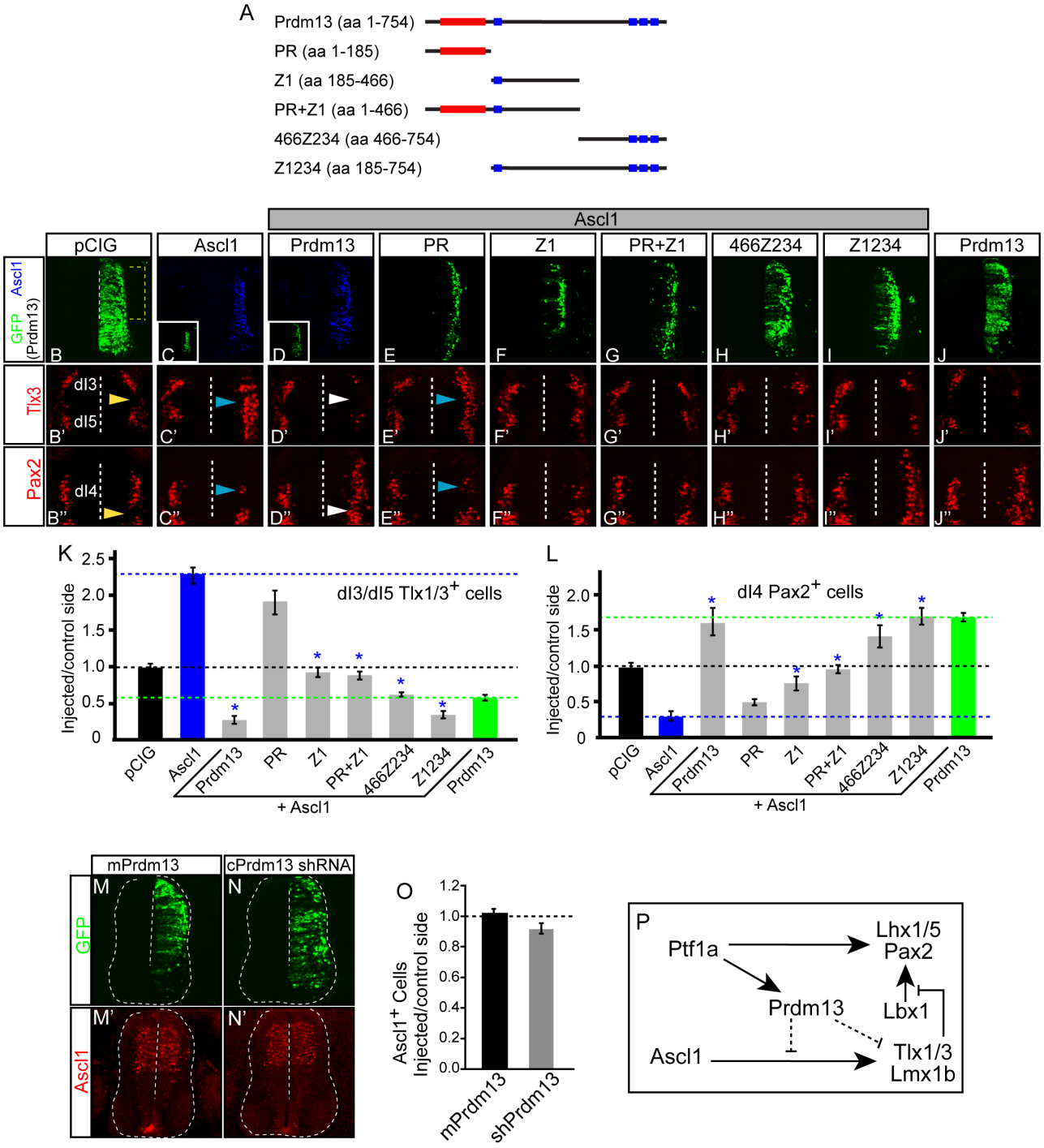
A
Prdm13 (aa 1-754)
PR (aa 1-185)
Z1 (aa 185-466)
PR+Z1 (aa 1-466)
466Z234 (aa 466-754)
Z1234 (aa 185-754)
Ascl1
pCIG
Ascl1
Prdm13
PR
Z1
PR+Z1
466Z234
Z1234
Prdm13
GFP (Prdm13) Ascl1
Tlx3
Pax2
dI3
dI5
dI4
K
dI3/dI5 Tlx1/3+ cells
Injected/control side
+ Ascl1
L
dI4 Pax2+ cells
mPrdm13
cPrdm13 shRNA
GFP
Ascl1
O
Ascl1+ Cells Injected/control side
mPrdm13
shPrdm13
P
Ptf1a
Lhx1/5
Pax2
Prdm13
Lbx1
Ascl1
Tlx1/3
Lmx1b

Figure 4-2. Prdm13 blocks Ascl1 activity through repression an activity requiring its Zinc fingers.

(A) Diagram of the Prdm13 mutations tested. PR domain (red boxes) and Zn finger domains (blue boxes) are indicated.
(B-J) Stage HH12-13 chick embryos were electroporated with empty pCIG vector (B), Ascl1 (C), Prdm13 (J), or Ascl1 plus Prdm13 and the mutated Prdm13 (D-I). Transverse sections through stage HH24-25 are shown with the electroporated side on the right. Ascl1 immunofluorescence detects the ectopically expressed protein (blue) and Prdm13 is indicated by the GFP signal. Dashed lines indicate location of the ventricle. Insets: GFP shows electroporation efficiency.
(B'-J', K) Dorsal neural tube sections from (B-J) show Tlx1/3 defining the dI3 and dI5 neuronal populations. Ectopic Ascl1 causes a dramatic increase in the number of $Tlx1/3^{+}$ neurons relative to control, whereas addition of Prdm13 reverses this phenotype and decreases the number of dI3/dI5 neurons. The ability of Prdm13 to block this activity of Ascl1 requires either the first zinc finger domain (F') or the last three zinc finger domains (H'). The Z1234 mutated Prdm13 is sufficient to function as the full length Prdm13 (I'). Data is quantitatively shown in (K).
(B"-J",L) Dorsal neural tube sections from from (B-J) show Pax2 defining the dI4 neurons. Ectopic Ascl1 causes a dramatic decrease in the number of these neurons relative to control, whereas addition of Prdm13 reverses this phenotype and increases the number of dI4 neurons. The ability of Prdm13 to block this activity of Ascl1 requires the last three zinc finger domains (Z234, H'', I''). The Z1234 mutated Prdm13 is sufficient to function as the full length Prdm13 (I''). Data is quantitatively shown in (L).
(K, L) The black dashed line indicates the control ratio of injected/control side of 1. The blue dashed line indicates the phenotype of the Ascl1. The green dashed line indicates the phenotype of the full-length Prdm13. More than 6 embryos were quantified for each condition and error bars are reported as standard error of the mean. Asterisks indicate significance with p-values<0.001.
(M-O) Endogenous Ascl1 expression is not altered when Prdm13 is either overexpressed (M') or knocked down (N') in chick neural tubes. (O) The number of $Ascl1^{+}$ cells does not change with manipulation of Prdm13 expression. p-value<0.001.
(P) Diagram summarizing the conclusion that Prdm13 antagonizes Ascl1 neuronal subtype specification activity.

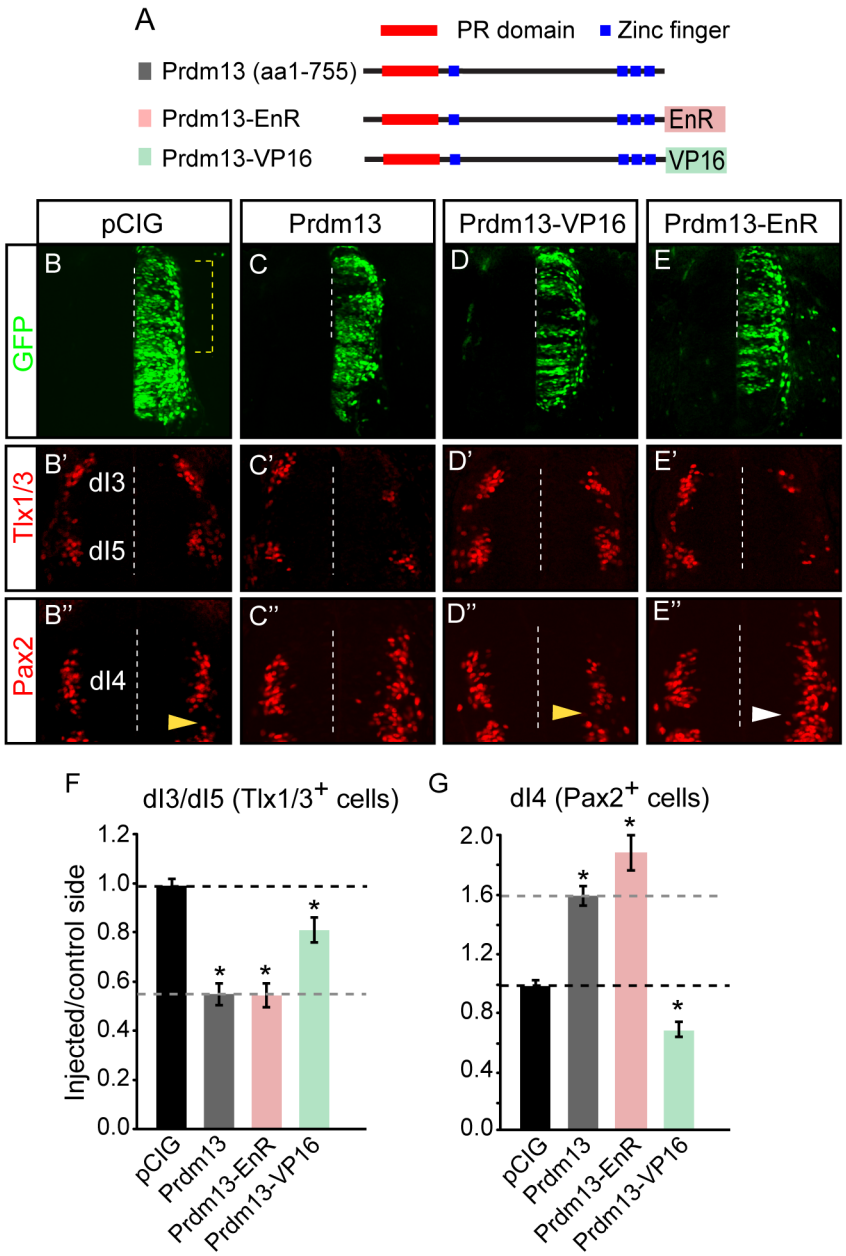

Figure 4-3. Prdm13 functions as a transcriptional repressor.

(A) Diagram of the Engrailed repressor (EnR) or activator VP16 that were fused in frame at the C-terminal end of Prdm13. EnR (pink boxes) and VP16 (green boxes) are indicated.
Stage HH12-13 chick embryos were electroporated with empty vector (control), Prdm13, and EnR or VP16 fused Prdm13. Transverse sections through stage HH24-25 are shown with the electroporated side on the right.
(B-E) GFP (green) shows electroporation efficiency along the dorsoventral axis. Dashed bracket in (B-E) is the region of the neural tube shown in (B'-E'').

(B'-E', F) Dorsal neural tube sections from (B-E) indicate the dI3 and dI5 neuronal populations marked by Tlx1/3. Dashed vertical line indicates the ventricle. (F) is the ratio of $Tlx1/3^+$ neurons on the electroporated side versus the control side showing that the Prdm13-EnR fusion mimics the Prdm13 phenotype to suppress Tlx1/3 (E'), whereas the Prdm13-VP16 does not (D').
(B"-E", G) Dorsal neural tube sections from (B-E) showing the dI4 neuronal population marked by Pax2. (G) is the ratio of $Pax2^+$ neurons above dI6 on the electroporated side versus the control side showing the Prdm13-EnR fusion mimics the Prdm13 phenotype to induce PAx2 (E"), whereas the Prdm13-VP16 does not, instead, it suppresses Pax2 (D''). Note that ectopic $Pax2^+$ cells (E'', white arrowheads) are found in the dI5 domain not normally expressing Pax2 (yellow arrowhead).

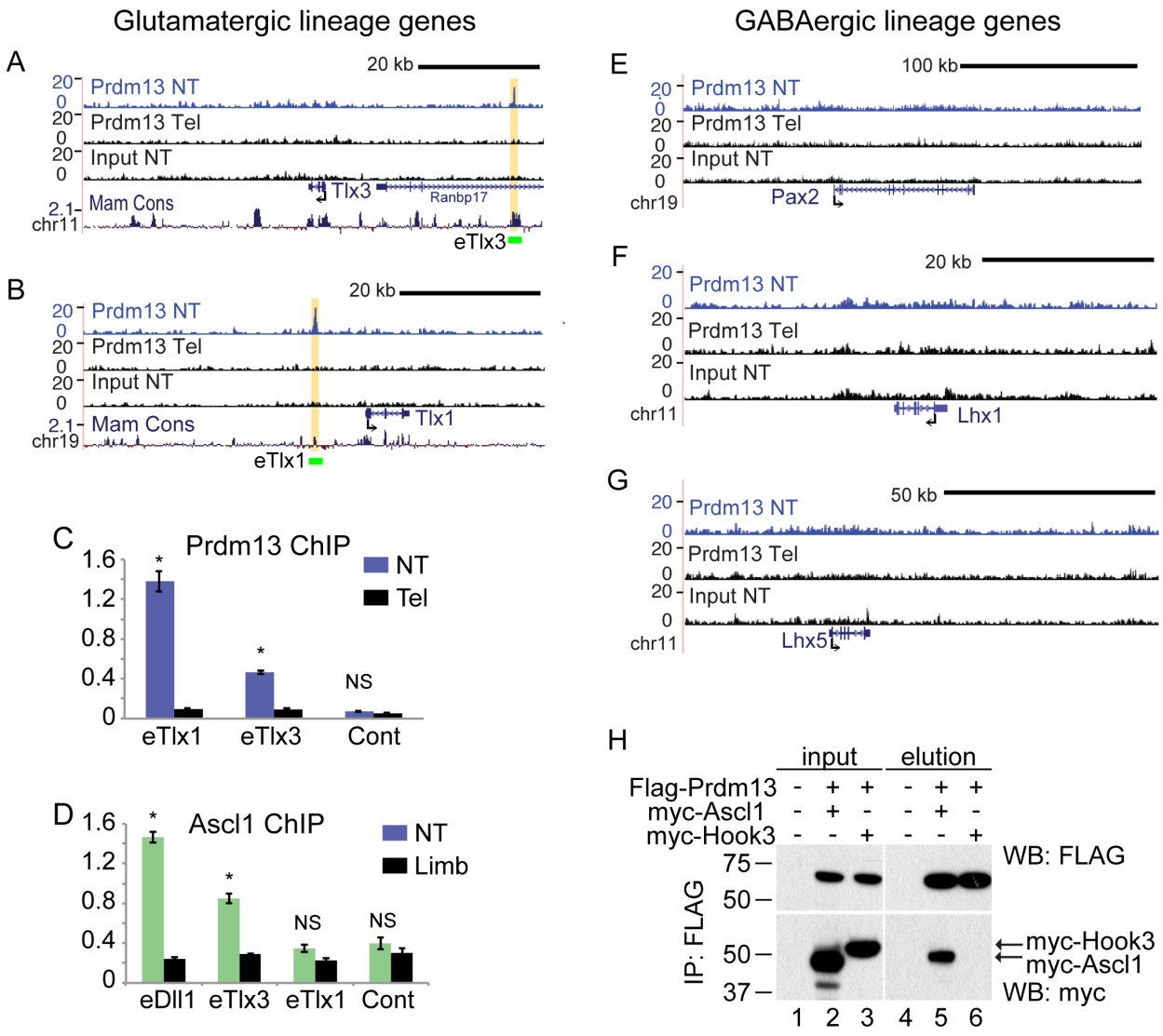

Figure 4-4. Prdm13 interacts with specific cis-elements of Tlx1 and Tlx3 with or without Ascl1.

UCSC Genome Browser showing mouse genomic regions surrounding glutamatergic lineage genes as *Tlx3* (A)**,** *and Tlx1* (B); and GABAergic lineage genes as *Pax2* (E), *Lhx1* (F), and *Lhx5* (G), including Prdm13 ChIP-seq data from neural tube (NT, blue), and two negative controls including Prdm13 ChIP-seq from telencephalon (Tel) and input from NT, all from E11.5 mouse embryos. Prdm13 occupies chromatin near the *Tlx1* and *Tlx3* genes at sequence conserved across mammals (yellow highlight), but no potential binding region near *Pax2* (E), *Lhx1* (F), or *Lhx5* (G). Green bars labeled *eTlx1* and *eTlx3* are the regions used in the GFP reporter constructs in (Fig. 4-5).
(C) ChIP-qPCR validating Prdm13 ChIP-seq data at the *eTlx1* and *eTlx3* loci in (A and B). Tel tissue is negative for Prdm13 and serves as a control for specificity of the antibody in this assay.
(D) ChIP-qPCR for Ascl1 at the *eTlx1* and *eTlx3* loci in (A and B). Limb tissue is negative for Ascl1 and serves as a control for specificity of the antibody in this assay. *eDll1* is a known target of Ascl1.
(H) Co-IP experiments of epitope tagged versions of the proteins transfected into HEK 293 cells indicate specific interaction between Ascl1 and Prdm13 (lane 5), but not the negative control, myc-Hook3 (lane 6).

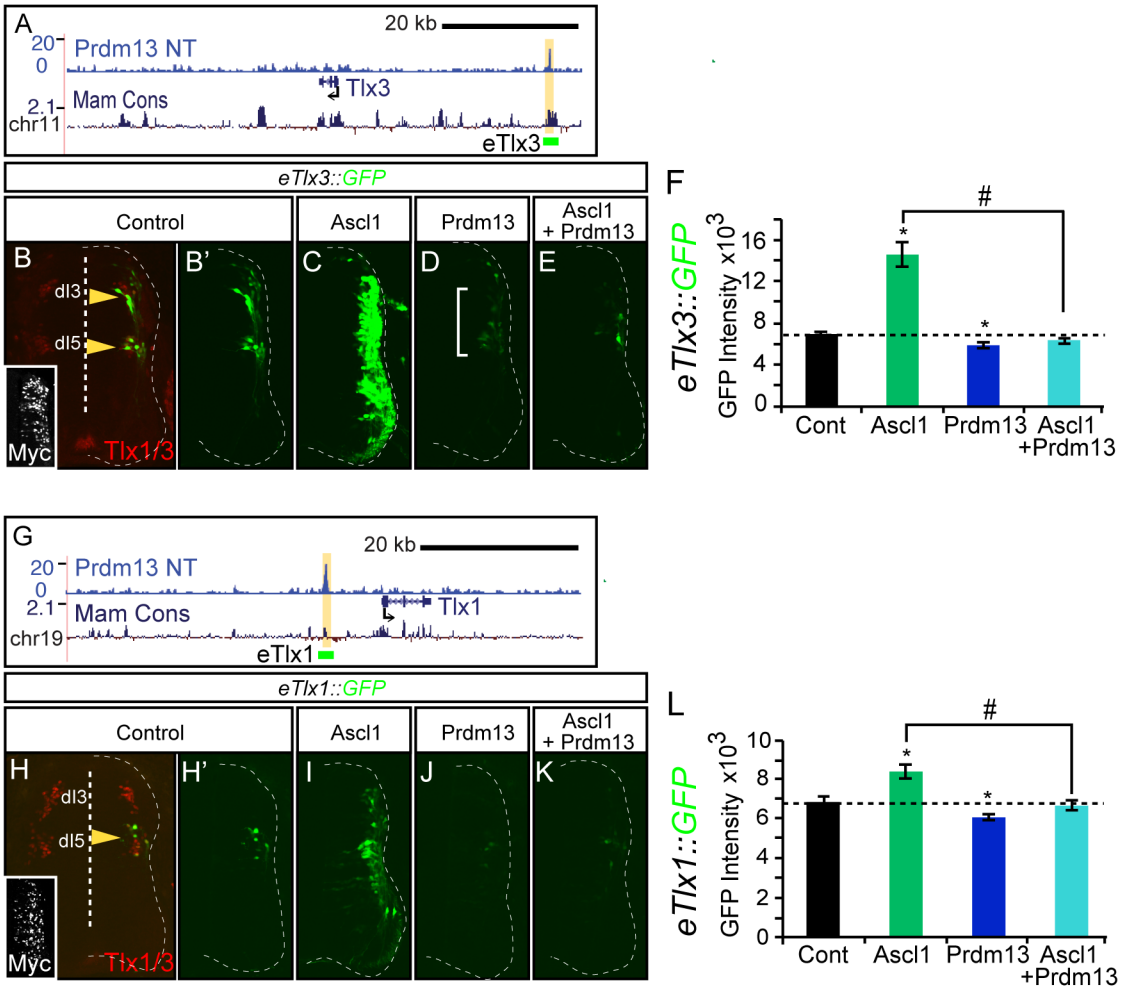

Figure 4-5. Prdm13 directly suppresses Tlx1 and Tlx3 through multiple mechanisms.

Chick neural tube electroporated with either *eTlx3*::GFP (A) or *eTlx1*::GFP (G) reporter and expression vectors for Ascl1 (C, I), Prdm13 (D, J), or both (E, K) as indicated. Only the electroporated side is shown and the neural tube is outlined with a dashed line. (B) The *eTlx3*::GFP signals are restricted and co-localized with dI3/dI5 markers, Tlx1/3 (yellow arrowheads). (C, F) Ascl1 dramatically induces *eTlx3::GFP* and this is blocked by Prdm13 (E, F). (H) The *eTlx1*::GFP signals are restricted to dI5 neurons (yellow arrowhead). (I, L) Induction by Ascl1 is more subtle than that seen with *eTlx3::GFP* but Prdm13 is still repressive (K, L). Inset: myc immunofluorescence indicates the electroporation efficiency. (F and L) shows the quantification of these data by measuring pixel intensity. Asterisk and # indicate a p-value<0.001 relative to control or between samples indicated.

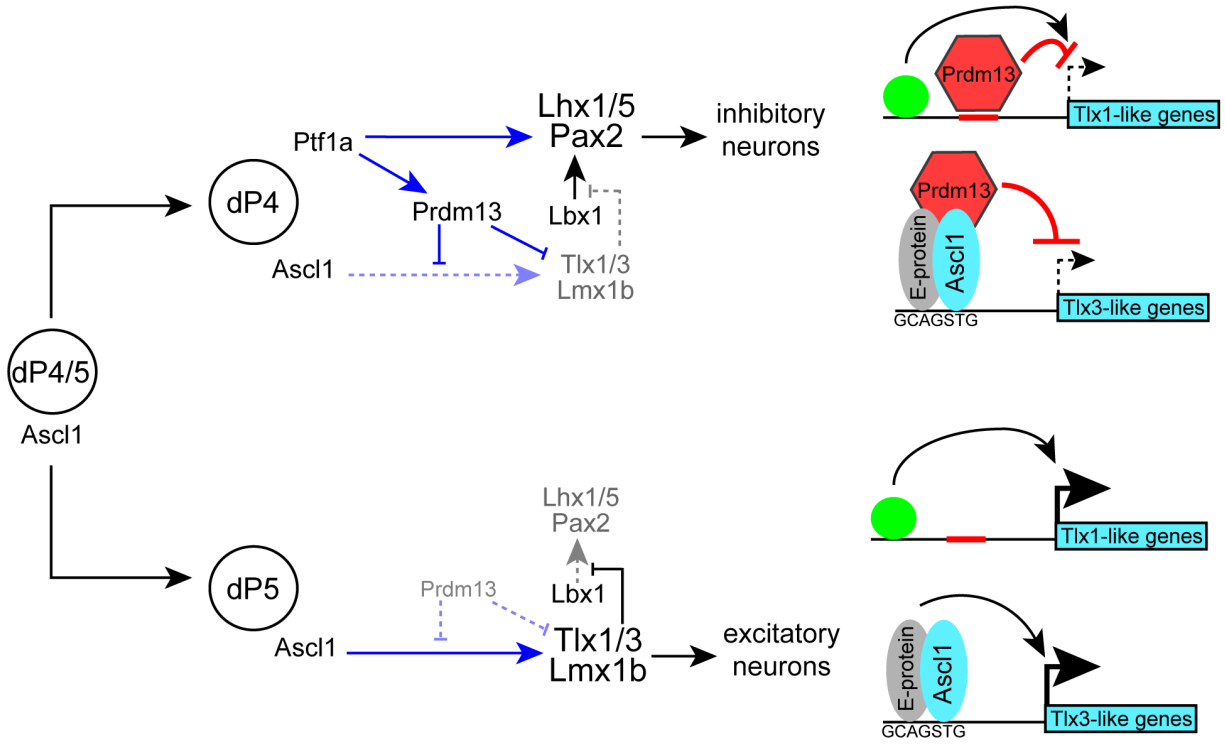

Figure 4-6. Transcriptional network controlling the balance of inhibitory and excitatory neurons in the dorsal spinal cord.

Progenitors in the ventricular zone express Ascl1. In the absence of Ptf1a, these cells become excitatory neurons (dP5 lineage) through Ascl1 induction of the HD factors Tlx1/3 and Lmx1b. Tlx1/3 repress the Lbx1-dependent induction of Pax2 and the inhibitory neuronal program. Ascl1 regulates *Tlx3* directly whereas *Tlx1* may be indirect. Ptf1a is upregulated in a subset of the Ascl1 progenitor cells directing their fate to inhibitory neurons (dP4 lineage) through induction the HD factors Pax2 and Lhx1/5. Additionally, Ptf1a directly increases levels of Prdm13 that in turn suppresses Tlx1 and Tlx3, ensuring a suppression of the glutamatergic program in the inhibitory neurons. Prdm13 works through at least two mechanisms; one being Ascl1-dependent involving a novel transcriptional repressor complex for *Tlx3*-like genes, and the other Ascl1-independent requiring some other activator (green circle) for *Tlx1*-like genes.

CHAPTER FIVE

Summary and Future direction

I. Conclusion and future direction

In my dissertation I have identified the mechanism by which a zinc finger transcription factor can repress the glutamatergic gene program in GABAergic neurons. In this study, I 1) identify a chromatin-remodeling transcription factor, Prdm13, as a direct downstream target of Ptf1a, 2) present the first functional data for Prdm13 as a regulator of the balance of inhibitory and excitatory neurons in the dorsal spinal cord, 3) identify Prdm13 as a direct repressor through specific cis-elements to suppress homeodomain factors *Tlx1* and *Tlx3* that specify the glutatmatergic fate, and 4) identify a mechanism for the repression through novel interactions with the bHLH factor Ascl1 providing, the first evidence for switching Ascl1 from activator to repressor. Thus, Prdm13 provides the missing link between the essential activities of the bHLH factors and the downstream homeodomain factors in neuronal sub-type specification. Given the importance of Ptf1a and Ascl1 in neural development, neural cancers, and for reprogramming somatic cells to neurons, understanding how Prdm13 cooperates with these factors provides a broader and deeper understanding not only in fundamentals of development biology, but also in several health issues, specifically stem cell research and cancer investigation.

a. Additional functions of Prdm13 in the dorsal spinal cord

The results of *Prdm13* in situ hybridization in the spinal cord revealed that the high *Prdm13* expression in the lateral cells is Ptf1a-dependent; it is expressed in the Ptf1a domain and it is lost in the *Ptf1a* mutant. However, *Prdm13* has some expression that is Ptf1a-independent, and this expression

comes on prior to Ptf1a expression. The Prdm13 expression stays on in the VZ till E13.5. These observations indicate a potential functional contribution of Prdm13, whereby it not only regulates the neuronal specification, but also might be involved in early neuronal proliferation and differentiation. Some of the PRDM members have shown important functions in regulating the proliferation and differentiation of progenitors. For example, Prdm1 represses c-myc transcription, which is consistent with the role of Prdm1 as a master regulator in B-cell (BCL, B-cell lymphoma cell) terminal differentiation (Yu et al., 2000). Both Prdm3 and Prdm16 play a critical role in a network that contains negative and positive feedback loops and integrates HSC renewal, quiescence, apoptosis, and differentiation of the hematopoietic stems cells (HSCs) (Aguilo et al., 2011; Chuikov et al.; Goyama et al., 2008; Zhang et al., 2011). Prdm6 functions as an epigenetic regulator of smooth muscle cells (SMC) phenotypic plasticity by suppressing differentiation and maintaining the proliferative potential of vascular SMCs via modulating local chromatin-remodeling activity (Davis et al., 2006; Wu et al., 2008).

Indeed, when Prdm13 is overexpressed in the chick neural tube, ectopic S-phase cells labeled by BrdU are found in the MZ. There are approximately 35 more $BrdU^+$ cells in the MZ when compared to the control side or the empty pCIG vector (Fig. 5-2A-C). However, the number of $BrdU^+$ cells in the VZ is not affected (Fig. 5-2A,B,D). Interestingly, a hint that Prdm13 may also function in neuronal proliferation and differentiation was seen when Prdm13 was co-expressed with Ascl1, as it disrupted Ascl1's ability to drive neuronal differentiation. Thus, Prdm13 may function to modulate Ascl1 activity (and other bHLH factors) in their role in neuronal differentiation as well as their role in controlling cell fate decisions in the dorsal spinal cord. A potential functional contribution of Prdm13 in regulating neuronal proliferation and differentiation needs to be further investigated.

Another interesting question in regards to the function of Prdm13 is whether it is also involved in specification of other interneurons in the dorsal spinal cord. The dorsal/ventral boundaries of Prdm13 look to match with progenitors from dI2 to dI6, and the programming that gives rise to dI2 and dI6 is not affected in the *Ptf1a* mutant. Furthermore, the mRNA expression levels of Prdm13 are not only enriched

in the dI4, but also highly expressed in the dI2 and dI6. Thus, it is possible that Prdm13 also regulates the other populations. Indeed, I did notice that the number of dI2 interneurons (defined by $Lhx1/5^{+}$; $Pax2^{-}$ cells) is decreased when Prdm13 is overexpressed in the chick neural tube, and in the Prdm13 knockdown there is a slight increase of dI2 interneurons that was not statistically significant (data not shown). These preliminary results suggest that Prdm13 not only suppresses the dI3 and dI5 neuronal cell fate, but also suppresses other populations of interneurons. Both the possible role of Prdm13 in neuronal differentiation and in specification of additional dorsal interneurons will be addressed in the future when a Prdm13 null mouse is generated.

b. Electrical activity modulates the excitatory/inhibitory balance in the spinal cord

One open question in the field is how levels of the neuronal specifying transcription factors are regulated. For example, relevant to studies here, how are Ptf1a levels regulated in the first place to parse out those cells that will become GABAergic. Recently, insight into this question of how neuronal specifying factors are regulated has come from studies in Xenopus, where electrical activity has been shown to play a critical role in neuronal specification early in neuronal development (Spitzer, 2006). In the developing Xenopus neural tube, spinal neurons spontaneously generate patterned Ca^{2+} spike activity, and these spikes are created by the Ca^{2+}-dependent action potentials that trigger Ca^{2+} release in a temporary developmental period (Gu et al., 1994). Altering the electrical activity by changing the patterns of Ca^{2+} spike activity is necessary and sufficient to modify neurotransmitter expression via intracellular signaling cascades during development (Spitzer et al., 2004). When electrical activity is experimentally decreased by modulating the inward rectifying potassium channel (Kir2.1) overexpression or by the local administration of Ca^{2+} or Na^{+} channel blockers, excitatory neurotransmitter expression such as glutamate increases, while inhibitory neurotransmitter expression such as GABA decreases. When electrical activity is increased by Na^{+} channel overexpression, the authors observed the reverse, a decrease in glutamate expression and an increase in GABA expression in the embryonic spinal cord of Xenopus (Borodinsky et al., 2004). They demonstrated that the Ca^{2+} fluxes are acting through a mechanism including

phosphorylation of cJun that represses transcription of Tlx3, a transcription factor critical for the specification of glutamatergic lineage (Marek et al., 2010). Indeed, I confirmed some of this model in the chick neural tube. When I ectopically expressed Kir2.1 in the chick spinal cord, a decrease of Ptf1a, Pax2, and GAD1 were observed in the electroporated side, but not the control side or with the mutated Kir2.1 as an additional control (data not shown). In contrast, there is a significant increase of *vGlut2* mRNA level. Since Ptf1a, Pax2, and GAD1 are markers for the GABAergic lineage, these results support the model that suppressing the electrical activity will shift the generation of glutamatergic over GABAergic neurons. In order to establish a balanced excitatory versus inhibitory neuronal population, the electrical activity-dependent mechanism regulates the neuronal cell fate decision in this homeostatic paradigm during neuronal development. In summary, not only the genetic components, but also modulation of neuronal development by earlier forms of activity is required to switch the phenotype of developing neurons at critical decision points. Thus, further study to identify the targets of electrical activity-dependent factors, possibly through regulation of Ptf1a levels, is important to understand the precise equilibrium of E/I balance during neuronal development.

c. Additional functional contributions of Prdm13 in CNS

Ptf1a not only functions in specifying the excitatory/inhibitory balance in the dorsal spinal cord, but it also controls the balance of GABAergic interneurons including Purkinje, stellate, basket, and Golgi cells with that of the glutamatergic granule cells in the cerebellum (Hoshino et al., 2005; Pascual et al., 2007). In addition, Ptf1a specifies the GABAergic and glycinergic horizontal cells and the majority of amacrine cell subtypes during retinogenesis (Dullin et al., 2007; Fujitani et al., 2006; Lelievre et al., 2011; Nakhai et al., 2007). Since Prdm13 is also expressed in these same regions, it is likely that Prdm13 also functions in these regions. In *Ptf1a* mutants, *Prdm13* is dramatically attenuated in these other domains as well. Therefore, similar to the functional contribution of Prdm13 in the dorsal spinal cord, where it suppresses the glutamatergic lineage genes and indirectly induces the GABAergic interneurons, Prdm13 may also mediate the neuronal cell fate decisions seen in the retina and cerebellum with Ptf1a.

Interestingly, in the retina, another PRDM family member, Prdm1 (Blimp1), functions to regulate cell fate decisions by specifying the photoreceptor fate over bipolar cell fate through suppressing Chx10, a HD factor required for the formation of bipolar cells (Brzezinski et al., 2010; Katoh et al., 2010). Thus, the retina may use multiple PRDM factors to generate the diversity of neurons found in this tissue. Here again the role of Prdm13 in these other regions of the nervous system will be addressed in the future when a Prdm13 null mouse is generated.

II. Possible problems and alternative strategies

a. What are the required cis-elements for regulating Prdm13 expression?

We know that Prdm13 is critical for regulating the neuronal specification in the spinal cord, but the trans-acting elements that regulate the expression of Prdm13 remain unclear. From the reporter assay, 2 of 5 enhancer regions of Prdm13 were shown to contain activity to drive reporter expression in chick neural tube (Peak 4 and 5). In the dorsal neural tube, Peak 4 mainly drives the expression in dI2, dI6, and a few cells in dI4; whereas Peak 5 drives the expression broadly throughout the dorsal part of neural tube. Interestingly, although the Peak 4 enhancer gives a similar expression as the endogenous Prdm13 expression pattern, there is no consensus PTF1 binding site found within this region. Furthermore, the co-expression of Ptf1a and these enhancer regions (Peak 4 and 5) does not increase the expression of the reporter (data not shown). Thus, these cis-elements were not sufficient for Ptf1a to drive the expression of *Prdm13* in the spinal cord, suggesting additional trans-elements might be involved in the transcriptional regulation through these cis-elements, and additional binding regions might exist for Ptf1a to interact for regulating Prdm13 transcriptional activity. Future experiments will need to be pursued to uncover the mechanisms controlling Prdm13 expression. For example, combining different genome wide deep sequencing results, such as ChIP-Seq for additional transcription factors, FAIRE-Seq (Formaldehyde-Assisted Isolation of Regulatory Elements) for open chromatin, and cross-species sequence comparisons could provide insights to address this question. Furthermore, additional mutations in consensus binding

sites within peak 5 followed by reporter assays could identify candidate upstream transcription factors. Together with *in vitro* EMSA experiments; one could identify the transcription factors that directly regulate the expression of Prdm13. These cis-elements could also be used in generating transgenic mice to determine the Prdm13 derived neurons. Thus, there is still much to do to uncover how Prdm13 is regulated and this will be essential for understanding how the E/I balance is mediated during embryonic development.

b. Does Prdm13 directly bind to DNA?

Most of the PRDM family members, such as Prdm1, 3, 5, 9, and 14, were shown to directly interact with DNA through the zinc finger domain (Fog et al., 2012). In contrast, Prdm8, which shows the highest similarity to Prdm13, does not directly bind DNA but rather binds chromatin in a complex with Bhlhb5 (Ross et al., 2012). Results from Prdm13 ChIP indicate it localizes with chromatin, but like Prdm8, it may do so indirectly. This is supported by several findings in my data. First, for efficient ChIP, a long-arm cross-linker compound treatment, EGS, ethylene glycol-bis (succinimidyl succinate) (Zeng et al., 2006) was required. This could reflect indirect interaction with the chromatin, or it could reflect the quality of the antibody for ChIP. Second, no zinc finger type binding motif was identified from the ChIP-Seq results in regions bound by Prdm13 (data not shown). If Prdm13 was a site specific DNA binding factor, one would expect to see enrichment of that site within the regions bound by Prdm13. Third, most of the triple or double zinc finger domains contain a well-conserved linker, TGEKP, in between adjacent zinc fingers, which is required for DNA interaction (Nunez et al., 2011; Wolfe et al., 2000). However, the linker in the second (Z2) and third (Z3) zinc finger domains of Prdm13 is TGYKP, which contains a difference of one amino acid when compared to the classic DNA binding linker. And importantly, I provide evidence for Prdm13 interacting with Ascl1 to repress Ascl1 target genes. These results do not exclude the possibility that Prdm13 also binds DNA directly, and this may be the mechanism for repressing Tlx1. Thus, it is still unclear whether Prdm13 represses its targets by direct and/or indirect binding to DNA.

c. Does Prdm13 recruit other histone modifying proteins for transcriptional regulation?

PRDM factors recruit histone modifying proteins to mediate their function (Fog et al., 2012), including factors as histone methyltransferases (HMTs) and/or histone deacetylases (HDACs). For example, Prdm6 functions as a transcription repressor by recruiting class I HDACs and the G9a, a ubiquitous HMT known to dimethylate histone H3k9 and H3K27 (Davis et al., 2006). Prdm1 interacts with a Lysine-specific demethylase Lsd1 (Kdm1a) forming a repressor complex, and binds to the specific enhancer region of *CIITA* gene to regulate cell differentiation (Su et al., 2009). However, little is known about the co-factors of Prdm13. By using a purified recombinant N-terminus of human Jarid1b (Kdm5b), a lysine-specific demethylase encoded by the *Kdm5b* gene as bait and a human brain cDNA expression library, Prdm13 is identified as one of the interaction proteins of Kdm5b. Therefore, recruiting Kdm5b might be one of the mechanisms used by Prdm13 to regulate transcription. However, there is no further evidence confirming the interaction of Prdm13 and Kdm5b. Moreover, other HMT and HDAC factors might also interact with Prdm13 to form a repressor complex. Thus, Co-IP or pull-down experiments with Kdm5b or other co-factors with Prdm13 will be necessary to understand how Prdm13 represses transcription. In addition, mass spectrometry could be utilized to identify novel interacting proteins if the candidate approach does not lead to interacting factors. Indeed, the Johnson lab is pursuing a strategy generating a GFP-Prdm13 fusion protein by targeting the Prdm13 gene in mouse. This fusion protein will be helpful for future biochemical experiments along these lines. Moreover, the series of mutated Prdm13 expression constructs I generated may be useful to determine what domain of the protein is being used for protein-protein interactions identified. These studies will reveal novel connections between chromatin remodeling factors with bHLH transcription factors important for neuronal subtype determination.

By addressing the regulation and function of Prdm13, I define molecular mechanisms controlling the delicate equilibrium between inhibitory and excitatory neurons for precise integration of sensory input. An imbalance in this neural circuitry may underlie disorders such as hypo- or hyperalgesia, balance and coordination. The possibility that I have identified a novel factor that modulates neuronal diversity in

multiple regions of the nervous system is informative, thus, providing impact for several health issues in stem/progenitor cell research, neurogenesis, and possibly neural cell-derived cancers.

Experimental procedures

The work presented in Figure. 5-1 was performed in collaboration with a graduate student, Yi-Hung Ou, who provided help with Co-immunoprecipitation experiments.

Co-immunoprecipitation

For Co-immunoprecipitating Ptf1a and Prdm13, HEK293T cells were co-transfected with Ptf1a and flag-tagged full length Prdm13 (Flag-Prdm13-FL), or one of two other mutated versions of Prdm13; one contained the PR domain (Flag-Prdm13-PR) and the other contained the four zinc finger domains (Flag-Prdm13-Z1234). Whole cell extracts were prepared in non-denaturing IP buffer (20 mM Tris HCl [pH 7.5], 10 mM $MgCl_2$, 2 mM EGTA, 10% Glycerol, 137 mM NaCl, 1% Triton X-100 (vol/vol), 0.5% Na Deoxycholate, 1 mM DTT, phosphatase and protease inhibitors [Roche]) were incubated with with 30 µl of anti-HA agarose beads (25% slurry, Santa Cruz) or anti-FLAG M2 beads (50% slurry, Sigma) overnight at 4 ˚C. Immunoprecipitates were washed three times in wash buffer (20 mM Tris HCl [pH 7.5], 10 mM $MgCl_2$, 2 mM EGTA, 10% Glycerol, 137 mM NaCl, 1% Triton X-100 (vol/vol), 0.5% Na Deoxycholate, 1 mM DTT, and 1 mM PMSF) then boiled in standard SDS sample buffer. Samples were separated by SDS-PAGE followed by immunoblot analysis.

BrdU labeling and staining

For BrdU labeling, each chick embryo was treated with 100 µl of 5mg/ml BrdU in PBS 2 hours before harvest. Sections were treated with 2 N HCl for 20 minutes, 0.1 M sodium borate (pH 8.5) for 20 minutes and incubated with mouse anti-BrdU antibody. Cell death was detected using rabbit anti-Caspase 3 (Abcam ab2302).

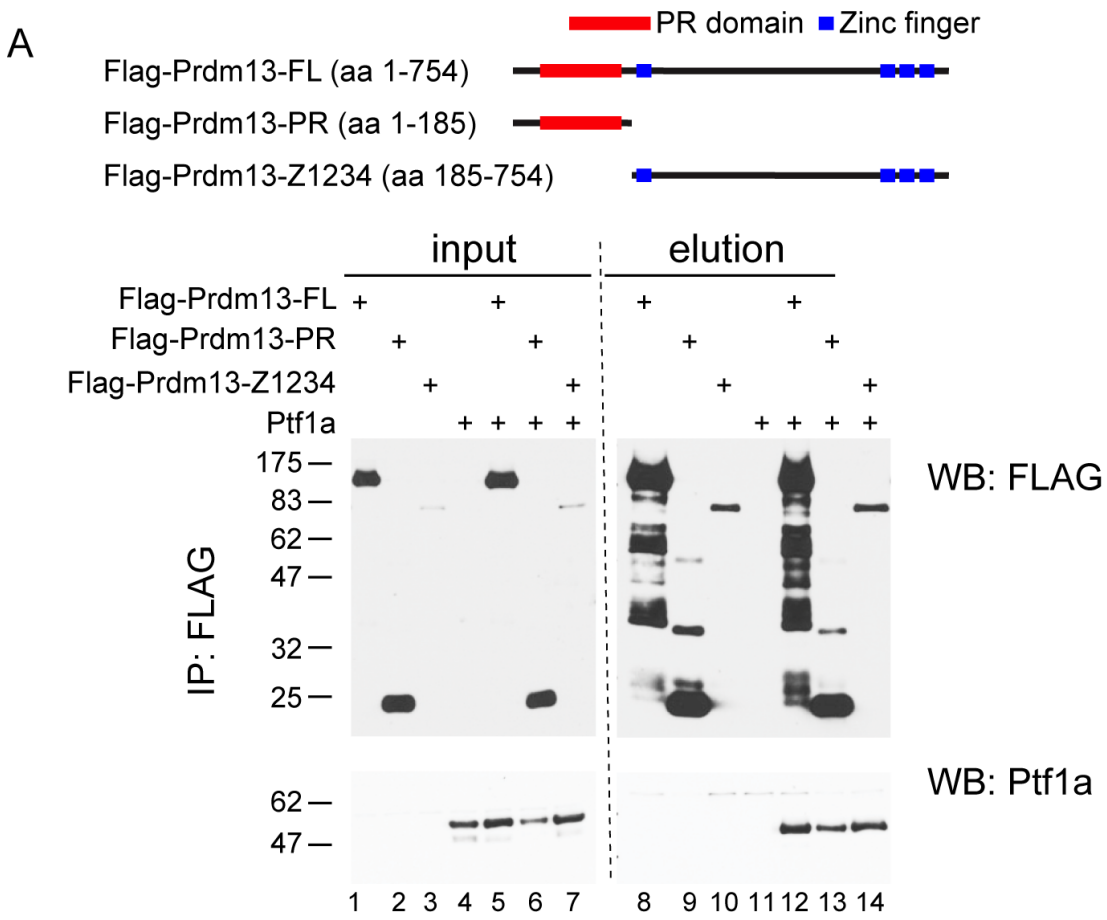

Figure 5-1. Prdm13 interacts with Ptf1a.

(A) Diagram of the flag tagged Prdm13 tested. PR domain (red boxes) and Zn finger domains (blue boxes) are indicated. Co-IP experiments of epitope tagged versions of the proteins transfected into HEK 293 cells indicate specific interaction between Ptf1a and Prdm13 (lane 12). Both of the truncated Prdm13, PR (line 13) and Z1234 (line14), can interact with Ptf1a. (Experiment performed by Yi-Hung Ou)

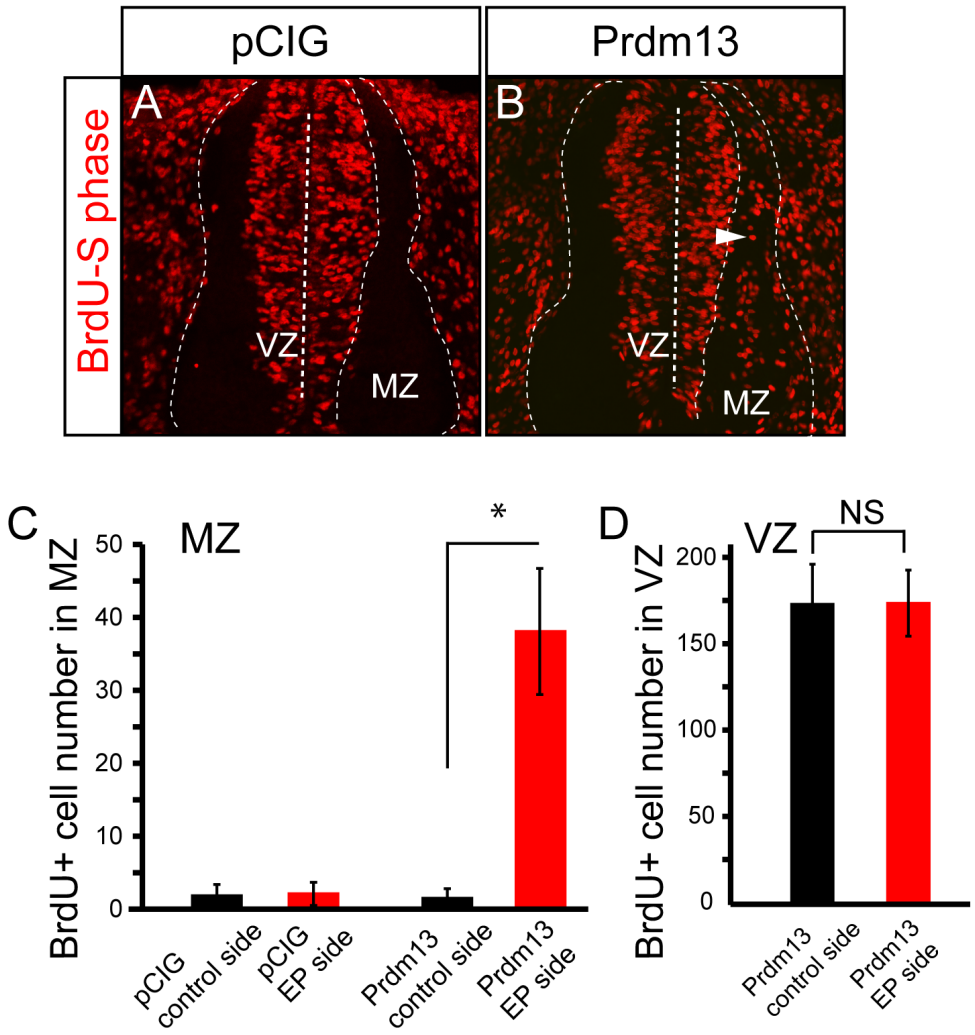

Figure 5-2. Overexpression of Prdm13 causes ectopic S-phase cells in the mantle zone (MZ) in chick neural tube.

Stage HH12-13 chick embryos were electroporated with empty vector (control) or Prdm13. BrdU was added 2 hours before harvest. Transverse sections through stage HH24-25 are shown with the electroporated side on the right.
(A-B) Neural tube sections of chick embryos indicate the proliferating cell (S-phase) marked by BrdU. Dashed lines out line the VZ and MZ in the spinal cord sections. Overexpression of Prdm13 causes ectopic S-phase cells existed in the MZ (B, white arrowhead).
(C-D) The numbers of the $Brdu^{+}$ cells in the MZ were quantified in (C). The numbers of the $Brdu^{+}$ cells from the overexpression of Prdm13 in the VZ were quantified in (D). More than 6 embryos were quantified for each condition. The asterisk indicates p-value<0.001. NS, not significant.

APPENDIX

I. Antibodies used

Name	Source	Use	Dilution		Ref
Ascl1	Johnson Lab generated	IHC	1:10000	guinea pig	(Kim et al., 2008)
Ptf1a	Johnson Lab generated	IHC	1:5000	guinea pig	(Hori et al., 2008)
Pax2	Zymed	IHC	1:1000	rabbit	
Tlx1/3	gift from T. Müller and C. Birchmeier	IHC	1:20,000	rabbit	
Islet1/2	gift from T. Jessell	IHC	1:5000	rabbit	(Tsuchida et al., 1994)
Lmx1b	gift from T. Müller and C. Birchmeier	IHC	1:2000	guinea pig	(Muller et al., 2002)
Lhx1/5	4F2, Developmental Studies Hybridoma Bank	IHC	1:100	mouse	
Brn3a	gift from E. Turner	IHC	1:500	guinea pig	(Quina et al., 2005)
Lbx1	gift from T. Müller and C. Birchmeier	IHC	1:10000	rabbit	
Caspase 3	Abcam ab2302	IHC	1:100	rabbit	
Ptf1a	gift from R. MacDonald	ChIP	2.4	rabbit	(Beres et

			μg/tube reaction		al., 2006)
Rbpj	Johnson lab generated using peptide sequence (CKKK)NSSQVPSNESNTNSE	ChIP	5 μL/tube reaction	rabbit	
Ascl1	BD Pharmigen, 556604	ChIP		mouse	
Prdm13	Johnson lab generated using bacterially expressed full length GST-tagged Prdm13	ChIP	10 μL/tube reaction	rabbit	
BrdU	BD Biosciences, 347580	IHC	1:25	mouse	

II. Chromatin Immunoprecipitation and Sequencing Library Preparation

Ptf1a, Rbpj and Prdm13 ChIPs

Solutions:

Buffer A (15 mM Hepes-Cl 7.6, 60 mM KCl, 15 mM NaCl, 0.2 mM EDTA, 0.2 mM EGTA, 0.34 M sucrose, 1 tab/10 mL Protease inhibitor tablet[a])

Buffer B (15 mM Hepes-Cl 7.6, 60 mM KCl, 15 mM NaCl, 2.1 M sucrose, 1 tab/10 mL Protease inhibitor tablet[a])

Buffer C (15 mM Hepes-Cl 7.6, 60 mM KCl, 15 mM NaCl, 0.34 M sucrose, 2 mM $MgCl_2$, 1 tab/10 mL Protease inhibitor tablet[a])

[a] Roche Complete, Mini cat #11836153001

ChIP sonication Buffer (1% Triton X-100, 0.1% Deoxycholate, 50 mM Tris 8.1, 150 mM NaCl, 5 mM EDTA). Just before use, add protease inhibitor tablet to each 10 ml.

High Salt Wash Buffer (1% Triton X-100, 0.1% Deoxycholate, 50 mM Tris-8.1, 500 mM NaCl, 5 mM EDTA)

LiCl Wash Buffer (250 mM LiCl, 0.5% NP-40, 0.5% Deoxycholate, 10 mM Tris-8.1, 1 mM EDTA)

TE Buffer (10mM Tris, 8.1, 1 mM EDTA)

Protein A/G Plus Agarose (Santa Cruz)

Proteinase K (19 mg/ml, Boehringer Mannheim # 1964372)

Elution Buffer (1% SDS, 0.1 M NaHCO3)

37% Formaldehyde (ACS reagent grade)

1.25 M glycine

ChIP protocol:

Neural tube, telencephalon, and limb tissues from E12.5 mouse embryos were dissected and placed in Buffer A on ice. Nuclei were liberated by dounce homogenization and purified by centrifugation through a sucrose gradient (Buffer A and Buffer B; 1:1). For the Prdm13 ChIP, the nuclei were incubated in 1.5 mM ethylene glycolbis (succinimidyl succinate) a long-arm cross-linker in Buffer C for 20 min at RT, prior to fixation in 1% formaldehyde for 10 minutes at 30 degrees C (Zeng et al., 2006). Fixation was terminated by adding glycine to a final concentration of 0.125M. Chromatin was sheared using a Diagenode Bioruptor for 28 minutes on high power with 30s:30s on:off cycles. 150-200 μg of neural tube or telencephalon/limb chromatin was immunoprecipitated with either 2.4 μg affinity purified rabbit anti-Ptf1a antibody (Beres et al., 2006), 5 μL of rabbit Rbpj antisera (laboratory generated, TX857), or 10 μL of rabbit Prdm13 antisera (laboratory generated, TX970), and 50 μL Protein A/G agarose beads (Santa Cruz). Captured bead:antibody complexes were washed twice with sonication buffer, three times with a high salt buffer, three times with LiCl buffer, and twice with TE buffer. Two 15 minute elutions were performed with 1% SDS, 0.1M $NaHCO_3$, 10mM Tris at room temperature. The immunoprecipitated

chromatin was purified using Qiagen's PCR cleanup kit and re-suspended in 60 μL elution buffer. Prior to sequencing, ChIP quality was determined by qPCR for known targets and negative control regions.

Independent libraries were prepared from neural tube and telencephalon ChIPs according to Illumina's protocol (NEBNext ChIP-Seq Sample Prep Master Mix Set 1). Amplification of the libraries was conducted using Invitrogen's Platinum *Pfx* polymerase for 12 cycles of 94ºC for 15 seconds, 62ºC for 30 seconds, 72ºC for seconds. Single-end sequencing of 36 bp (Ptf1a) or 40 bp (Rbpj) were conducted on the Illumina GAIIx or 50 bp (Prdm13) was conducted on the Illumina HiSeq 2000 sequencer.

Ascl1 ChIP

Solutions:

Fix solution (11% Formaldehyde, 0.1 M NaCL, 1 mM EDTA pH 8.0, 0.05 mM EGTA 8.0, 1 M Hepes 8.0)

10x IP buffer (0.2 M Hepes 8.0, 0.2 M NaCl, 0.02 M EDTA 8.0)

Working IP Buffer (1x IP buffer, 0.1% Trition X-100, 1mg/ml BSA)

Wash Buffer (50 mM Hepes 7.6, 1 mM EDTA 8.0, 1.0% NP-40, 0.7% Deoxycholate, 512 mM LiCl)

Elution buffer (10 mM Tris 8, 1.0% SDS)

ChIP Protocol

E12.5 Neural tube or limb tissue was dissected and placed in cold PBS. Nuclei were liberated by dounce homogenization, 1/10 volume of fixation solution was added to the nuclei for rotated for 10 minutes. Fixation was stopped by adding 1/20 volume of 2.5M glycine (non-buffered), and incubated for 5 minutes at RT. Nuclei were spun at 1.2K rpm at 4 degrees C or at the low speed sufficient to pellet the sample for 5 minutes. The nuclei pellet with rinsed with cold PBS and re-spun at 1.2K rpm at+4C or at the low speed sufficient to pellet the sample for additional 5 minutes. The pellet was then re-suspended in 300ul

of IP buffer. Chromatin was sheared in the IP buffer using a Diagenode Bioruptor for 28 minutes on high power with 30s:30s on:off cycles. 250 μg of neural tube or limb chromatin was immunoprecipitated with 5.0 μg affinity purified mouse anti-Ascl1 (BD Pharmigen) antibody, and 50 μL and Sheep anti-Mouse IgG Dynabeads (Invitrogen) overnight at 4 degrees C. Captured bead:antibody complexes were washed seven times with wash buffer and twice with TE buffer. Chromaton elution was performed by adding 500ul of elution buffer to the bead:antibody complexes and rotated at 65 degrees. The immunoprecipitated chromatin was purified using Qiagen's PCR cleanup kit and re-suspended in 60 μL Qiagen's elution buffer.

III. mRNA Isolation and Sequencing Library Preparation

Mouse neural tubes were dissected from E11.5 *12.4kbPtf1a::mcherrry* embryos either wildtype or null for Ptf1a and placed into DMEM/F12 on ice and dissociated in 0.25% trypsin for 15 minutes at 37 degrees C. Trypsin activity was quenched with 2% fetal bovine serum, and mcherry positive cells were purified from the resulting single cell suspension by fluorescence activated cell sorting (FACS). Total RNA from FACS sorted neural tube populations were extracted and purified with Zymo's Mini RNA Isolation Kit. mRNA was purified, reverse transcribed and amplified for sequencing with Illumina's mRNA-Seq kit according to manufacturer's instructions. Two independent libraries were sequenced for each cell population.

IV. Bioinformatics

ChIP-Seq Peak Calling

Sequence reads were mapped to the mm9 assembly of the mouse genome using Bowtie (Langmead et al., 2009). Reads that had greater than two base pair mismatches or aligned to more than one place in the reference genome were removed. In addition, duplicate reads were removed for further analysis. Unique read numbers were normalized to 10 million total reads for comparison across experiments. Peak calling

was performed by Homer (Heinz et al., 2010), the FDR cutoff was set at 0.001 and peaks were required to have greater than a 4-fold read enrichment over local background and control sample. Control samples used for Ptf1a ChIP-Seq was a Ptf1a ChIP in the telencephalon, RbpJ ChIP-seq was compared to input sample, and Prdm13 was compared to both Prdm13 ChIP in the telencephalon and input sample.

RNA-Seq Analysis

Sequence reads were aligned to the mm9 build of the mouse genome using TopHat v1.4.1 (Trapnell et al., 2009). Default settings were used with the following exceptions: -G option (instructs TopHat to initially map reads onto a supplied reference transcriptome) and –no-novel-juncs option, which ignores putative splice junctions occurring outside of known gene models. Expression levels were determined by the FPKM method using Cuffdiff v1.3.0 with the same reference gene annotation file (from RefSeq) used in the TopHat alignment (Trapnell et al., 2010). Upper quartile normalization (-N option) was performed to more accurately estimate levels of low-abundance transcripts, and multiple read correction (-u option) was selected to better distribute reads mapping to multiple genomic locations. The minimum number of alignments needed for significance testing was set to 1 (-c option). All other settings were left at default values.

V. GFP enhancer reporter assay

Sections were imaged using a Zeiss LSM510 confocal microscope. For Fig. 6, E-H or I-L, the endogenous GFP fluorescence gain and offset was kept constant and 16-bit tiff images taken on the same slide and day within one set of chick electroporation experiments of an enhancer-GFP construct plus control, Prdm13, Ascl1, or both. Mean GFP pixel intensity/cell of GFP signal was processed using ImageJ. Significant differences between control and experimental samples were calculated using a two-

tailed two-sample equal variance (homoscedastic) Student's t test (* indicates P <, 0.001) in Microsoft Excel. SEM is shown.

VI. Primers

Primers for ChIP-qPCR:

Gene name	F	R
Kirrel2 ORF (Cont, Fig. 6B)	AGAGGACATGGTGGTGCTGTTGG	TGAGCAGAGACCAGCTCACCTG
eTlx1	GGAGCCTCCTCCCTCAATCGGT	CACCAGCGTCCGCTCTGCCA
eTlx3	TGCACCAGTAGCAGGTGCCAG	AGGCCGGCACCAGAAACAATCG
DII1 M (eDll1)	GCGTGGCTGTCATTAAGG	GGTGCTGTCTGCATTACC
DII1 N (Cont, Fig. 6C)	ATGACACGCCTTTAGACG	AGCTGTGGGAGTATAGAGAC

Oligonucleotides for generating the shRNA:

Target gene name	Target sequence
Ptf1a	1. AAGTGTAACTTAAGATTCGGA 2. AAGAAAATCATCATCTGCCAC
Prdm13	1. AAGAAGCCCTTGGGAACAAAG 2. AAGCTGTACTCCCGCAAGTAC
DSred control	AAGGTGAAGTTCATCGGCGTG

Primers for generating ISH probes:

Probe name	F	R
cPrdm13	TCGTCTGTTCCTGTACTGCGGC	CGTCGGTGAAGCAGACGTCCAC
mPrdm13	TACATCTGCTGGTACTGCTGG	GCGCTCCACAGGGAGCCCGGG

Primers for generating GFP reporter constructs:

Enhancer::GFP	F	R
eTlx1::GFP	GCACGCTTGCACAAGTAGTA	CACTCGGGTCACTGCACTT
eTlx3::GFP	GTACTGTCATTCACAGCAATAGTT	TTACCCCTACCCCTCACACC

Primers for genotyping Ptf1a null:

Genotyping	F	R	Band size
Wild-type	TGAGGAAGATTTCTTCACCGAC CAGTCCTC	CGGTAGCAGTATTCGTGT AGCTGGTG	133bp
Mutant	GGACATGTTCAGGGATCGCCA GGCG	GCATAACCAGTGAAACA GCATTGCTG	300bp

BIBLIOGRAPHY

Aguilo, F., Avagyan, S., Labar, A., Sevilla, A., Lee, D.F., Kumar, P., Lemischka, I.R., Zhou, B.Y., and Snoeck, H.W. (2011). Prdm16 is a physiologic regulator of hematopoietic stem cells. Blood *117*, 5057-5066.

Aldinger, K.A., and Elsen, G.E. (2008). Ptf1a is a molecular determinant for both glutamatergic and GABAergic neurons in the hindbrain. J Neurosci *28*, 338-339.

Ancelin, K., Lange, U.C., Hajkova, P., Schneider, R., Bannister, A.J., Kouzarides, T., and Surani, M.A. (2006). Blimp1 associates with Prmt5 and directs histone arginine methylation in mouse germ cells. Nat Cell Biol *8*, 623-630.

Anderson, S.A., Eisenstat, D.D., Shi, L., and Rubenstein, J.L. (1997a). Interneuron migration from basal forebrain to neocortex: dependence on Dlx genes. Science *278*, 474-476.

Anderson, S.A., Qiu, M., Bulfone, A., Eisenstat, D.D., Meneses, J., Pedersen, R., and Rubenstein, J.L. (1997b). Mutations of the homeobox genes Dlx-1 and Dlx-2 disrupt the striatal subventricular zone and differentiation of late born striatal neurons. Neuron *19*, 27-37.

Batista, M.F., and Lewis, K.E. (2008). Pax2/8 act redundantly to specify glycinergic and GABAergic fates of multiple spinal interneurons. Dev Biol *323*, 88-97.

Baudat, F., Buard, J., Grey, C., Fledel-Alon, A., Ober, C., Przeworski, M., Coop, G., and de Massy, B. (2010). PRDM9 is a major determinant of meiotic recombination hotspots in humans and mice. Science *327*, 836-840.

Beres, T.M., Masui, T., Swift, G.H., Shi, L., Henke, R.M., and MacDonald, R.J. (2006). PTF1 is an organ-specific and Notch-independent basic helix-loop-helix complex containing the mammalian Suppressor of Hairless (RBP-J) or its paralogue, RBP-L. Mol Cell Biol *26*, 117-130.

Berg, I.L., Neumann, R., Lam, K.W., Sarbajna, S., Odenthal-Hesse, L., May, C.A., and Jeffreys, A.J. (2010). PRDM9 variation strongly influences recombination hot-spot activity and meiotic instability in humans. Nat Genet *42*, 859-863.

Bertrand, N., Castro, D.S., and Guillemot, F. (2002). Proneural genes and the specification of neural cell types. Nat Rev Neurosci *3*, 517-530.

Bikoff, E.K., Morgan, M.A., and Robertson, E.J. (2009). An expanding job description for Blimp-1/PRDM1. Curr Opin Genet Dev *19*, 379-385.

Borodinsky, L.N., Root, C.M., Cronin, J.A., Sann, S.B., Gu, X., and Spitzer, N.C. (2004). Activity-dependent homeostatic specification of transmitter expression in embryonic neurons. Nature *429*, 523-530.

Brayer, K.J., and Segal, D.J. (2008). Keep your fingers off my DNA: protein-protein interactions mediated by C2H2 zinc finger domains. Cell biochemistry and biophysics *50*, 111-131.

Brohl, D., Strehle, M., Wende, H., Hori, K., Bormuth, I., Nave, K.A., Muller, T., and Birchmeier, C. (2008). A transcriptional network coordinately determines transmitter and peptidergic fate in the dorsal spinal cord. Dev Biol *322*, 381-393.

Brzezinski, J.A.t., Lamba, D.A., and Reh, T.A. (2010). Blimp1 controls photoreceptor versus bipolar cell fate choice during retinal development. Development *137*, 619-629.

Bulfone, A., Wang, F., Hevner, R., Anderson, S., Cutforth, T., Chen, S., Meneses, J., Pedersen, R., Axel, R., and Rubenstein, J.L. (1998). An olfactory sensory map develops in the absence of normal projection neurons or GABAergic interneurons. Neuron *21*, 1273-1282.

Casarosa, S., Fode, C., and Guillemot, F. (1999). Mash1 regulates neurogenesis in the ventral telencephalon. Development *126*, 525-534.

Caspary, T., and Anderson, K.V. (2003). Patterning cell types in the dorsal spinal cord: what the mouse mutants say. Nat Rev Neurosci *4*, 289-297.

Castro, D.S., Skowronska-Krawczyk, D., Armant, O., Donaldson, I.J., Parras, C., Hunt, C., Critchley, J.A., Nguyen, L., Gossler, A., Gottgens, B., *et al*. (2006). Proneural bHLH and Brn proteins coregulate a neurogenic program through cooperative binding to a conserved DNA motif. Dev Cell *11*, 831-844.

Cheng, H.Y., Chen, X.W., Cheng, L., Liu, Y.D., and Lou, G. DNA methylation and carcinogenesis of PRDM5 in cervical cancer. J Cancer Res Clin Oncol *136*, 1821-1825.

Cheng, L., Arata, A., Mizuguchi, R., Qian, Y., Karunaratne, A., Gray, P.A., Arata, S., Shirasawa, S., Bouchard, M., Luo, P., *et al*. (2004). Tlx3 and Tlx1 are post-mitotic selector genes determining glutamatergic over GABAergic cell fates. Nat Neurosci *7*, 510-517.

Cheng, L., Samad, O.A., Xu, Y., Mizuguchi, R., Luo, P., Shirasawa, S., Goulding, M., and Ma, Q. (2005). Lbx1 and Tlx3 are opposing switches in determining GABAergic versus glutamatergic transmitter phenotypes. Nat Neurosci *8*, 1510-1515.

Chittka, A., Nitarska, J., Grazini, U., and Richardson, W.D. (2012). Transcription Factor Positive Regulatory Domain 4 (PRDM4) Recruits Protein Arginine Methyltransferase 5 (PRMT5) to Mediate Histone Arginine Methylation and Control Neural Stem Cell Proliferation and Differentiation. J Biol Chem *287*, 42995-43006.

Chuikov, S., Levi, B.P., Smith, M.L., and Morrison, S.J. Prdm16 promotes stem cell maintenance in multiple tissues, partly by regulating oxidative stress. Nat Cell Biol *12*, 999-1006.

Cockell, M., Stevenson, B.J., Strubin, M., Hagenbuchle, O., and Wellauer, P.K. (1989). Identification of a cell-specific DNA-binding activity that interacts with a transcriptional activator of genes expressed in the acinar pancreas. Mol Cell Biol *9*, 2464-2476.

Corbin, J.G., and Butt, S.J. (2011). Developmental mechanisms for the generation of telencephalic interneurons. Dev Neurobiol *71*, 710-732.

Crews, S.T. (1998). Control of cell lineage-specific development and transcription by bHLH-PAS proteins. Genes Dev *12*, 607-620.

Dahm, L., Klugmann, F., Gonzalez-Algaba, A., and Reuss, B. Tamoxifen and raloxifene modulate gap junction coupling during early phases of retinoic acid-dependent neuronal differentiation of NTera2/D1 cells. Cell Biol Toxicol.

Davis, C.A., Haberland, M., Arnold, M.A., Sutherland, L.B., McDonald, O.G., Richardson, J.A., Childs, G., Harris, S., Owens, G.K., and Olson, E.N. (2006). PRISM/PRDM6, a transcriptional repressor that promotes the proliferative gene program in smooth muscle cells. Mol Cell Biol *26*, 2626-2636.

Deneault, E., Cellot, S., Faubert, A., Laverdure, J.P., Frechette, M., Chagraoui, J., Mayotte, N., Sauvageau, M., Ting, S.B., and Sauvageau, G. (2009). A functional screen to identify novel effectors of hematopoietic stem cell activity. Cell *137*, 369-379.

Deng, Q., and Huang, S. (2004). PRDM5 is silenced in human cancers and has growth suppressive activities. Oncogene *23*, 4903-4910.

Derunes, C., Briknarova, K., Geng, L., Li, S., Gessner, C.R., Hewitt, K., Wu, S., Huang, S., Woods, V.I., Jr., and Ely, K.R. (2005). Characterization of the PR domain of RIZ1 histone methyltransferase. Biochem Biophys Res Commun *333*, 925-934.

Ding, Y.Q., Yin, J., Kania, A., Zhao, Z.Q., Johnson, R.L., and Chen, Z.F. (2004). Lmx1b controls the differentiation and migration of the superficial dorsal horn neurons of the spinal cord. Development *131*, 3693-3703.

Dovat, S., Ronni, T., Russell, D., Ferrini, R., Cobb, B.S., and Smale, S.T. (2002). A common mechanism for mitotic inactivation of C2H2 zinc finger DNA-binding domains. Genes Dev *16*, 2985-2990.

Duan, Z., Person, R.E., Lee, H.H., Huang, S., Donadieu, J., Badolato, R., Grimes, H.L., Papayannopoulou, T., and Horwitz, M.S. (2007). Epigenetic regulation of protein-coding and microRNA genes by the Gfi1-interacting tumor suppressor PRDM5. Mol Cell Biol *27*, 6889-6902.

Dullin, J.P., Locker, M., Robach, M., Henningfeld, K.A., Parain, K., Afelik, S., Pieler, T., and Perron, M. (2007). Ptf1a triggers GABAergic neuronal cell fates in the retina. BMC Dev Biol *7*, 110.

Eckert, D., Biermann, K., Nettersheim, D., Gillis, A.J., Steger, K., Jack, H.M., Muller, A.M., Looijenga, L.H., and Schorle, H. (2008). Expression of BLIMP1/PRMT5 and concurrent histone H2A/H4 arginine 3 dimethylation in fetal germ cells, CIS/IGCNU and germ cell tumors. BMC Dev Biol *8*, 106.

Ellenberger, T., Fass, D., Arnaud, M., and Harrison, S.C. (1994). Crystal structure of transcription factor E47: E-box recognition by a basic region helix-loop-helix dimer. Genes Dev *8*, 970-980.

Eom, G.H., Kim, K., Kim, S.M., Kee, H.J., Kim, J.Y., Jin, H.M., Kim, J.R., Kim, J.H., Choe, N., Kim, K.B., *et al*. (2009). Histone methyltransferase PRDM8 regulates mouse testis steroidogenesis. Biochem Biophys Res Commun *388*, 131-136.

Ferre-D'Amare, A.R., Pognonec, P., Roeder, R.G., and Burley, S.K. (1994). Structure and function of the b/HLH/Z domain of USF. EMBO J *13*, 180-189.

Ferre-D'Amare, A.R., Prendergast, G.C., Ziff, E.B., and Burley, S.K. (1993). Recognition by Max of its cognate DNA through a dimeric b/HLH/Z domain. Nature *363*, 38-45.

Fitzgerald, M. (2005). The development of nociceptive circuits. Nat Rev Neurosci *6*, 507-520.

Fode, C., Ma, Q., Casarosa, S., Ang, S.L., Anderson, D.J., and Guillemot, F. (2000). A role for neural determination genes in specifying the dorsoventral identity of telencephalic neurons. Genes Dev *14*, 67-80.

Fog, C.K., Galli, G.G., and Lund, A.H. (2012). PRDM proteins: Important players in differentiation and disease. Bioessays *34*, 50-60.

Fruhbeck, G., Sesma, P., and Burrell, M.A. (2009). PRDM16: the interconvertible adipo-myocyte switch. Trends Cell Biol *19*, 141-146.

Fujitani, Y., Fujitani, S., Luo, H., Qiu, F., Burlison, J., Long, Q., Kawaguchi, Y., Edlund, H., MacDonald, R.J., Furukawa, T., *et al*. (2006). Ptf1a determines horizontal and amacrine cell fates during mouse retinal development. Development *133*, 4439-4450.

Fumasoni, I., Meani, N., Rambaldi, D., Scafetta, G., Alcalay, M., and Ciccarelli, F.D. (2007). Family expansion and gene rearrangements contributed to the functional specialization of PRDM genes in vertebrates. BMC Evol Biol *7*, 187.

Glasgow, S.M., Henke, R.M., Macdonald, R.J., Wright, C.V., and Johnson, J.E. (2005). Ptf1a determines GABAergic over glutamatergic neuronal cell fate in the spinal cord dorsal horn. Development *132*, 5461-5469.

Gowan, K., Helms, A.W., Hunsaker, T.L., Collisson, T., Ebert, P.J., Odom, R., and Johnson, J.E. (2001). Crossinhibitory activities of Ngn1 and Math1 allow specification of distinct dorsal interneurons. Neuron *31*, 219-232.

Goyama, S., Yamamoto, G., Shimabe, M., Sato, T., Ichikawa, M., Ogawa, S., Chiba, S., and Kurokawa, M. (2008). Evi-1 is a critical regulator for hematopoietic stem cells and transformed leukemic cells. Cell Stem Cell *3*, 207-220.

Gross, M.K., Dottori, M., and Goulding, M. (2002). Lbx1 specifies somatosensory association interneurons in the dorsal spinal cord. Neuron *34*, 535-549.

Gu, X., Olson, E.C., and Spitzer, N.C. (1994). Spontaneous neuronal calcium spikes and waves during early differentiation. J Neurosci *14*, 6325-6335.

Gyory, I., Wu, J., Fejer, G., Seto, E., and Wright, K.L. (2004). PRDI-BF1 recruits the histone H3 methyltransferase G9a in transcriptional silencing. Nat Immunol *5*, 299-308.

Hamburger, V., and Hamilton, H.L. (1992). A series of normal stages in the development of the chick embryo. 1951. Dev Dyn *195*, 231-272.

Hayashi, K., Yoshida, K., and Matsui, Y. (2005). A histone H3 methyltransferase controls epigenetic events required for meiotic prophase. Nature *438*, 374-378.

Heinz, S., Benner, C., Spann, N., Bertolino, E., Lin, Y.C., Laslo, P., Cheng, J.X., Murre, C., Singh, H., and Glass, C.K. (2010). Simple combinations of lineage-determining transcription factors prime cis-regulatory elements required for macrophage and B cell identities. Mol Cell *38*, 576-589.

Helms, A.W., Battiste, J., Henke, R.M., Nakada, Y., Simplicio, N., Guillemot, F., and Johnson, J.E. (2005). Sequential roles for Mash1 and Ngn2 in the generation of dorsal spinal cord interneurons. Development *132*, 2709-2719.

Helms, A.W., and Johnson, J.E. (2003). Specification of dorsal spinal cord interneurons. Curr Opin Neurobiol *13*, 42-49.

Henke, R.M., Savage, T.K., Meredith, D.M., Glasgow, S.M., Hori, K., Dumas, J., MacDonald, R.J., and Johnson, J.E. (2009). Neurog2 is a direct downstream target of the Ptf1a-Rbpj transcription complex in dorsal spinal cord. Development *136*, 2945-2954.

Hohenauer, T., and Moore, A.W. (2012). The Prdm family: expanding roles in stem cells and development. Development *139*, 2267-2282.

Holmstrom, S.R., Deering, T., Swift, G.H., Poelwijk, F.J., Mangelsdorf, D.J., Kliewer, S.A., and MacDonald, R.J. (2011). LRH-1 and PTF1-L coregulate an exocrine pancreas-specific transcriptional network for digestive function. Genes Dev *25*, 1674-1679.

Hori, K., Cholewa-Waclaw, J., Nakada, Y., Glasgow, S.M., Masui, T., Henke, R.M., Wildner, H., Martarelli, B., Beres, T.M., Epstein, J.A., *et al*. (2008). A nonclassical bHLH Rbpj transcription factor complex is required for specification of GABAergic neurons independent of Notch signaling. Genes Dev *22*, 166-178.

Horn, K.H., Warner, D.R., Pisano, M., and Greene, R.M. (2009). PRDM16 expression in the developing mouse embryo. Acta Histochem.

Hoshino, M., Nakamura, S., Mori, K., Kawauchi, T., Terao, M., Nishimura, Y.V., Fukuda, A., Fuse, T., Matsuo, N., Sone, M., *et al*. (2005). Ptf1a, a bHLH transcriptional gene, defines GABAergic neuronal fates in cerebellum. Neuron *47*, 201-213.

Huang, M., Huang, T., Xiang, Y., Xie, Z., Chen, Y., Yan, R., Xu, J., and Cheng, L. (2008). Ptf1a, Lbx1 and Pax2 coordinate glycinergic and peptidergic transmitter phenotypes in dorsal spinal inhibitory neurons. Dev Biol *322*, 394-405.

Huang, S. (2002). Histone methyltransferases, diet nutrients and tumour suppressors. Nature reviews Cancer *2*, 469-476.

Huang, S., Shao, G., and Liu, L. (1998). The PR domain of the Rb-binding zinc finger protein RIZ1 is a protein binding interface and is related to the SET domain functioning in chromatin-mediated gene expression. J Biol Chem *273*, 15933-15939.

Iuchi, S. (2001). Three classes of C2H2 zinc finger proteins. Cell Mol Life Sci *58*, 625-635.

Jenuwein, T. (2001). Re-SET-ting heterochromatin by histone methyltransferases. Trends Cell Biol *11*, 266-273.

Johnson, J.E., Birren, S.J., and Anderson, D.J. (1990). Two rat homologues of Drosophila achaete-scute specifically expressed in neuronal precursors. Nature *346*, 858-861.

Johnson, J.E., Birren, S.J., Saito, T., and Anderson, D.J. (1992). DNA binding and transcriptional regulatory activity of mammalian achaete-scute homologous (MASH) proteins revealed by interaction with a muscle-specific enhancer. Proc Natl Acad Sci U S A *89*, 3596-3600.

Kageyama, R., and Nakanishi, S. (1997). Helix-loop-helix factors in growth and differentiation of the vertebrate nervous system. Curr Opin Genet Dev *7*, 659-665.

Kajimura, S., Seale, P., Kubota, K., Lunsford, E., Frangioni, J.V., Gygi, S.P., and Spiegelman, B.M. (2009). Initiation of myoblast to brown fat switch by a PRDM16-C/EBP-beta transcriptional complex. Nature *460*, 1154-1158.

Kajimura, S., Seale, P., and Spiegelman, B.M. (2010). Transcriptional control of brown fat development. Cell Metab *11*, 257-262.

Kajimura, S., Seale, P., Tomaru, T., Erdjument-Bromage, H., Cooper, M.P., Ruas, J.L., Chin, S., Tempst, P., Lazar, M.A., and Spiegelman, B.M. (2008). Regulation of the brown and white fat gene programs through a PRDM16/CtBP transcriptional complex. Genes Dev *22*, 1397-1409.

Katoh, K., Omori, Y., Onishi, A., Sato, S., Kondo, M., and Furukawa, T. (2010). Blimp1 suppresses Chx10 expression in differentiating retinal photoreceptor precursors to ensure proper photoreceptor development. J Neurosci *30*, 6515-6526.

Kawaguchi, Y., Cooper, B., Gannon, M., Ray, M., MacDonald, R.J., and Wright, C.V. (2002). The role of the transcriptional regulator Ptf1a in converting intestinal to pancreatic progenitors. Nat Genet *32*, 128-134.

Kim, E.J., Battiste, J., Nakagawa, Y., and Johnson, J.E. (2008). Ascl1 (Mash1) lineage cells contribute to discrete cell populations in CNS architecture. Mol Cell Neurosci *38*, 595-606.

Kim, K.C., Geng, L., and Huang, S. (2003). Inactivation of a histone methyltransferase by mutations in human cancers. Cancer Res *63*, 7619-7623.

Kinameri, E., Inoue, T., Aruga, J., Imayoshi, I., Kageyama, R., Shimogori, T., and Moore, A.W. (2008). Prdm proto-oncogene transcription factor family expression and interaction with the Notch-Hes pathway in mouse neurogenesis. PLoS One *3*, e3859.

Kouzarides, T. (2002). Histone methylation in transcriptional control. Curr Opin Genet Dev *12*, 198-209.

Krapp, A., Knofler, M., Frutiger, S., Hughes, G.J., Hagenbuchle, O., and Wellauer, P.K. (1996). The p48 DNA-binding subunit of transcription factor PTF1 is a new exocrine pancreas-specific basic helix-loop-helix protein. EMBO J *15*, 4317-4329.

Krapp, A., Knofler, M., Ledermann, B., Burki, K., Berney, C., Zoerkler, N., Hagenbuchle, O., and Wellauer, P.K. (1998). The bHLH protein PTF1-p48 is essential for the formation of the exocrine and the correct spatial organization of the endocrine pancreas. Genes Dev *12*, 3752-3763.

Kriegstein, A., and Alvarez-Buylla, A. (2009). The glial nature of embryonic and adult neural stem cells. Annu Rev Neurosci *32*, 149-184.

Krishna, S.S., Majumdar, I., and Grishin, N.V. (2003). Structural classification of zinc fingers: survey and summary. Nucleic Acids Res *31*, 532-550.

Kuo, T.C., and Calame, K.L. (2004). B lymphocyte-induced maturation protein (Blimp)-1, IFN regulatory factor (IRF)-1, and IRF-2 can bind to the same regulatory sites. J Immunol *173*, 5556-5563.

Lai, H.C., Klisch, T.J., Roberts, R., Zoghbi, H.Y., and Johnson, J.E. (2011). In vivo neuronal subtype-specific targets of Atoh1 (Math1) in dorsal spinal cord. J Neurosci *31*, 10859-10871.

Langmead, B., Trapnell, C., Pop, M., and Salzberg, S.L. (2009). Ultrafast and memory-efficient alignment of short DNA sequences to the human genome. Genome Biol *10*, R25.

Lelievre, E.C., Lek, M., Boije, H., Houille-Vernes, L., Brajeul, V., Slembrouck, A., Roger, J.E., Sahel, J.A., Matter, J.M., Sennlaub, F.*, et al*. (2011). Ptf1a/Rbpj complex inhibits ganglion cell fate and drives the specification of all horizontal cell subtypes in the chick retina. Dev Biol *358*, 296-308.

Liu, C., Ma, W., Su, W., and Zhang, J. (2012). Prdm14 acts upstream of islet2 transcription to regulate axon growth of primary motoneurons in zebrafish. Development.

Liu, Y., and Ma, Q. (2011). Generation of somatic sensory neuron diversity and implications on sensory coding. Curr Opin Neurobiol *21*, 52-60.

Livne-Bar, I., Pacal, M., Cheung, M.C., Hankin, M., Trogadis, J., Chen, D., Dorval, K.M., and Bremner, R. (2006). Chx10 is required to block photoreceptor differentiation but is dispensable for progenitor proliferation in the postnatal retina. Proc Natl Acad Sci U S A *103*, 4988-4993.

Lo, L.C., Johnson, J.E., Wuenschell, C.W., Saito, T., and Anderson, D.J. (1991). Mammalian achaete-scute homolog 1 is transiently expressed by spatially restricted subsets of early neuroepithelial and neural crest cells. Genes Dev *5*, 1524-1537.

Longo, A., Guanga, G.P., and Rose, R.B. (2008). Crystal structure of E47-NeuroD1/beta2 bHLH domain-DNA complex: heterodimer selectivity and DNA recognition. Biochemistry *47*, 218-229.

Ma, P.C., Rould, M.A., Weintraub, H., and Pabo, C.O. (1994). Crystal structure of MyoD bHLH domain-DNA complex: perspectives on DNA recognition and implications for transcriptional activation. Cell *77*, 451-459.

Ma, Q., Sommer, L., Cserjesi, P., and Anderson, D.J. (1997). Mash1 and neurogenin1 expression patterns define complementary domains of neuroepithelium in the developing CNS and are correlated with regions expressing notch ligands. J Neurosci *17*, 3644-3652.

Ma, Z., Swigut, T., Valouev, A., Rada-Iglesias, A., and Wysocka, J. (2011). Sequence-specific regulator Prdm14 safeguards mouse ESCs from entering extraembryonic endoderm fates. Nat Struct Mol Biol *18*, 120-127.

Marek, K.W., Kurtz, L.M., and Spitzer, N.C. (2010). cJun integrates calcium activity and tlx3 expression to regulate neurotransmitter specification. Nat Neurosci *13*, 944-950.

Marin, O., Anderson, S.A., and Rubenstein, J.L. (2000). Origin and molecular specification of striatal interneurons. J Neurosci *20*, 6063-6076.

Massari, M.E., and Murre, C. (2000). Helix-loop-helix proteins: regulators of transcription in eucaryotic organisms. Mol Cell Biol *20*, 429-440.

Masui, T., Long, Q., Beres, T.M., Magnuson, M.A., and MacDonald, R.J. (2007). Early pancreatic development requires the vertebrate Suppressor of Hairless (RBPJ) in the PTF1 bHLH complex. Genes Dev *21*, 2629-2643.

Masui, T., Swift, G.H., Hale, M.A., Meredith, D.M., Johnson, J.E., and Macdonald, R.J. (2008). Transcriptional autoregulation controls pancreatic Ptf1a expression during development and adulthood. Mol Cell Biol *28*, 5458-5468.

McCormick, D.A., and Contreras, D. (2001). On the cellular and network bases of epileptic seizures. Annu Rev Physiol *63*, 815-846.

Megason, S.G., and McMahon, A.P. (2002). A mitogen gradient of dorsal midline Wnts organizes growth in the CNS. Development *129*, 2087-2098.

Meredith, D.M., Deering, T., Casey, B., Savage, T.K., Mayer, P.R., Borromeo, M.D., Shen, C., Swift, G.H., MacDonald, R.J., and Johnson, J.E. (submitted). Program specificity for Ptf1a in pancreas versus neural tube development is mediated by collaborating cofactors and chromatin accessibility

Meredith, D.M., Masui, T., Swift, G.H., MacDonald, R.J., and Johnson, J.E. (2009). Multiple transcriptional mechanisms control Ptf1a levels during neural development including autoregulation by the PTF1-J complex. J Neurosci *29*, 11139-11148.

Merkle, F.T., and Alvarez-Buylla, A. (2006). Neural stem cells in mammalian development. Curr Opin Cell Biol *18*, 704-709.

Merot, Y., Retaux, S., and Heng, J.I. (2009). Molecular mechanisms of projection neuron production and maturation in the developing cerebral cortex. Semin Cell Dev Biol *20*, 726-734.

Mizuguchi, R., Kriks, S., Cordes, R., Gossler, A., Ma, Q., and Goulding, M. (2006). Ascl1 and Gsh1/2 control inhibitory and excitatory cell fate in spinal sensory interneurons. Nat Neurosci *9*, 770-778.

Mortazavi, A., Williams, B.A., McCue, K., Schaeffer, L., and Wold, B. (2008). Mapping and quantifying mammalian transcriptomes by RNA-Seq. Nat Methods *5*, 621-628.

Muller, T., Anlag, K., Wildner, H., Britsch, S., Treier, M., and Birchmeier, C. (2005). The bHLH factor Olig3 coordinates the specification of dorsal neurons in the spinal cord. Genes Dev *19*, 733-743.

Muller, T., Brohmann, H., Pierani, A., Heppenstall, P.A., Lewin, G.R., Jessell, T.M., and Birchmeier, C. (2002). The homeodomain factor lbx1 distinguishes two major programs of neuronal differentiation in the dorsal spinal cord. Neuron *34*, 551-562.

Murre, C., Bain, G., van Dijk, M.A., Engel, I., Furnari, B.A., Massari, M.E., Matthews, J.R., Quong, M.W., Rivera, R.R., and Stuiver, M.H. (1994). Structure and function of helix-loop-helix proteins. Biochim Biophys Acta *1218*, 129-135.

Murre, C., McCaw, P.S., and Baltimore, D. (1989a). A new DNA binding and dimerization motif in immunoglobulin enhancer binding, daughterless, MyoD, and myc proteins. Cell *56*, 777-783.

Murre, C., McCaw, P.S., Vaessin, H., Caudy, M., Jan, L.Y., Jan, Y.N., Cabrera, C.V., Buskin, J.N., Hauschka, S.D., Lassar, A.B.*, et al*. (1989b). Interactions between heterologous helix-loop-helix proteins generate complexes that bind specifically to a common DNA sequence. Cell *58*, 537-544.

Nakada, Y., Hunsaker, T.L., Henke, R.M., and Johnson, J.E. (2004). Distinct domains within Mash1 and Math1 are required for function in neuronal differentiation versus neuronal cell-type specification. Development *131*, 1319-1330.

Nakhai, H., Sel, S., Favor, J., Mendoza-Torres, L., Paulsen, F., Duncker, G.I., and Schmid, R.M. (2007). Ptf1a is essential for the differentiation of GABAergic and glycinergic amacrine cells and horizontal cells in the mouse retina. Development *134*, 1151-1160.

Nguyen, M.M., Nguyen, M.L., Caruana, G., Bernstein, A., Lambert, P.F., and Griep, A.E. (2003). Requirement of PDZ-containing proteins for cell cycle regulation and differentiation in the mouse lens epithelium. Mol Cell Biol *23*, 8970-8981.

Nishida, K., Hoshino, M., Kawaguchi, Y., and Murakami, F. (2010). Ptf1a directly controls expression of immunoglobulin superfamily molecules Nephrin and Neph3 in the developing central nervous system. J Biol Chem *285*, 373-380.

Nishikawa, K., Nakashima, T., Hayashi, M., Fukunaga, T., Kato, S., Kodama, T., Takahashi, S., Calame, K., and Takayanagi, H. (2010). Blimp1-mediated repression of negative regulators is required for osteoclast differentiation. Proc Natl Acad Sci U S A *107*, 3117-3122.

Nishikawa, N., Toyota, M., Suzuki, H., Honma, T., Fujikane, T., Ohmura, T., Nishidate, T., Ohe-Toyota, M., Maruyama, R., Sonoda, T., *et al*. (2007). Gene amplification and overexpression of PRDM14 in breast cancers. Cancer Res *67*, 9649-9657.

Nunez, N., Clifton, M.M., Funnell, A.P., Artuz, C., Hallal, S., Quinlan, K.G., Font, J., Vandevenne, M., Setiyaputra, S., Pearson, R.C., *et al*. (2011). The multi-zinc finger protein ZNF217 contacts DNA through a two-finger domain. J Biol Chem *286*, 38190-38201.

Obata, J., Yano, M., Mimura, H., Goto, T., Nakayama, R., Mibu, Y., Oka, C., and Kawaichi, M. (2001). p48 subunit of mouse PTF1 binds to RBP-Jkappa/CBF-1, the intracellular mediator of Notch signalling, and is expressed in the neural tube of early stage embryos. Genes Cells *6*, 345-360.

Parnavelas, J.G. (2002). The origin of cortical neurons. Braz J Med Biol Res *35*, 1423-1429.

Pascual, M., Abasolo, I., Mingorance-Le Meur, A., Martinez, A., Del Rio, J.A., Wright, C.V., Real, F.X., and Soriano, E. (2007). Cerebellar GABAergic progenitors adopt an external granule cell-like phenotype in the absence of Ptf1a transcription factor expression. Proc Natl Acad Sci U S A *104*, 5193-5198.

Persico, A.M., and Bourgeron, T. (2006). Searching for ways out of the autism maze: genetic, epigenetic and environmental clues. Trends Neurosci *29*, 349-358.

Pillai, A., Mansouri, A., Behringer, R., Westphal, H., and Goulding, M. (2007). Lhx1 and Lhx5 maintain the inhibitory-neurotransmitter status of interneurons in the dorsal spinal cord. Development *134*, 357-366.

Quina, L.A., Pak, W., Lanier, J., Banwait, P., Gratwick, K., Liu, Y., Velasquez, T., O'Leary, D.D., Goulding, M., and Turner, E.E. (2005). Brn3a-expressing retinal ganglion cells project specifically to thalamocortical and collicular visual pathways. J Neurosci *25*, 11595-11604.

Rallu, M., Corbin, J.G., and Fishell, G. (2002). Parsing the prosencephalon. Nat Rev Neurosci *3*, 943-951.

Rao, M., Baraban, J.H., Rajaii, F., and Sockanathan, S. (2004). In vivo comparative study of RNAi methodologies by in ovo electroporation in the chick embryo. Dev Dyn *231*, 592-600.

Razin, S.V., Borunova, V.V., Maksimenko, O.G., and Kantidze, O.L. (2012). Cys2His2 zinc finger protein family: classification, functions, and major members. Biochemistry (Mosc) *77*, 217-226.

Rose, S.D., Kruse, F., Swift, G.H., MacDonald, R.J., and Hammer, R.E. (1994). A single element of the elastase I enhancer is sufficient to direct transcription selectively to the pancreas and gut. Mol Cell Biol *14*, 2048-2057.

Rose, S.D., and MacDonald, R.J. (1997). Evolutionary silencing of the human elastase I gene (ELA1). Hum Mol Genet *6*, 897-903.

Ross, S.E. (2011). Pain and itch: insights into the neural circuits of aversive somatosensation in health and disease. Curr Opin Neurobiol *21*, 880-887.

Ross, S.E., McCord, A.E., Jung, C., Atan, D., Mok, S.I., Hemberg, M., Kim, T.K., Salogiannis, J., Hu, L., Cohen, S., *et al*. (2012). Bhlhb5 and prdm8 form a repressor complex involved in neuronal circuit assembly. Neuron *73*, 292-303.

Schneider, R., Bannister, A.J., and Kouzarides, T. (2002). Unsafe SETs: histone lysine methyltransferases and cancer. Trends Biochem Sci *27*, 396-402.

Seale, P., Bjork, B., Yang, W., Kajimura, S., Chin, S., Kuang, S., Scime, A., Devarakonda, S., Conroe, H.M., Erdjument-Bromage, H., *et al*. (2008). PRDM16 controls a brown fat/skeletal muscle switch. Nature *454*, 961-967.

Seale, P., Conroe, H.M., Estall, J., Kajimura, S., Frontini, A., Ishibashi, J., Cohen, P., Cinti, S., and Spiegelman, B.M. (2011). Prdm16 determines the thermogenic program of subcutaneous white adipose tissue in mice. J Clin Invest *121*, 96-105.

Seale, P., Kajimura, S., Yang, W., Chin, S., Rohas, L.M., Uldry, M., Tavernier, G., Langin, D., and Spiegelman, B.M. (2007). Transcriptional control of brown fat determination by PRDM16. Cell Metab *6*, 38-54.

Segurel, L., Leffler, E.M., and Przeworski, M. (2011). The case of the fickle fingers: how the PRDM9 zinc finger protein specifies meiotic recombination hotspots in humans. PLoS Biol *9*, e1001211.

Sellick, G.S., Barker, K.T., Stolte-Dijkstra, I., Fleischmann, C., Coleman, R.J., Garrett, C., Gloyn, A.L., Edghill, E.L., Hattersley, A.T., Wellauer, P.K., *et al*. (2004). Mutations in PTF1A cause pancreatic and cerebellar agenesis. Nat Genet *36*, 1301-1305.

Smith, S.T., and Jaynes, J.B. (1996). A conserved region of engrailed, shared among all en-, gsc-, Nk1-, Nk2- and msh-class homeoproteins, mediates active transcriptional repression in vivo. Development *122*, 3141-3150.

Soriano, P. (1999). Generalized lacZ expression with the ROSA26 Cre reporter strain. Nat Genet *21*, 70-71.

Spitzer, N.C. (2006). Electrical activity in early neuronal development. Nature *444*, 707-712.

Spitzer, N.C., Root, C.M., and Borodinsky, L.N. (2004). Orchestrating neuronal differentiation: patterns of Ca2+ spikes specify transmitter choice. Trends Neurosci *27*, 415-421.

Stevens, J.D., Roalson, E.H., and Skinner, M.K. (2008). Phylogenetic and expression analysis of the basic helix-loop-helix transcription factor gene family: genomic approach to cellular differentiation. Differentiation *76*, 1006-1022.

Su, S.T., Ying, H.Y., Chiu, Y.K., Lin, F.R., Chen, M.Y., and Lin, K.I. (2009). Involvement of histone demethylase LSD1 in Blimp-1-mediated gene repression during plasma cell differentiation. Mol Cell Biol *29*, 1421-1431.

Tavares, I., and Lima, D. (2007). From neuroanatomy to gene therapy: searching for new ways to manipulate the supraspinal endogenous pain modulatory system. J Anat *211*, 261-268.

Timmer, J., Johnson, J., and Niswander, L. (2001). The use of in ovo electroporation for the rapid analysis of neural-specific murine enhancers. Genesis *29*, 123-132.

Trapnell, C., Pachter, L., and Salzberg, S.L. (2009). TopHat: discovering splice junctions with RNA-Seq. Bioinformatics *25*, 1105-1111.

Trapnell, C., Williams, B.A., Pertea, G., Mortazavi, A., Kwan, G., van Baren, M.J., Salzberg, S.L., Wold, B.J., and Pachter, L. (2010). Transcript assembly and quantification by RNA-Seq reveals unannotated transcripts and isoform switching during cell differentiation. Nat Biotechnol *28*, 511-515.

Triezenberg, S.J., Kingsbury, R.C., and McKnight, S.L. (1988). Functional dissection of VP16, the trans-activator of herpes simplex virus immediate early gene expression. Genes Dev *2*, 718-729.

Tsuchida, T., Ensini, M., Morton, S.B., Baldassare, M., Edlund, T., Jessell, T.M., and Pfaff, S.L. (1994). Topographic organization of embryonic motor neurons defined by expression of LIM homeobox genes. Cell *79*, 957-970.

Verma-Kurvari, S., Savage, T., Gowan, K., and Johnson, J.E. (1996). Lineage-specific regulation of the neural differentiation gene MASH1. Dev Biol *180*, 605-617.

Vincent, S.D., Dunn, N.R., Sciammas, R., Shapiro-Shalef, M., Davis, M.M., Calame, K., Bikoff, E.K., and Robertson, E.J. (2005). The zinc finger transcriptional repressor Blimp1/Prdm1 is dispensable for early axis formation but is required for specification of primordial germ cells in the mouse. Development *132*, 1315-1325.

Walenta, J.H., Didier, A.J., Liu, X., and Kramer, H. (2001). The Golgi-associated hook3 protein is a member of a novel family of microtubule-binding proteins. J Cell Biol *152*, 923-934.

Watanabe, Y., Toyota, M., Kondo, Y., Suzuki, H., Imai, T., Ohe-Toyota, M., Maruyama, R., Nojima, M., Sasaki, Y., Sekido, Y., *et al*. (2007). PRDM5 identified as a target of epigenetic silencing in colorectal and gastric cancer. Clin Cancer Res *13*, 4786-4794.

Wiebe, P.O., Kormish, J.D., Roper, V.T., Fujitani, Y., Alston, N.I., Zaret, K.S., Wright, C.V., Stein, R.W., and Gannon, M. (2007). Ptf1a binds to and activates area III, a highly conserved region of the Pdx1 promoter that mediates early pancreas-wide Pdx1 expression. Mol Cell Biol *27*, 4093-4104.

Wildner, H., Muller, T., Cho, S.H., Brohl, D., Cepko, C.L., Guillemot, F., and Birchmeier, C. (2006). dILA neurons in the dorsal spinal cord are the product of terminal and non-terminal asymmetric progenitor cell divisions, and require Mash1 for their development. Development *133*, 2105-2113.

Willis, W.D., Jr. (2007). The somatosensory system, with emphasis on structures important for pain. Brain Res Rev *55*, 297-313.

Wolfe, S.A., Nekludova, L., and Pabo, C.O. (2000). DNA recognition by Cys2His2 zinc finger proteins. Annu Rev Biophys Biomol Struct *29*, 183-212.

Wu, Y., Ferguson, J.E., 3rd, Wang, H., Kelley, R., Ren, R., McDonough, H., Meeker, J., Charles, P.C., Wang, H., and Patterson, C. (2008). PRDM6 is enriched in vascular precursors during development and inhibits endothelial cell proliferation, survival, and differentiation. Journal of molecular and cellular cardiology *44*, 47-58.

Xie, M., Shao, G., Buyse, I.M., and Huang, S. (1997). Transcriptional repression mediated by the PR domain zinc finger gene RIZ. J Biol Chem *272*, 26360-26366.

Xu, Y., Lopes, C., Qian, Y., Liu, Y., Cheng, L., Goulding, M., Turner, E.E., Lima, D., and Ma, Q. (2008). Tlx1 and Tlx3 coordinate specification of dorsal horn pain-modulatory peptidergic neurons. J Neurosci *28*, 4037-4046.

Yamamoto, N., Yamamoto, S., Inagaki, F., Kawaichi, M., Fukamizu, A., Kishi, N., Matsuno, K., Nakamura, K., Weinmaster, G., Okano, H., *et al*. (2001). Role of Deltex-1 as a transcriptional regulator downstream of the Notch receptor. J Biol Chem *276*, 45031-45040.

Yang, N., Ng, Y.H., Pang, Z.P., Sudhof, T.C., and Wernig, M. (2011). Induced neuronal cells: how to make and define a neuron. Cell Stem Cell *9*, 517-525.

Yu, J., Angelin-Duclos, C., Greenwood, J., Liao, J., and Calame, K. (2000). Transcriptional repression by blimp-1 (PRDI-BF1) involves recruitment of histone deacetylase. Mol Cell Biol *20*, 2592-2603.

Zeng, P.Y., Vakoc, C.R., Chen, Z.C., Blobel, G.A., and Berger, S.L. (2006). In vivo dual cross-linking for identification of indirect DNA-associated proteins by chromatin immunoprecipitation. Biotechniques *41*, 694, 696, 698.

Zhang, Y., Stehling-Sun, S., Lezon-Geyda, K., Juneja, S.C., Coillard, L., Chatterjee, G., Wuertzer, C.A., Camargo, F., and Perkins, A.S. (2011). PR-domain-containing Mds1-Evi1 is critical for long-term hematopoietic stem cell function. Blood *118*, 3853-3861.

Zhou, W., Chen, H., and Zhang, L. (2009). The PcG protein hPc2 interacts with the N-terminus of histone demethylase JARID1B and acts as a transcriptional co-repressor. BMB Rep *42*, 154-159.